

| | |
|------------------|----|
| Title Page | 1 |
| Contents | 11 |
| Acknowledgements | 1 |

INVESTIGATION INTO THE EFFECTS OF FROTH

HEIGHT IN A FLOTATION CELL

| | |
|-------------------------------------|----|
| 3.1 Effect of Froth on Flotation | 8 |
| 3.2 Behaviour of Froth Columns | 10 |
| by | |
| 3.2.1 Breakage and Drainage of Foam | 10 |
| 3.2.2 Mass Balance for Foam | 11 |
| 3.2.3 Drainage Velocity | 12 |
| IAN JAMES BARKER B. Sc. (Eng.) | |
| 3.2.4 Operation at Steady State | 13 |
| 3.2.5 Froth Drainage | 13 |
| 3.4 Measurement of Liquid Fraction | 15 |
| 3.4.1 Flotation | 16 |

This thesis is submitted in partial fulfillment of the requirements of the degree of Master of Science in Engineering in the Department of Chemical Engineering at the University of Natal, Durban.

| | |
|--------------------------------------|----|
| Fig.1 Cutaway View of Cell | 23 |
| Fig.2 Photograph of Cell | 24 |
| 4.1.2 Mixing Tank System | 25 |
| 4.1.3 Controls on Mixing Tank System | 25 |
| 4.2 Experimental Procedure | 25 |
| Fig.3 System Flowchart | 26 |
| 4.3 Conductivity Measurements | 28 |

Durban, 1971.

CONTENTS

| | |
|---|----|
| Title Page | i |
| Contents | ii |
| Acknowledgements | 1 |
| 1. Introduction and Summary | 2 |
| 2. Literature Survey | 4 |
| 3. Theory: | 8 |
| 3.1 Effect of Froth on Flotation | 8 |
| 3.2 Behaviour of Froth Columns | 10 |
| 3.2.1 Breakage and Drainage of Foam | 10 |
| 3.2.2 Mass Balance for Foam | 11 |
| 3.2.3 Drainage Velocity | 12 |
| 3.2.4 Operation at Steady State | 12 |
| 3.2.5 Froth Breakage | 13 |
| 3.2.6 Measurement of Liquid Fraction | 15 |
| 3.3 Entrainment | 16 |
| 3.3.1 Triangular Diagram | 16 |
| 3.2.2 Entrainment Model | 18 |
| 4. Apparatus and Experimental Procedure | 22 |
| 4.1.1 Flotation Cell | 22 |
| Fig.1 Cutaway View of Cell | 23 |
| Fig.2 Photograph of Cell | 24 |
| 4.1.2 Mixing Tank System | 25 |
| 4.1.3 Controls on Mixing Tank System | 25 |
| 4.2 Experimental Procedure | 25 |
| Fig.3 System Flowsheet | 26 |
| 4.3 Conductivity Measurements | 28 |

ACKNOWLEDGEMENTS

| | | |
|-------|--|----|
| 4.4 | Investigation of Entrainment Using Silica Slurry | 29 |
| 5. | Results | 30 |
| 5.1 | Direct Effects of Froth Height | 30 |
| 5.1.1 | Effects on Grade | 31 |
| 5.1.2 | Effects on Solids Density | 32 |
| 5.1.3 | Effects on Particle Size Distribution | 33 |
| 5.2 | Froth Breakage from Conductivity Measurements | 34 |
| 5.3 | Entrainment | 37 |
| 6. | Discussion | 40 |
| 6.1 | Summary of Experimental Results | 40 |
| 6.2 | Link with Flotation Model | 40 |
| 6.2.1 | Optimisation | 44 |
| 6.3 | Conductivity Measurements | 45 |
| 6.4 | Entrainment | 47 |
| 7. | Conclusions | 48 |

Appendices:

(Experimental Results and Graphs in Appendices A to D):

| | | |
|----|---|----------|
| A. | Effect of froth height on grade, weight % solids, solids flow, water flow | A1 - A14 |
| B. | Effect of froth height on particle size distribution | B1 - B11 |
| C. | Results of conductivity measurements on froth | C1 - C8 |
| D. | Entrainment Study | D1 - D6 |
| E. | Study of controllers on mixing tanks | E1 - E12 |
| F. | References | F1 - F3 |
| G. | Nomenclature | G1 - G3 |

ACKNOWLEDGEMENTSCHAPTER I

I wish to express my gratitude to the following people for their help and guidance in this project:

Professor E.T. Woodburn and the staff, both academic and workshop, of the Department of Chemical Engineering at the University of Natal.

Dr. R.P. King, my supervisor for this project.

The National Institute for Metallurgy, who generously provided financial assistance and services for this project.

My fellow students, particularly those of the flotation research group in the Department.

The many people, both in the academic field and out, who helped in some way with this project.

The many people, both in the academic field and out, who helped in some way with this project. This group is concerned with the general modelling of the Flotation process, together with the study of individual sub-processes (such as the effect of froth height in a flotation cell).

The aim of this investigation was to study the effects of froth height on grade in a flotation cell, and then to model this mathematically in a manner suitable for inclusion into the general model for the Flotation process which was being built up by the research group.

To do this, a special cell was built in which the thickness of the froth layer could be easily adjusted and measured. Some work was done in which the froth height was varied and samples of the slurry streams taken. This formed the basis of the investigation. From analyses of these samples, and measurements

CHAPTER I

INTRODUCTION AND SUMMARY

Flotation is a process commonly used to upgrade or separate minerals in the mining industry. Although the process itself is superficially simple, modelling has proved difficult mainly because of the large number of variables and the interactions between them. It has been the object of much research to get a better understanding of the process, so enabling nearer optimum operation of existing plants and better design of new plants.

This particular investigation formed part of a larger and more general study of flotation being performed by the National Institute for Metallurgy Research Group in the Chemical Engineering Department of the University of Natal. This group is concerned with the general modelling of the flotation process, together with the study of individual sub-processes (such as the effect of froth height) in a flotation cell.

The aim of this investigation was to study the effects of froth height on grade in a flotation cell, and then to model this mathematically in a manner suitable for inclusion into the general model for the flotation process which was being built up by the research group.

To do this, a special cell was built in which the thickness of the froth layer could be easily adjusted and measured. Runs were then done in which the froth height was varied and samples of the slurry streams taken. This formed the basis of the investigation. From analyses of these samples, and measurements

taken / ...

taken during the runs, the direct effects of froth height were determined. Apatite ore was used for these runs, as it is the main one used by the Research Group.

In addition to the direct effects of froth height, the behaviour of the froth column was determined for some of the runs from measurements of the electrical conductivity. It was possible by this means to compare rates of breakage for different types of froth.

Finally, entrainment was investigated directly by the investigation of a depressed silica slurry.

All the data from these experiments are presented together in appendices A to D. Detailed descriptions and discussions are in the main body of the thesis. Graphs accompany data in the appendices.

Apart from the work done directly on froth, a study of the controls on the existing slurry mixing tanks was carried out in an attempt to reduce some of the observed experimental scatter. A summary of this study, and some of the conclusions drawn from it, are presented in appendix E.

In addition to the experimental work, a short literature survey was carried out in the fields of interest. This provided an idea of some of the past and present thinking on these matters, as a guide in the work.

CHAPTER 2.

LITERATURE SURVEY

(See list of references, appendix F)

The literature surveyed for this investigation can be divided into two groups :-

- (1) Articles and books on flotation proper, especially where the subject matter included reference to froth.
- (2) Literature on froths and foams. This was done in order to get an understanding of the behaviour of froth.

No references to the effect of froth height on flotation cell performance were found in the literature.

Flotation as a mineral extraction process has been used for over half a century, and a fair number of articles and books have been written on the subject. Much of the writing has been on the various subprocesses related to flotation.

Reference to a text such as Klassen and Mokrousov (ref 15) or, on the modelling side, Arbiter and Harris (ref 1) will provide a large list of references.

Modelling of the flotation process has taken several forms to date. Arbiter and Harris list four types of model. Probably the most common type is based on an analogy with chemical kinetics, and involves a rate constant, k . This can be used to explain why an increase in grade in the contents of the cell results in an increase in froth grade. A distributed rate constant has also been used to relate batch and continuous flotation (e.g. Loveday, ref 19). The model being developed by the Research Group at the University of Natal (see King et al, ref 14) is an advancement on this, and involves a distributed rate constant which is

also / ...

also a function of particle size and grade.

Up to now, models which have included froth height have not been formulated with the prime object of determining the effect of froth height, nor have they been specifically tested for such an effect. It appeared in many cases, and intuitively it seemed reasonable, that the froth layer did have an effect, but the exact nature of this effect was unknown. Klassen and Mokrousov included a chapter on froth in their book. This was mostly a fairly qualitative discussion, but quoted some results which showed that an increase in grade occurred when the froth on a flotation cell was sprayed gently with water, apparently because of secondary enrichment. Maksimov and Khainman (ref 20) gave results of an experiment which showed that up to 80% of the particles entering the froth layer returned to the pulp again.

Only two models which included the effects of froth have been found in literature :-

(1) Arbiter and Harris (ref 1, see also Harris, Jowett and Ghosh ref 8, and Harris and Rimmer, ref 9) postulated that the rate of return from the froth was proportional to the product of froth volume and solids concentration. A mass balance yields:

$$\begin{aligned} \text{Rate of flotation} &= k \times (\text{cell conc.}) \times (\text{cell vol.}) \\ &\quad - k' \times (\text{froth conc.}) \times (\text{froth vol.}) \end{aligned}$$

(2) Bushell (ref 3) postulated that the rate at which solids returned from the froth was proportional to the rate at which solids entered the froth. This simply reduces to a modified rate constant in an ordinary rate constant model.

It should be noted here that neither of the above models

included / ...

included any effects on the liquid flow, and also that neither was tested directly for the effect of froth height.

A phenomenon associated with the froth layer in a flotation cell is entrainment, especially entrainment of gangue particles. This is possible if the particles of less floatable material become trapped within the interstices of the rising bubbles. Again, like froth height, entrainment has not been studied much. Jowett (ref 13) investigated it experimentally, but found that, although the phenomenon appears to exist, his simple theory could not adequately explain it for complex systems.

In 1953 Bikerman published a book (ref 2), entitled "Foams: theory and industrial applications." In this book, he summarised all the work which had been done in this field up to 1953. Froth flotation featured prominently as a major industrial application in the use of foam. It is interesting to note that the study of foams dates back quite a long way. Bikerman lists a number of references to work done by Plateau (of "Plateau border" fame) over 100 years ago.

The study of foam drainage and also foam stability (these two terms are often confused) is touched on by Bikerman. Most of the equations given are semi-empirical, and indicate the lack of research in this field up to 1953. More recently, further attempts have been made to model drainage. Jakobi, Woodcock and Grove (ref 12) are the first of this group. Haas and Johnson (ref 7) later presented experimental results for continuous operation of foam columns, and compared their model with that of Jakobi. Leonard and Lemlich (ref 17) took a more sophisticated view, and analysed the flow through channels the shape of Plateau borders, using a

computer / ...

computer to calculate results from their model.

So far, the theories form two distinct groups : Jakobi's type where the liquid flow, L , is proportional to the cube of the liquid fraction f , and the other type as used by Haas and Johnson, and Leonard and Lemlich, where L is proportional to f^2 . In terms of drainage velocity, v_d , ($=L/f$) the models become

$$v_d = K_1 f^2 \quad \underline{2.1}$$

and

$$v_d = K_2 f \quad \underline{2.2}$$

Rubin, La Mantia and Gaden (ref 22) discuss the theories and present experimental results which appear to agree with equation 2.2. Hoffer and Rubin (ref 10) discuss the flow regimes which are attainable, and point out that equation 2.2 will hold in the "plug flow" region, which they say should occur when $f < 0.26$.

In the field of froth stability there has been little work done. Ross, (ref 21) in a very readable article, derives the ideal gas law as it applies to foams and shows how it is possible to represent bubble coalescence and foam breakage on a potential energy diagram. The chapter on froths in Klassen and Mokrousov discusses froth stability rather qualitatively.

A subject closely linked with froth stability is the modus operandi of surfactants, frothers and anti-frothers. This subject is also not well understood. Both Bikerman and Klassen and Mokrousov include discussions on this, mainly from the point of view of individual compounds. Livshits and Dudenkov (ref 18) discuss the effects on froth stability of compounds formed between collectors and various ions present in a flotation cell. Data and discussions on the common chemicals used in flotation can be found in the commercial literature of most mining chemical manufacturers.

CHAPTER 3

THEORY

The theory for this project is divided into three sections:

- (1) Modelling the effects of froth height on grade.
- (2) Studying the behaviour of froth columns.
- (3) Studying entrainment of solids in the froth.

3.1 EFFECT OF FROTH HEIGHT ON FLOTATION

The flotation theory (see ref. 14) being developed by the research group is a distributed parameter model using a first order rate constant, k . Each particle in the flotation cell is regarded as being of a particular size D , a grade g , and having a flotation rate constant k . There will be a distribution of these parameters over the solids in the cell. A distribution function $f(k,g,D)$ is then defined such that $f(k,g,D) \cdot dk \cdot dg \cdot dD$ is the mass fraction of solids in the range k to $k + dk$, g to $g + dg$ and D to $D + dD$.

The rate of flotation of solids is dependent also on the aeration of the cell and the behaviour in the froth layer. The rate of attachment of solids in an element of k - g - D space to the bubbles is given by:

$$k \cdot f(k,g,D) \cdot (A' \cdot s) \cdot \phi(D) \cdot w \cdot dk \cdot dg \cdot dD$$

where $A' \cdot s$ is the product of bubble surface area \times fraction of this surface area which is uncovered by solids;

w is the mass of solids in the cell;

$\phi(D)$ is a function of D which accounts for the effects that particle size has over and above $f(k,g,D)$.

Process/.....

Processes occurring in the froth layer might also treat each type of particle differently. (For example, if solids were becoming detached in the froth, it would seem reasonable that gangue particles might fall off first, thus leading to enrichment in the froth). The most convenient way to model the effects of froth height in the context of the above model is to define a function, R , which is not only a function of froth height, h , but is also dependent on k , g , and D , and describes the fraction returning from the froth for solids lying in a given element of k - g - D space.

The overall rate of flotation of solids is then given by

$$\int_0^{\infty} \int_0^1 \int_0^{\infty} (1 - R(k, g, D, h)) \cdot (k f(k, g, D) A' S \phi(D) W) dk dg dD.$$

From here, it is possible to develop a model for the behaviour of the flotation cell under both batch and continuous operation. Reference 14 describes this in detail.

Returning to the effects of froth height, it is now a matter of determining the form of R ; in particular the interactions of the four variables in its argument list. Note the following in this respect:

- (1) The effects of froth height on grade reveal the interactions of g and h .
- (2) The effects of froth height on particle size distribution reveal the interactions of D and h .
- (3) The effects of froth height on total solids does not reflect any interactions over those mentioned above. It only reflects an average of the dependence of R on h .
- (4) The model does not allow for any effects of froth height on water overflow or weight percent solids in the froth.

R is/....

breakage R is dependent on the processes occurring in the froth layer, and as these are largely unknown, it is necessary to have experimental results before considering what form is most suitable for $R(k, g, D, h)$. Consider, however, the two models for froth height found in the literature (see section 2) expressed in terms of the above model:

(i) Harris' model Return rate proportional to product volume and solids concentration, i.e. total solids in froth.

Total solids in froth = rate of flotation \times holding time in froth

$$= (\text{rate of flotation}) \times (\text{froth volume}) / (\text{Air rate} \times (1-f))$$

$\therefore R(k, g, D, h) = k' \times (\text{total solids in froth}) / (\text{rate of flotation})$

$$= k' \times \{A \times h\} / Q_A (1-f)$$

Where k' is proportionality constant,

A is the surface area covered by froth,

Q_A is the air rate

f is the liquid fraction of the froth ($\neq f(k, g, D)$)

(ii) Bushell's model Return rate proportional to flotation rate,

$$\therefore R(k, g, D, h) = \text{constant.}$$

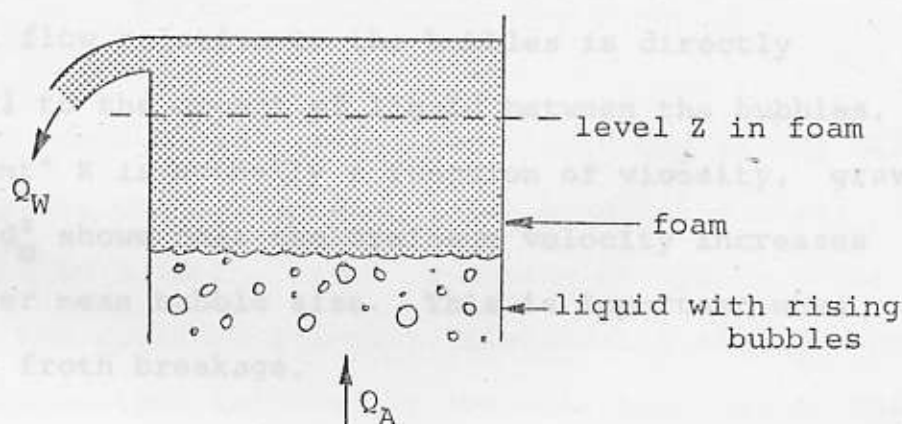
3.2 BEHAVIOUR OF FROTH COLUMNS

3.2.1 BREAKAGE AND DRAINAGE OF FOAM

As mentioned in the literature survey, foam drainage and foam breakage are two often confused terms. This is possibly because both processes release water from the body of the foam. A body of foam consists of air bubbles separated by thin liquid lamellae. The triangular intersections of these lamellae are called Plateau borders, and they accommodate most of the water held in the foam. Froth

breakage is caused by rupture of the liquid lamellae so that water is released from both the lamellae and the Plateau borders which disappear as a result of the rupture. Drainage, on the other hand, results from the interstitial liquid, because it is a liquid, draining down between the bubbles. In view of there being no suitable theory available in the literature for studying froth breakage, the following theory was developed.

3.2.2. MASS BALANCE FOR FOAM



Consider the foam column shown in the figure. The foam is generated from bubbles rising to the surface of the liquid in the cell. It then rises up the column and is removed at the top. A mass balance for liquid over the top of the foam column down to any level x yields:

Overflow = amount brought up through bubbles rising
- amount draining back.

$$\text{i.e. } Q_W = \left(\frac{Q_A}{(1-f)} \right) \cdot f - v_d \cdot A \cdot f$$

$$\text{or } v_d = \frac{Q_A}{A(1-f)} - \frac{Q_W}{Af}$$

3.2.2.1

(see appendix G for nomenclature).

In an/...

In an experiment, Q_A , Q_W and A are easily measured. The drainage velocity, v_d , is thus a function of f by equation 3.2.2.1.

3.2.3 DRAINAGE VELOCITY

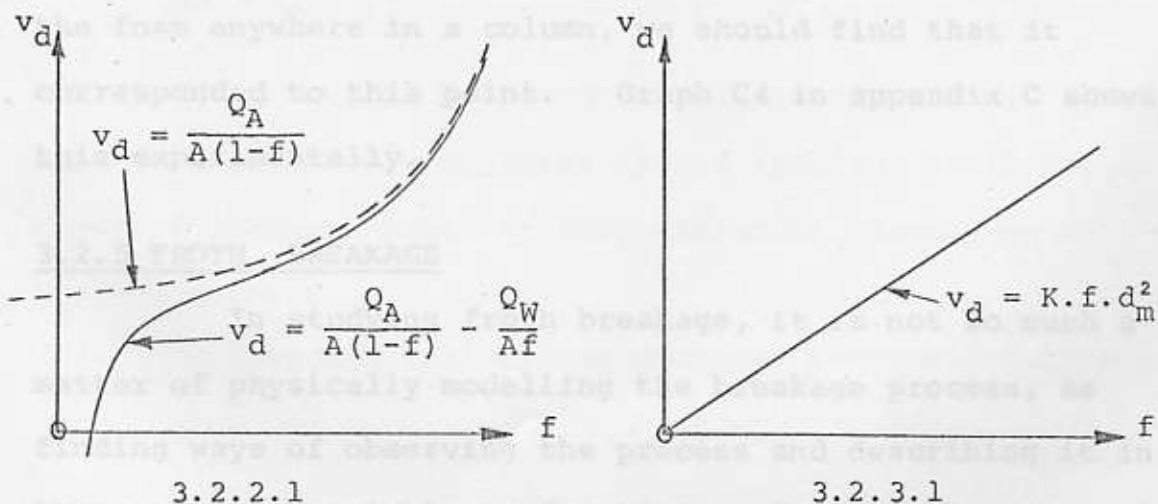
As discussed in the literature survey, a number of studies of froth drainage have been made (refs. 2, 7, 10, 12, 16, 17 and 22). Several models have been tried, and one seems to fit the experimental results on drainage fairly well. This model can be summarised by:

$$v_d = K \cdot f \cdot d_m^2 \quad 3.2.3.1$$

This shows that the average velocity at which the liquid will flow relative to the bubbles is directly proportional to the amount of liquid between the bubbles. The "constant" K is actually a function of viscosity, gravity, etc. The d_m^2 shows that the drainage velocity increases with a larger mean bubble size. This is important when considering froth breakage.

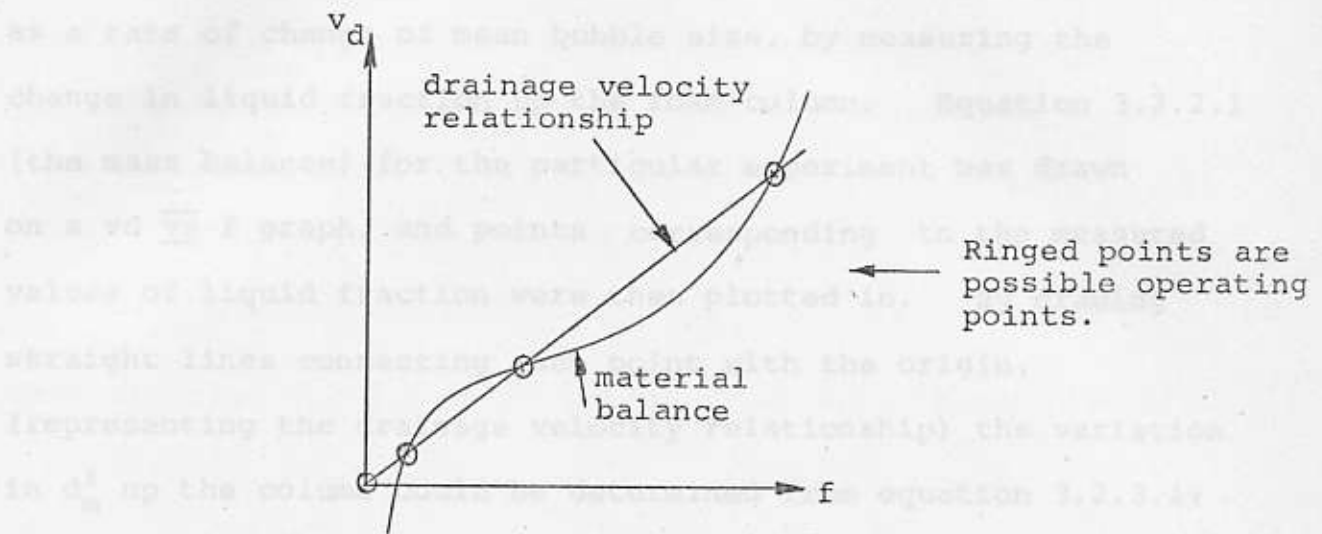
3.2.4. OPERATION AT STEADY STATE

Consider first, plots of equations 3.2.2.1 and 3.2.3.1 for a particular experiment:



In practice/...

In practice, both the material balance and drainage velocity relationship must be obeyed. Only the points where the two lines intersect are allowable operating points at steady state:



Of these three points, the middle one is the only stable operating point. Consider, for example, a small increase in f in a froth column operating at such a point. Immediately the drainage velocity relationship allows a greater rate of drainage than required by the mass balance, so that the extra liquid drains away, and the column returns to the original value of f .

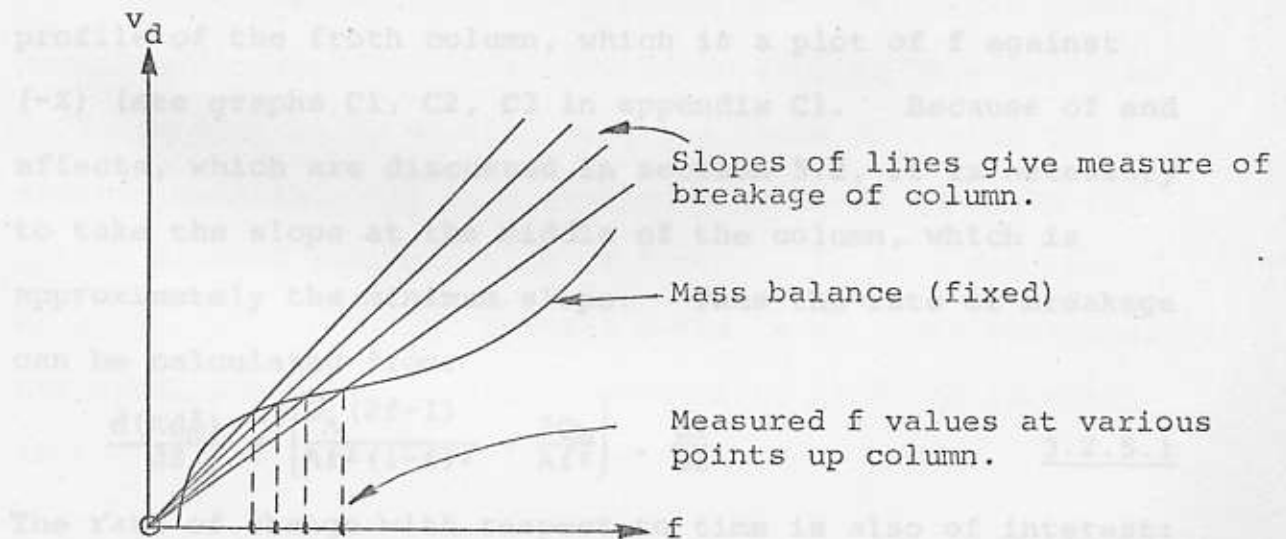
If we could measure the liquid fraction, f , of the foam anywhere in a column, we should find that it corresponded to this point. Graph C4 in appendix C shows this experimentally.

3.2.5 FROTH BREAKAGE

In studying froth breakage, it is not so much a matter of physically modelling the breakage process, as finding ways of observing the process and describing it in terms of some variable or function. For example, it could be observed in terms of such things as a decrease in

potential energy, (Ross, ref. 21) or a change in bubble size distribution, or an increase in drainage due to the release of water.

In this investigation, froth breakage was determined as a rate of change of mean bubble size, by measuring the change in liquid fraction up the foam column. Equation 3.2.2.1 (the mass balance) for the particular experiment was drawn on a v_d vs f graph, and points corresponding to the measured values of liquid fraction were then plotted in. By drawing straight lines connecting each point with the origin, (representing the drainage velocity relationship) the variation in d_m^2 up the column could be determined from equation 3.2.3.1: (see graph C4 in appendix C).



(It should be noted here that although two froth columns might show comparable liquid fraction profiles, their rates of breakage could be very different, depending on the mass balances).

Although this method provided a visual picture of

froth/...

froth column behaviour, it was easier to obtain data on rates of breakage by the following formulae, 3.2.5.1 and 3.2.5.2, from a liquid fraction profile of the column.

It is convenient to express the rate of bubble breakage up a froth column as the rate of change of Kd_m^2 . The constant K , from equation 3.2.3.1, is included as it is both unnecessary and difficult to evaluate separately.

From equation 3.2.3.1, this can be written

$$\frac{d(Kd_m^2)}{dz} = \frac{d(vd/f)}{dz} = \frac{d(vd/f)}{df} \cdot \frac{df}{dz}$$

From equation 3.2.2.1, vd/f can be found and differentiated:

$$\frac{d(vd/f)}{df} = \frac{d}{df} \left(\frac{Q_A}{Af(1-f)} - \frac{Q_W}{Af^2} \right) = \frac{Q_A(2f-1)}{Af^2(1-f)^2} + \frac{2Q_W}{Af^3}$$

The value of $\frac{df}{dz}$ can be obtained from the liquid fraction profile of the froth column, which is a plot of f against $(-Z)$ (see graphs C1, C2, C3 in appendix C). Because of end effects, which are discussed in section 5.2, it is necessary to take the slope at the middle of the column, which is approximately the minimum slope. Thus the rate of breakage can be calculated from:

$$\frac{d(Kd_m^2)}{dz} = \left(\frac{Q_A(2f-1)}{Af^2(1-f)^2} + \frac{2Q_W}{Af^3} \right) \cdot \frac{df}{dz} \quad 3.2.5.1$$

The rate of change with respect to time is also of interest:

$$\frac{d(Kd_m^2)}{dt} = \left(\frac{Q_A(2f-1)}{Af^2(1-f)^2} + \frac{2Q_W}{Af^3} \right) \cdot \frac{df}{dz} \cdot \frac{Q_A}{A(1-f)} \quad 3.2.5.2$$

$\left(\frac{Q_A}{A(1-f)} \right)$ is $\frac{dz}{dt}$, the rate at which the froth column rises.

Equation 3.2.5.2. gives the rate of breakage recorded by an observer moving with the froth column.)

3.2.6 MEASUREMENT OF LIQUID FRACTION

In this investigation, electrical conductivity was used/...

used to determine f in the foam column. A light probe was also tried, but a number of difficulties, particularly calibration, made conductivity a superior method.

The problem of calibration with conductivity still remained. The ratio of foam conductivity to bulk liquid conductivity is related to the liquid fraction, but not directly. Bikerman discusses the approach to this problem taken by various authors. The graph given by Clark (ref. 4) which is purely a plot of experimental results, was used as it appeared to be the most useful correlation. This graph is reproduced in graph C5 in appendix C. Clark gives the accuracy of his correlation as $\pm 4\%$.

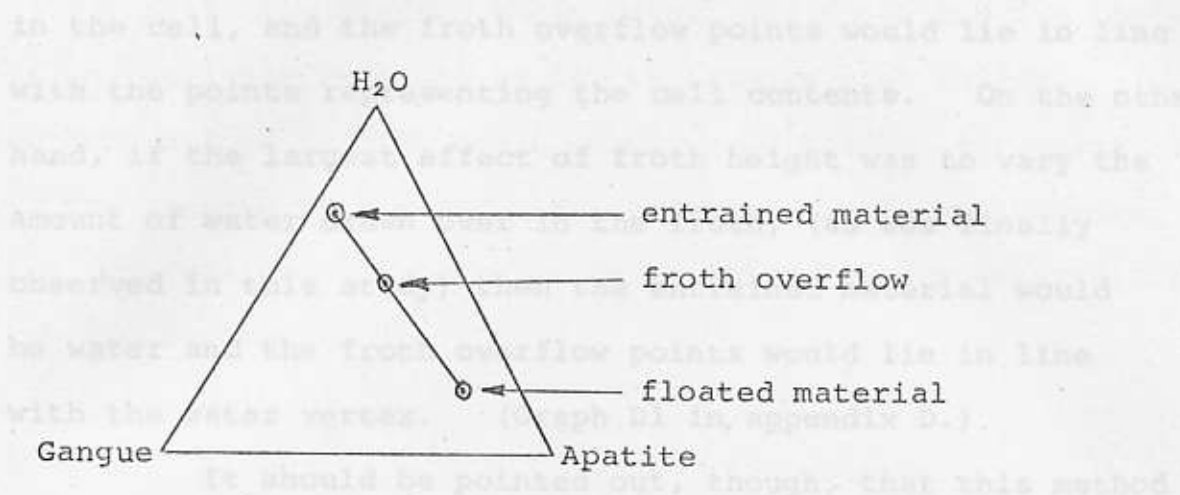
3.3. ENTRAINMENT

Entrainment is the phenomenon of unfloated material becoming enmeshed in the rising froth bubbles in a flotation cell, so that it is carried over the froth weir with the floated material. It is a problem because it can lead to gangue mineral contamination of froth. It is a function of froth height through several paths, e.g. froth breakage, drainage, bubble size, etc. Generally, as froth height increases, so entrainment should decrease.

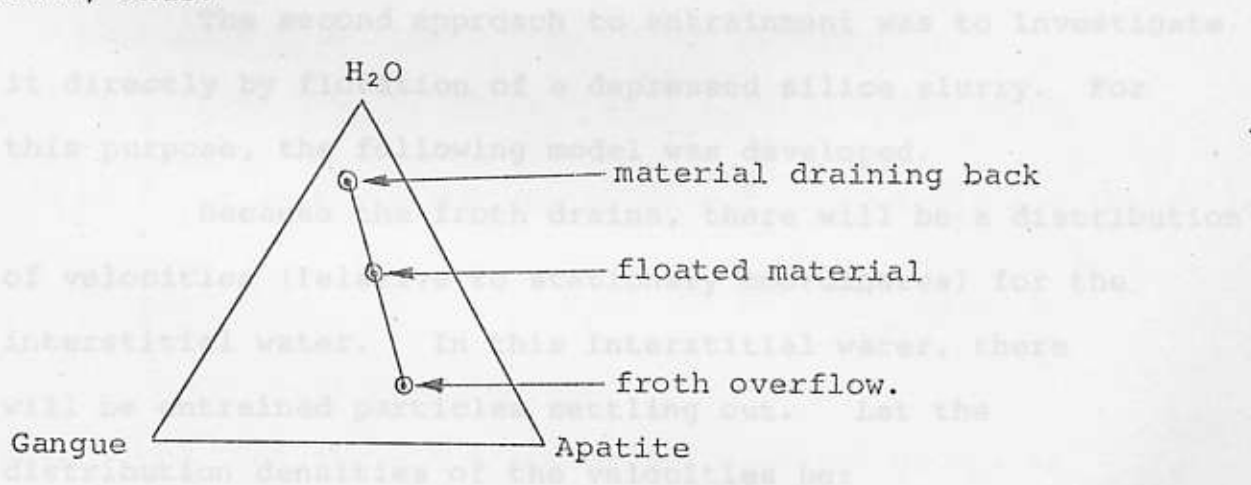
3.3.1 TRIANGULAR DIAGRAM

The first approach to entrainment was to try to detect it in the flotation of apatite ore. The slurry, being a mixture of apatite, gangue and water, could be represented by a point on a triangular diagram with these species as coordinates. Thus the contents of the cell, the froth, and the feed would each be represented by separate points. If entrainment were the only effect present, the froth overflow would contain a mixture of floated material and entrained/...

entrained material, and would lie on a line connecting these two points, thus:



On the other hand, if the froth were releasing material back into the cell, then the floated material would be the sum of the froth overflow and the material draining back. Consequently it would lie on the line joining the two points representing the overflow and material draining back, thus:



Unfortunately, it is possible to sample only the froth overflow. If the floated material and entrainment material remained reasonably constant during a run, then the points representing the froth overflow at various froth heights would be distributed along a line, the direction of which would be characteristic of the phenomenon occurring.

If the/...

If the solids from the cell were being entrained, then these would be of the same composition as the material in the cell, and the froth overflow points would lie in line with the points representing the cell contents. On the other hand, if the largest effect of froth height was to vary the amount of water drawn over in the froth, (as was finally observed in this study) then the entrained material would be water and the froth overflow points would lie in line with the water vertex. (Graph D1 in appendix D.)

It should be pointed out, though, that this method is not a conclusive method of detecting entrainment because of the large number of interfering effects and the inability to sample pure floated or entrained material, but it does give a rough indication.

3.3.2 ENTRAINMENT MODEL

The second approach to entrainment was to investigate it directly by flotation of a depressed silica slurry. For this purpose, the following model was developed.

Because the froth drains, there will be a distribution of velocities (relative to stationary coordinates) for the interstitial water. In this interstitial water, there will be entrained particles settling out. Let the distribution densities of the velocities be:

$f_W(u)$ for water

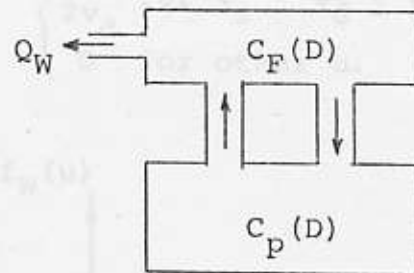
$f_D(u)$ for a particle of Stokes diameter D (i.e. the diameter of an equivalent sphere having the same terminal velocity).

If u_S is the Stokes velocity for a particle of diameter D , then

$$f_D(u)/\dots$$

$$f_D(u) = F_W(u + u_s) \quad \text{and } u_s \text{ are known, } C_F \text{ and } C_P \text{ are}$$

In the diagram shown below, the froth and the contents of the cell are regarded as two reservoirs with solids concentrations $C_F(D)dD$ and $C_P(D)dD$ respectively, for particles in the range D to $D + dD$. Material is transferred between the two reservoirs and the froth overflow removes material from the top reservoir.



Total interchange flow area = $A.f$, where f is the liquid fraction.

$$\begin{aligned} \therefore \text{Rate of removal from top reservoir} &= Q_W C_F(D) dD \\ &= \text{Nett mass flow from bottom to top reservoir} \\ &= Af \int_0^\infty f_D(u) u C_P(D) dD du + Af \int_{-\infty}^0 f_D(u) u C_F(D) dD du \\ &= Af \left[\int_0^\infty f_W(u + u_s) u C_P(D) dD du + \int_{-\infty}^0 f_W(u + u_s) u C_F(D) dD du \right] \\ &= Af \left[\int_{u_s}^\infty f_W(u') (u' - u_s) C_P(D) dD du' + \int_{-\infty}^{u_s} f_W(u') (u' - u_s) C_F(D) dD du' \right] \end{aligned}$$

Define the "entrainment fraction" of diameter D , E_D , as

$$E_D = C_F(D)/C_P(D)$$

This is the fraction of particles of a particular size in the tank which are entrained into the froth. (Expressed as a ratio of concentrations). Then, rewriting the above equation,

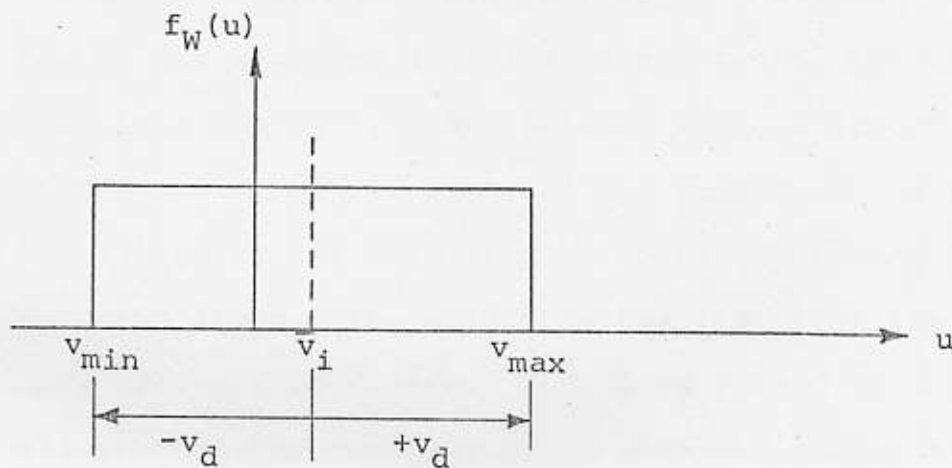
$$\frac{Q_W E_D}{A.f} = \int_{u_s}^\infty f_W(u') (u' - u_s) du' + E_D \int_{-\infty}^{u_s} f_W(u') (u' - u_s) du' \quad (A)$$

In this formula, A and u_s are known, Q_W and f can be measured, so that with an assumed f_W , E_D can be calculated for each size D .

On the basis that drainage occurs through capillary-like "Plateau borders" in laminar flow, assume that $f_W(u)$ is the same as for laminar flow through a pipe, but with the wall (i.e. the bubbles) moving

$$f_W(u) = \begin{cases} \frac{1}{2v_d} & \text{for } \bar{v}_i - v_d \leq u \leq \bar{v}_i + v_d \\ 0 & \text{for other } u. \end{cases}$$

i.e.



Where: \bar{v}_i is the mean interstitial velocity = Q_W/Af

$$\begin{aligned} v_{\max} &= \bar{v}_i + v_d, \text{ is the velocity of the rising bubbles} \\ &= Q_A/A(1-f) \end{aligned}$$

Equation (A) then becomes:

$$\begin{aligned} \bar{v}_i E_D &= \int_{u_s}^{v_{\max}} \frac{(u' - u_s)}{2v_d} du' + E_D \int_{v_{\min}}^{u_s} \frac{(u' - u_s)}{2v_d} du' \\ &= \frac{(u_s - v_{\max})^2}{2(v_{\max} - v_{\min})} - E_D \frac{(u_s - v_{\min})^2}{2(v_{\max} - v_{\min})} \end{aligned}$$

$$\text{i.e. } E_D = \frac{(v_{\max} - u_s)^2}{2(v_{\max} - v_{\min}) \bar{v}_i + (u_s - v_{\min})^2} \text{ for } v_{\min} \leq u_s \leq v_{\max}$$

3.3.2.1

Stokes velocity can be calculated from

$$u_s = \frac{D^2 g}{18\mu} (\rho_s - \rho_L) \quad \text{3.3.2.2}$$

(Note/ ...)

(Note how $E_D = 1$ for $D = 0$, i.e. dissolved matter is fully entrained).

An actual foam column will consist of a number, say n , of the stages as shown above. Then, entrainment $= E_D^n$. As froth height increases, so n will increase and nett entrainment will decrease. The problem is then to correlate h and n .

The flotation cell used in this investigation was specially designed and built so that the froth height could be easily varied and measured. Figure 1 shows a diagram of this cell. Slurry was admitted from the mixing tanks through a pipe dipping down into the cell. Air entered through the porous sparger at the bottom of the cell and was dispersed and stirred up with the slurry by the impeller. The froth formed flowed unaided over the froth weir, while the tailings left the cell via the overflow weir and sand gate. Windows fitted on both sides of the cell enabled the contents to be observed during a run.

Figure 2 shows a photograph of this cell mounted in its frame. The froth and tailings streams leaving the cell flowed into a receiving drum mounted directly below, and thence to drain. This enabled the streams to be sampled easily.

Froth height control was achieved by means of the sliding overflow weir. This could be moved up and down manually from the top of the cell, and held in position by a thumb screw on the extending rod. The resulting level of the interface between the pulp and the froth was measured on the scale attached to the window, and the weir adjusted accordingly. The froth weir was

APPARATUS AND EXPERIMENTAL PROCEDURE.

The apparatus used for this investigation was associated with the flotation pilot plant used by the N.I.M. Research Group. The mixing tanks and controls were the same, but a different cell was employed.

4.1.1 FLOTATION CELL.

The flotation cell used in this investigation was specially designed and built so that the froth height could be easily varied and measured. Figure 1 shows a diagram of this cell. Slurry was admitted from the mixing tanks through a pipe dipping down into the cell. Air entered through the porous sparger at the bottom of the cell and was dispersed and stirred up with the slurry by the impeller. The froth formed flowed unaided over the froth weir, while the tailings left the cell via the overflow weir and sand gate. Windows fitted on both sides of the cell enabled the contents to be observed during a run.

Figure 2 shows a photograph of this cell mounted in its frame. The froth and tailings streams leaving the cell flowed into a receiving drum mounted directly below, and thence to drain. This enabled the streams to be sampled easily.

Froth height control was achieved by means of the sliding overflow weir. This could be moved up and down manually from the top of the cell, and held in position by a thumbscrew on the extending rod. The resulting level of the interface between the pulp and the froth was measured on the scale attached to the window, and the weir adjusted accordingly. The froth weir was

fixed, / ...

FIGURE 1. CUTAWAY VIEW OF VARIABLE FROTH HEIGHT
FLOTATION CELL.

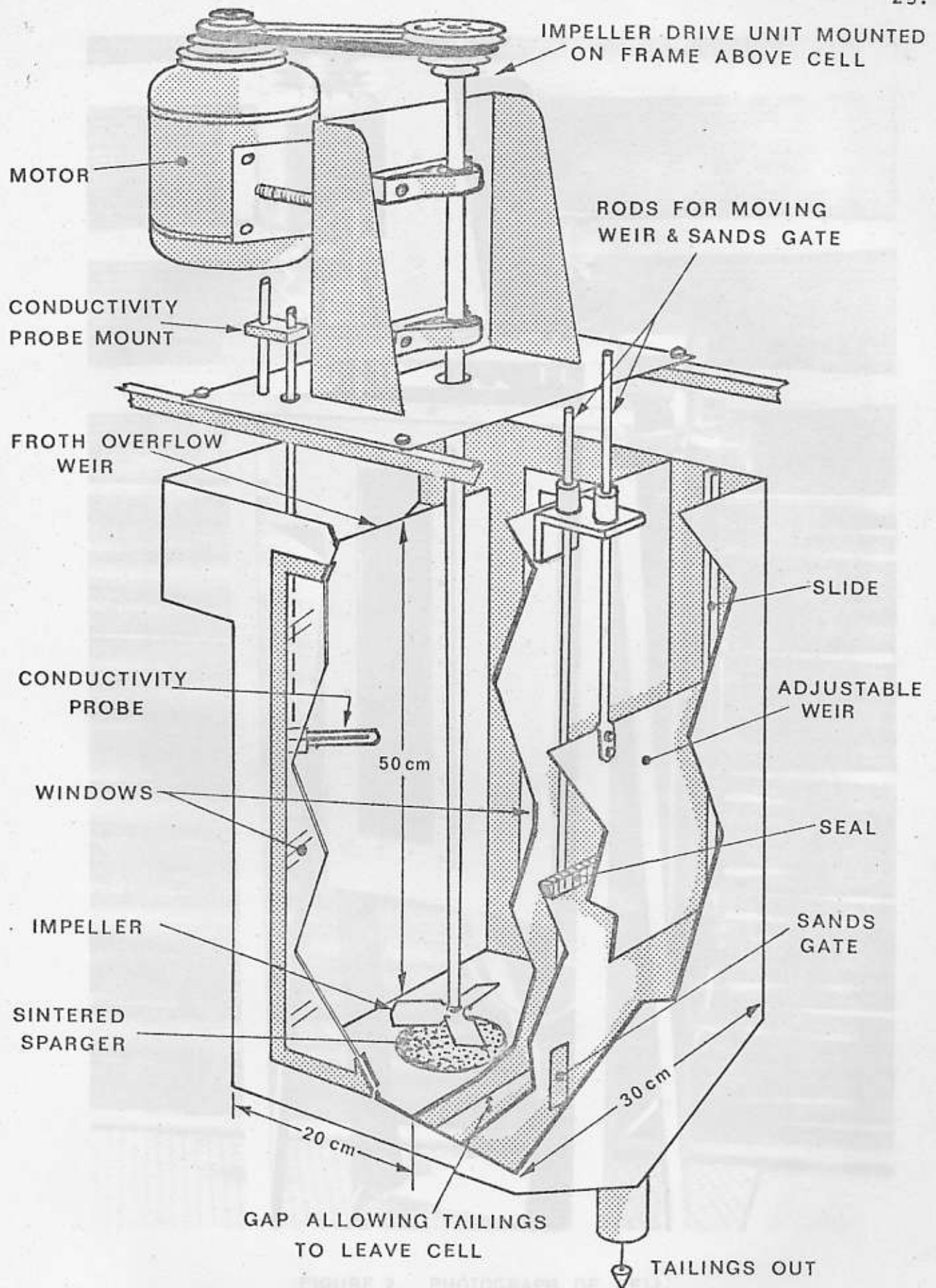


FIGURE 1. CUTAWAY VIEW OF VARIABLE FROTH HEIGHT
FLOTATION CELL.

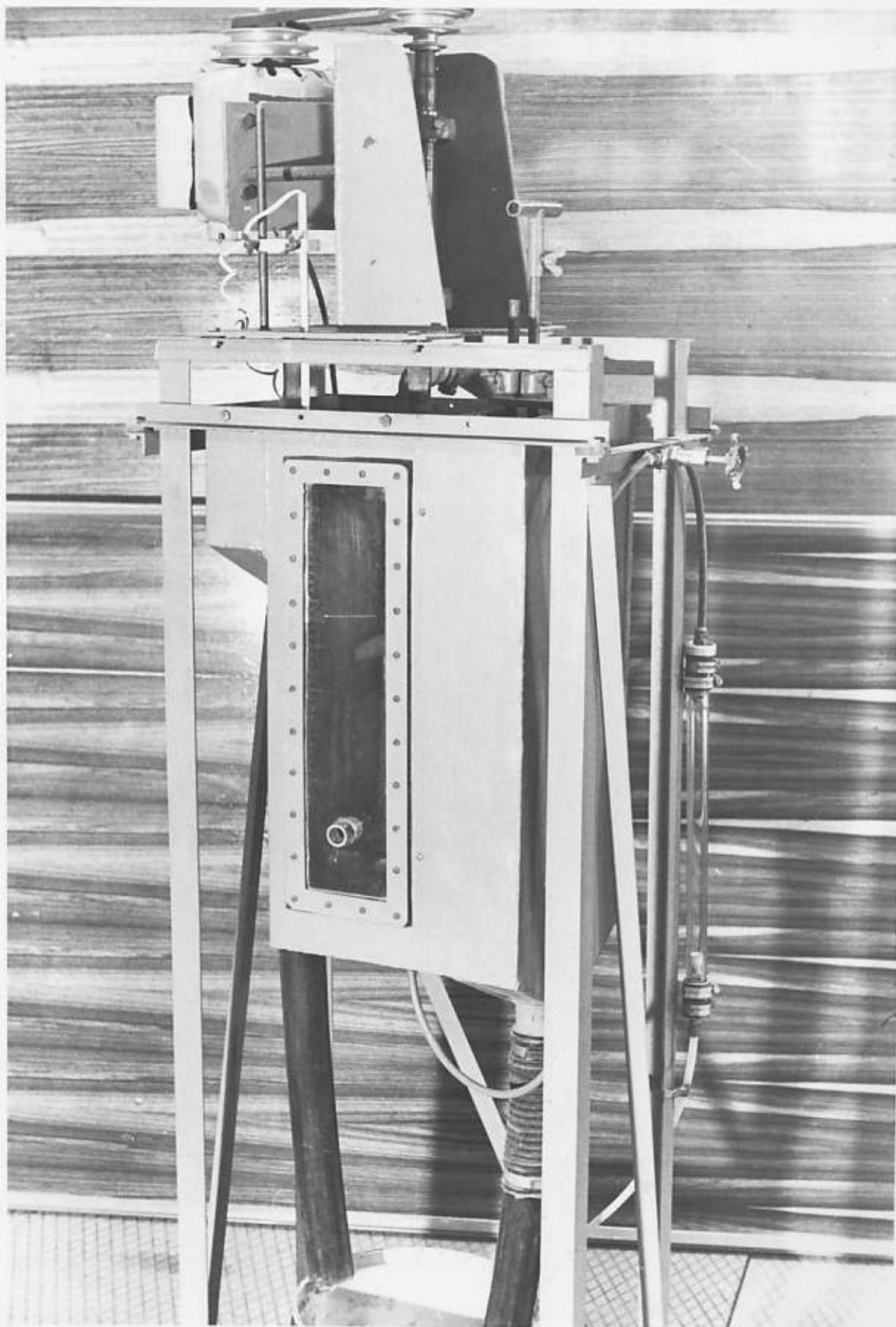


FIGURE 2. PHOTOGRAPH OF CELL.

fixed, so that the froth height was controlled by the tailings weir.

4.1.2 MIXING TANK SYSTEM.

The tanks used for mixing and preparing the slurry were those attached to the pilot flotation plant. Figure 3 is a flowchart which outlines the system. The output from the top mixing tank could be pumped to either the pilot plant or the variable height cell.

The basic system consisted of two stirred tanks, an upper and a lower, with fairly fast recirculation between them. Solids were added to the bottom tank, while water entered at the top. The required additives were fed to the bottom tank.

It was possible, although it was only done once, to recycle the froth and tailings from the cell back to the mixing tanks. It was also possible to control some of the variables manually, so that, for example, a batch of slurry could be made up by filling the tanks with water and admitting enough solids to achieve the required density.

4.1.3 CONTROLS ON MIXING TANK SYSTEM.

As shown in the flowchart, the system was equipped with a number of automatic controls which enabled the slurry preparation to be done automatically during a run. During the experimenting, a lot of difficulty was experienced with these controls, and as a result, an investigation was made into the dynamics of the system. The results of this investigation are given in appendix E.

4.2 EXPERIMENTAL PROCEDURE.

To start with, for runs A, B, C and D, the slurry was mixed up in a batch, conditioned, and pumped through the cell and

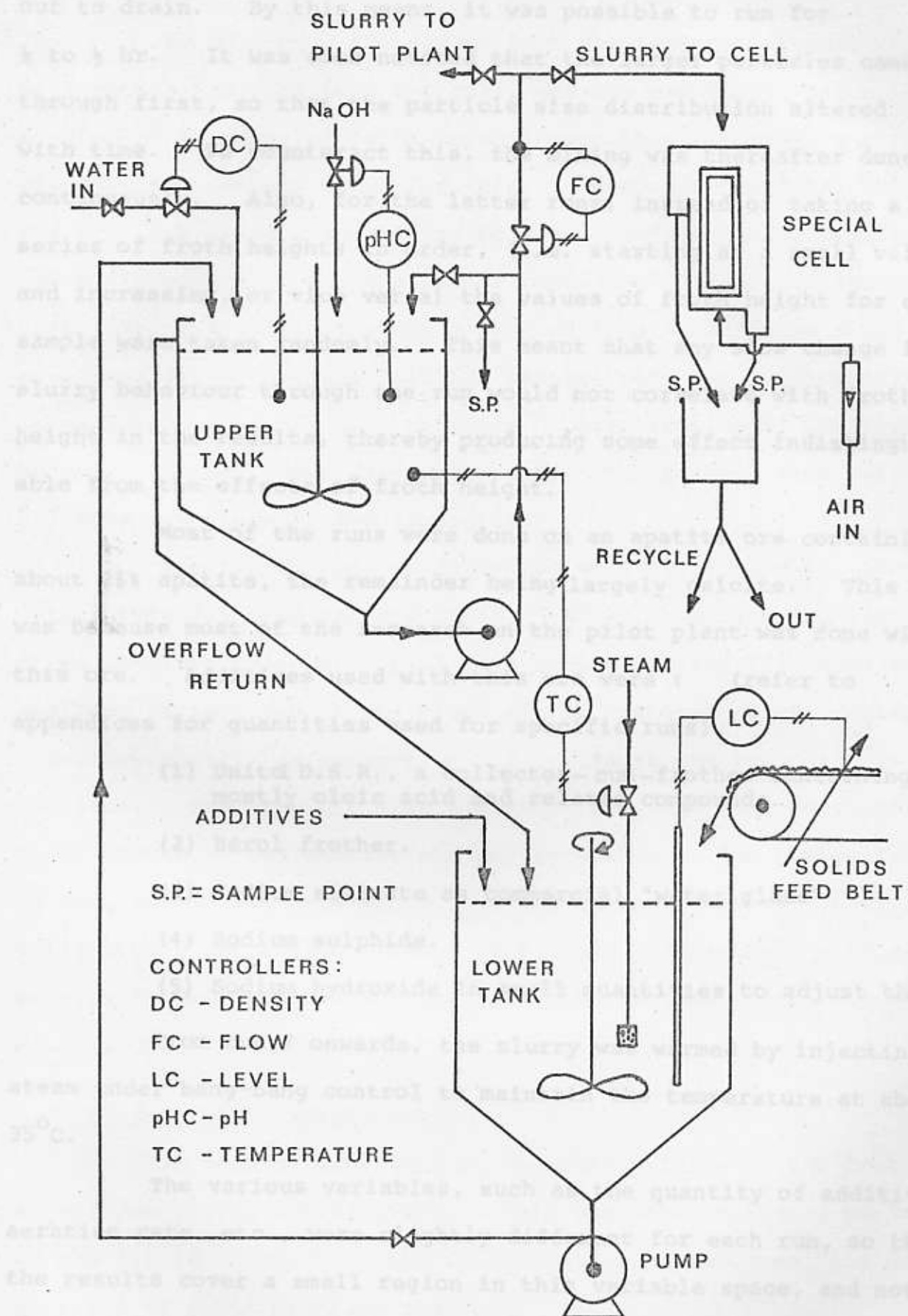


FIGURE 3. SYSTEM FLOWSHEET.

out to drain. By this means, it was possible to run for $\frac{1}{4}$ to $\frac{1}{2}$ hr. It was soon noticed that the larger particles came through first, so that the particle size distribution altered with time. To counteract this, the mixing was thereafter done continuously. Also, for the latter runs, instead of taking a series of froth heights in order, (i.e. starting at a small value and increasing, or vice versa) the values of froth height for each sample were taken randomly. This meant that any slow change in slurry behaviour through the run would not correlate with froth height in the results, thereby producing some effect indistinguishable from the effects of froth height.

Most of the runs were done on an apatite ore containing about 25% apatite, the remainder being largely calcite. This was because most of the research on the pilot plant was done with this ore. Additives used with this ore were : (refer to appendices for quantities used for specific runs)

- (1) Unitol D.S.R., a collector-cum-frother containing mostly oleic acid and related compounds.
- (2) Berol frother.
- (3) Sodium silicate as commercial "water glass"
- (4) Sodium sulphide.
- (5) Sodium hydroxide in small quantities to adjust the pH.

From run F onwards, the slurry was warmed by injecting steam under bang-bang control to maintain the temperature at about 35°C.

The various variables, such as the quantity of additives, aeration rate, etc., were slightly different for each run, so that the results cover a small region in this variable space, and not just a single point. This was useful as it gave a broader basis to the results.

To / ...

To do a run, the slurry from the mixing tanks was fed at a controlled rate into the cell, and the air supply and stirrer started. A number of froth heights were then selected, and froth and tailings samples taken for each. For each froth height, the cell was given a short time to settle before taking samples and measurements. For the latter runs, the contents of the cell were sampled directly through a pipe protruding into the cell, as it was found that the tailings samples were not sufficiently representative of the cell contents. Feed samples of the slurry entering the cell were also collected. The results from all the runs are given in the appendices.

The slurry samples collected were first weighed, then the solids were filtered off and dried. After measuring the mass of dried samples, they were split into suitably sized fractions to be analysed as required. The grade of the apatite ore was determined colourimetrically as percent P_2O_5 . (42.4% corresponding to pure apatite). The particle size distributions were done on standard Tyler sieves by wet washing and dry screening. The solids fraction of each sample was determined from the masses recorded, as were the total liquid and solids flows. The grade and particle size analyses were performed by the laboratories at the National Institute for Metallurgy.

4.3 CONDUCTIVITY MEASUREMENTS.

In runs H, I, J, and K, the conductivity of the froth at various levels was recorded. This was done so that a profile of the liquid fraction of the froth could be determined, and data on rates of froth breakage obtained.

A special conductivity probe was constructed for use in the cell. The electrodes were made of etched nickel wire,

and / ...

and were flat to measure the conductivity in a given horizontal plane. The probe could be moved up and down on its support to any required level in the froth. (see back to figure 1)

A conventional a.c. conductivity bridge was used to take measurements.

The liquid fraction in the froth was calculated from the ratio of froth conductivity to bulk liquid conductivity, using the correlation given in Clark, (ref 4) reproduced in graph C5. Consequently the cell constant of the probe was not needed.

4.4 INVESTIGATION OF ENTRAINMENT USING SILICA SLURRY.

One run, Run I, was done on a depressed silica slurry with the object of investigating entrainment. For this run, a batch of silica slurry was made up and recycled continuously through the cell and back to the mixing tanks. A cooling coil in the mixing tanks kept the system at an even temperature. Two additives were used for this run : Dowfroth 250 as frother and hydrofluoric acid as depressant. The slurry was conditioned for 2 hours before experimenting.

Sampling and taking measurements was much the same as for apatite ore flotation. Tank and froth samples were taken from the cell. The conductivity of the froth was also recorded. The tank samples were filtered and weighed as with apatite ore. The froth samples, however, because of the very fine particles in low concentration were settled, decanted, and evaporated to dryness. Particle size distributions were determined by sieving on U.S. standard sieves. Two air flows were tried, but the lower yielded such small samples that the particle size distributions were determined only for the higher.

5.1 DIRECT EFFECTS OF FROTH HEIGHT

This subsection the results presented in appendices

CHAPTER 5

RESULTS

The investigations took the form of a number of runs on the specially constructed cell. Most runs were done under a specific set of conditions with a specific object in view, which varied between runs. (Froth height was generally the only parameter which was varied during a run). The data from these runs are grouped together according to subject matter in appendices A to D, under the respective headings.

Appendix A tabulates the data from the runs done on apatite ore, and displays the direct effects of froth height (e.g. effect on grade) in graphical form.

Appendix B shows the particle size distributions for some of the samples taken. As well as being tabulated, these are also presented in the form of distribution histograms for easy comparison between froth heights.

Appendix C presents the results of conductivity measurements taken during some of the runs. The data for froth drainage are given here.

Appendix D deals with entrainment. The results for the run done on silica, together with the quantitative results from the theory, are compared here.

Many of the graphs in the appendices are intended for comparison purposes. For this reason, several groups of results are often presented on a single page but on separate axes.

5.1 DIRECT EFFECTS OF FROTH HEIGHT

This embraces the results presented in appendices

A and B/.....

A and B. In appendix A, the results for runs A, B, C, D, E, F, G and K are tabulated. Each table is preceded by a short paragraph describing the run and giving essential details. The results are summarised in graphs A1, A2, A3 and A4, showing the effect of varying froth height on grade, solids density, solids flow and water flow respectively. In appendix B, the particle size distributions for runs B, C, D and E are given together with the graphs comparing the size distributions of the froth and tailings samples over the range of froth heights used (graphs B1 to B4).

In each case, there is a fair experimental scattering of results, more in some cases than others, which made it difficult to detect slight trends. It was found difficult to reduce the scatter without spending considerable time modifying the apparatus and studying the system being used (see appendix E).

5.1.1 EFFECTS ON GRADE

From graph A1, it is clear that froth height has a negligible effect on grade for the apatite ore flotation under investigation. In this graph, for each run, the points representing the froth grade are ringed (O), and the corresponding points representing the contents of the cell are crossed (X). Thus there is a pair of points for each froth height. A horizontal line (i.e. no change in grade with froth height) drawn through the average of the points for each run, shows that the effect on grade of varying froth height was either smaller than could be determined within the scatter, or was in fact/...

in fact nil. In most cases, a high or low froth grade is reflected by a corresponding high or low grade for the contents of the cell, but is independent of froth height. The variations in the averages between runs are mainly due to different operating conditions; particularly differences in the additive concentrations.

5.1.2. EFFECTS ON SOLIDS DENSITY

Graph A2 shows (in a similar layout to graph A1) the effect of froth height on solids density. As solids density is a combination of liquid and solids flows, graphs A3 and A4 were plotted to show these variables separately. Graph A3 is then the solids overflow rate shown as a function of froth height, and graph A4 the water flow rate.

The points on graph A2 appear much the same as graph A1. The points are scattered, and variations in the cell solids density are reflected in the froth density. In this case, however, the pairs of points at smaller froth heights are slightly closer together than similar pairs occurring at greater froth heights. The difference is particularly noticable in run K, but in this case is probably due largely to scatter. Straight lines have been drawn in through the points for each run to show the effect up. The straight lines do not represent any particular model, but it is impossible to detect any further deviation because of the scatter.

In graph A3, there is a slight downward trend in total solids flow for some runs, and a slight upward trend in others. When read in conjunction with graph A2, it can be seen that these upward trends in solids flow are associated

with/...

with somewhat larger trends in the concentration of solids in the cell. It can therefore be concluded that solids flow does decrease slightly with increasing froth height.

Graph A4, as would be expected from the cumulative trends of graphs A2 and A3, shows a decrease in liquid flow with froth height. Again the lines drawn in on each plot are intended only as a guide to show the effect, and are not the graphs of a model. In this case, however, there is a marked change in the slope at small froth heights (see run C for example). For some runs the effect is more noticeable than in others, which may be caused by varying froth behaviour between runs. More will be said about this effect in section 5.2, when discussing the results of the conductivity measurements.

5.1.3 EFFECTS ON PARTICLE SIZE DISTRIBUTION

The particle size distributions in appendix B were determined by sieving the solids samples on standard Tyler sieves. They are presented as density histograms against a linear particle size scale. A mean distribution density between aperture sizes was determined so that the area under the line on the graph was equal to the weight percent/100 for each size fraction. The distributions are thus stepped, with discontinuities at the particle sizes corresponding to each sieve.

On the graphs, the froth and tailings samples for each froth height are presented on the same pair of axes. The areas enclosed by the froth distributions are shaded for contrast.

From/...

From these results, it appears that particle size distribution is not affected by varying froth height, although scatter makes this hard to detect. Looking at the set of distributions for any run, there are no nett trends with froth height which recur between runs. The distributions all show the same general shape, with the froth samples centered around smaller particle sizes (37 to 53 micron) than the tailings samples (74 to 108 micron).

Again, like grade and solids density, the contents of the cell have the largest effect on the froth. The unwanted scatter is mainly at low particle sizes, and is due to both the variation in feed to the cell, and the method of sample analysis. As the feed coming to the cell varied, so the froth and tailings varied. In some cases, it is possible to see two distinct "lumps" in the distributions, particularly the tailings. It is also possible that the random nature of the process and the collapse of froth might add significantly to the scatter because of the relatively small size of the cells. As the distributions are normalised, i.e. enclosed area equals unity, the larger particle sizes are affected by large variations in the fines region, and this makes comparison between plots difficult.

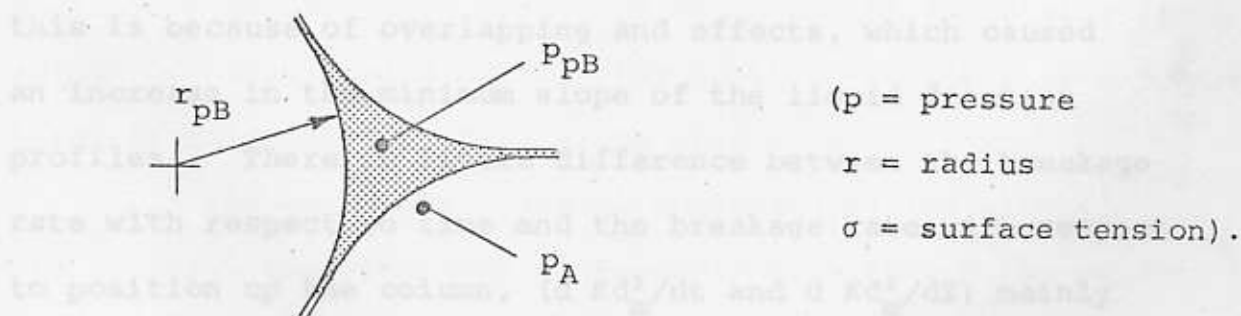
5.2 FROTH BREAKAGE FROM CONDUCTIVITY MEASUREMENTS

The results from the conductivity measurements on the suppressed silica slurry (run I) and the apatite ore (runs J and K) flotation froths are tabulated in appendix C. Graph C1 shows the liquid fraction profiles of the froth on the silica slurry, while graphs C2 and C3 show the profiles for the apatite ore flotation. Graph C4 shows the corresponding v_d vs. f plots/...

plots with the mass balance curves drawn in, and the operating points plotted (see section 3.2). Table C(i) on page 7 of appendix C compares rates of froth breakage for silica and apatite ore calculated from the conductivity results.

In all three profiles, graphs C1, C2 and C3, the liquid fraction changes up the column. All the curves have the same general shape, although the froth from the silica is of higher mean liquid fraction than the apatite ore froth. The proximity of interfaces makes the liquid fraction curves turn up near the base of the column, and turn down towards the top.

This end effect, i.e. the change in slope of the profiles near the interfaces (which was referred to in section 3.2.5) is explained theoretically through the drainage velocity relationship, $v_d = K.f.d_m^2$. The constant K was shown by Leonard and Lemlich to be slightly dependent on the rate of change of liquid fraction up the column, df/dz . A sharp interface would imply infinitely negative K and v_d . As v_d also has to obey the mass balance relationship, this is impossible, and so f has a finite rate of change over a region near the interface. It can also be explained in terms of the actual drainage process as follows. Consider



a Plateau border as in the figure. The pressures are related by $p_A - p_{pB} = 2\sigma/r_{pB}$. The pressure variations in p_A are

relatively/...

relatively small compared to the difference $P_A - P_{PB}$. P_{PB} will thus change with $2\sigma/r_{PB}$, in which r_{PB} is in turn affected by the quantity of water enclosed in the Plateau border (i.e. f). There are thus forces other than gravity causing the interstitial liquid to flow, especially near an interface where there is a marked change in f .

Graph C4 shows the large difference between the two types of froth. In each case, the operating points (see theory) on the v_d vs. f plot occur on the same part of the curves, except that those of the apatite ore lie more to the left and near to the limiting case of a tangential velocity relationship line. The froth on the silica slurry is also less stable than that on the apatite ore slurry, as revealed by the larger changes in slope over the froth column of the drainage velocity relationship lines (not actually shown on the graphs) which would connect the operating points to the origin.

The calculated rates of breakage given in table C(i) are higher for the silica slurry by a factor of 5 to 10 over the apatite ore slurry. The scatter of values reflects the random nature of froth collapse. The rate of breakage appears to increase at low froth heights, but this is because of overlapping and effects, which caused an increase in the minimum slope of the liquid fraction profiles. There is little difference between the breakage rate with respect to time and the breakage rate with respect to position up the column, ($d Kd_m^2/dt$ and $d Kd_m^2/dZ$) mainly because of the relatively small variation in the air flowrates chosen. As the silica slurry froth was not particularly

unstable/...

unstable, it can be concluded that the froth from the apatite ore slurry was a particularly stable type of froth, and one would therefore expect any effects associated with its breakage to be small.

The observed shape of the Q_W vs. froth height curves (graph A4 in appendix A) also shows a result of the overlapping and effects. At fairly large froth column heights, Q_W decreases slowly with increasing froth height, corresponding to the slight breakage as can be seen in the graphs above. When the froth column becomes shorter, the two end effects start to overlap. The shallower froth layer then exhibits a capillary action, drawing the water up from the pulp and producing an increase in Q_W .

5.3 ENTRAINMENT

Graph D1 of appendix D shows data from run F done on apatite ore, plotted on a triangular diagram in an attempt to detect entrainment. The points representing the froth do indeed fall roughly on a line, but not in the direction of the cell contents as would be the case for solids entrainment. Instead they lie in the direction of the water vertex, which, together with the graphs of appendix A, indicate that the major effect of froth height is to vary the amount of water coming over in the froth. As would be expected there is no change in grade along this line.

The experiment done on depressed silica slurry, run I, forms the remainder of appendix D, although the conductivity results from this run are in appendix C.

In this run, two air rates were chosen, and froth height was varied for each. Only the samples for the higher rate were analysed for particle size distribution, and hence

entrainment/...

entrainment fraction. Theoretical curves of entrainment fraction for one theoretical stage were also calculated (equation 3.3.2.1) from the water flow data for the higher air rate, and these are compared on graph D2. Values of the points on the theoretical curves are also tabulated in table D(iii). For each size fraction, the mean entrainment fraction is the concentration ratio of that size in the overflow to the cell contents. The mean experimental values of entrainment fraction were calculated for each size fraction from the particle size analyses and the weight percent of solids in the samples collected. The experimental graphs of entrainment fraction are thus stepped, like the particle size distributions of appendix B.

Again in these results, there is a fair amount of scatter, which is particularly noticeable in the experimental entrainment fraction graphs. It can be seen in table D(i) that the weight percent of solids in the froth overflow is very much smaller than the solids concentration in a typical apatite ore concentrate, for a comparable cell concentration. This would imply that entrainment can account for at the most 3% of the solids passing over with the froth for normal flotation. It is still doubtful how much of the silica coming over was purely entrainment and not flotation, as there is little change of entrainment fraction with froth height in graph D2. Although the slurry was heavily depressed, it is still possible that there may have been some flotation occurring. The theory predicts that the number of "stages", n , in the froth column will increase with froth height and that entrainment fraction should decrease to the power n . (The theoretical curves plotted

in graph/...

in graph D2 are for $n = 1$.)

Graph D2 also shows that the entrainment fraction for large particle size is greater than predicted by the theory. This is partially because of the errors involved in analysis at these larger fractions, but may also have been caused by either the large particles becoming trapped in the relatively smaller Plateau borders in the froth, or by flotation. (The radius of a Plateau border which would just trap a 200 micron particle is 0.065 cm, which is of the right order of magnitude).

(3) The effect of froth height on particle size distribution is undetectable.

(4) Apatite ore froth is a particularly stable type of froth.

(5) Entrainment, although it probably does exist, plays a negligible part in flotation.

(6) Froth height has a very definite effect on water overflow rate, even in the case of apatite ore flotation. The interrelationship is not simple, and involves several other variables.

(7) Study of the flotation process together with its associated process of froth breakage, is prone to produce noisy results, particularly on a small scale, because of the inherently random nature of these processes.

It is perhaps unfortunate that the effect of froth height on grade, which was the subject of this investigation, turned out to be zero.

6.2 Link with Flotation Model

The function λ , describing the fraction of the solid

CHAPTER 6

DISCUSSION

6.1 SUMMARY OF EXPERIMENTAL RESULTS

The experimental results show the following

- (1) The effect of froth height on grade is nil for apatite ore flotation.
- (2) The effect of froth height on total solids flow is slight, but there is a definite decrease for increasing froth height.
- (3) The effect of froth height on particle size distribution is undetectable.
- (4) Apatite ore froth is a particularly stable type of froth.
- (5) Entrainment, although it probably does exist, plays a negligible part in flotation.
- (6) Froth height has a very definite effect on water overflow rate, even in the case of apatite ore flotation. The interrelationship is not simple, and involves several other variables.
- (7) Study of the flotation process together with its associated process of froth breakage, is prone to produce noisy results, particularly on a small scale, because of the inherently random nature of these processes.

It is perhaps unfortunate that the effect of froth height on grade, which was the subject of this investigation, turned out to be zero.

6.2 Link with Flotation Model

The function R , describing the fraction of the solids

entering/...

entering the froth which returns to the cell, was postulated as a function of four variables, $R(k,g,D,h)$. The only thing that was found experimentally to vary with froth height, so far as this model is concerned, was the total solids flow. It appeared that the process occurring in the froth treated all types of solids in the same way - possibly a bulk return phenomenon, with small pockets of solids returning en masse to the pulp. This could have resulted from stagnation, caused by sections of the mineral-laden froth near the surface draining to below a critical liquid fraction when the solids form a ridged scum which does not flow easily.

The experimental results showed directly that R is not a function of g and D , leaving only h and k . The model itself postulates that there is a distribution of k values for the solids in the cell, and that for beneficial flotation, the gangue must have a lower mean than the apatite. Thus if there were an interaction between k and h , the grade in the froth would vary. It is practically impossible to tell whether R is a function of k independently of h , just as it is impossible to analyse directly for k values in a given sample of solids. Also, if R were a function of k in this way, it would be indistinguishable from a slightly modified k distribution for the solids in the cell. This makes it unnecessary to include it in R . As pointed out in section 4.2, the various variables such as air rate, additive concentrations, etc., varied slightly between runs, so that the independence of R on k , g and D is general, and does not apply to only one point in the variable space. Thus R for apatite ore flotation with the general flotation model which was discussed is a/...

is a function only of h , i.e. $R(k, g, D, h) = R(h)$.

$R(h)$ is still a function which is dependent on a large number of other variables which do not appear in the model, particularly the froth characteristics such as liquid fraction, breakage rate and rheology. The flotation model does not include a description of the water overflow behaviour. Fortunately however, these variables were held reasonably constant during each run.

In graph A3, the dependence of solids flow on froth height was reduced to a linear relationship, i.e.

$$R(h) = \text{constant} \times h.$$

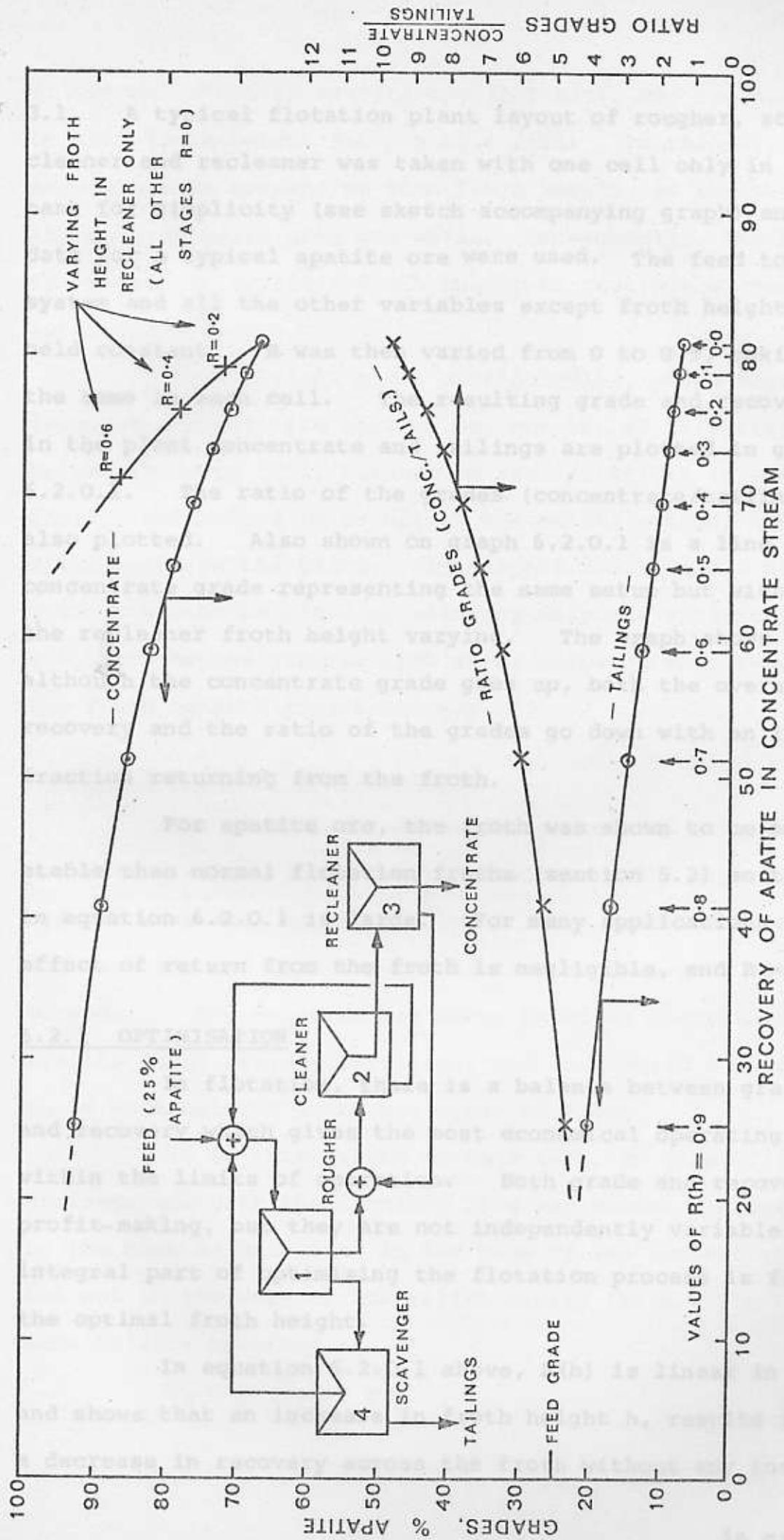
It was pointed out that because of the scatter and the small variation of solids flow with froth height, further deviations from this straight line could not be detected. If one extrapolates this line over the entire region of possible operation, then

$$R(h) = h/h_0, \quad 0 < h \leq h_0 \quad \underline{6.2.0.1}$$

where h_0 is the minimum froth height at which there is no solids overflow. This is a function of the other variables, but for a given run where only the froth height is varied, h_0 will stay constant.

Note how this model is related to Harris' model in section 2. He proposed that the rate of return from the froth was proportional to the product of froth volume and solids concentration in the froth.

Equation 6.2.0.1 provides a suitable form for R which may be used with the model for flotation. Graph 6.2.0.1 shows some results obtained when this froth model was used with the general flotation model which was discussed in section



GRAPH 6.2.0.1. FLOTATION MODEL. RESULTS OBTAINED BY VARYING FROTH HEIGHT IN SIMULATED PLANT.

3.1. A typical flotation plant layout of rougher, scavenger, cleaner and recleaner was taken with one cell only in each bank for simplicity (see sketch accompanying graph) and data for a typical apatite ore were used. The feed to the system and all the other variables except froth height were held constant. R was then varied from 0 to 0.9, making it the same in each cell. The resulting grade and recovery in the plant concentrate and tailings are plotted in graph 6.2.0.1. The ratio of the grades (concentrate/tailings) is also plotted. Also shown on graph 6.2.0.1 is a line of concentrate grade representing the same setup but with only the recleaner froth height varying. The graph shows that, although the concentrate grade goes up, both the overall recovery and the ratio of the grades go down with an increasing fraction returning from the froth.

For apatite ore, the froth was shown to be more stable than normal flotation froths (section 5.2) so that h_o in equation 6.2.0.1 is large. For many applications the effect of return from the froth is negligible, and $R \approx 0$.

6.2.1 OPTIMISATION

In flotation, there is a balance between grade and recovery which gives the most economical operating point within the limits of operation. Both grade and recovery are profit-making, but they are not independently variable. An integral part of optimising the flotation process is finding the optimal froth height.

In equation 6.2.0.1 above, $R(h)$ is linear in h , and shows that an increase in froth height h , results in a decrease in recovery across the froth without any increase

in grade/...

in grade. Thus in apatite ore flotation, the optimum lies at zero froth height for a single cell. Practically, it is impossible to operate at zero froth height, as the pulp from the cell splashes over the weir. Consequently, the best is to operate at as low a froth height as possible without splashing over.

In a typical plant configuration, where there are feedback streams, the optimum may not lie at zero froth height in every cell, because of specifications in product quality which have to be met. The actual optimal settings will depend on the plant. In graph 6.2.0.1, a far higher grade could be obtained by allowing only the recleaner froth height to become greater than zero, compared with varying all the froth heights simultaneously.

6.3 CONDUCTIVITY MEASUREMENTS

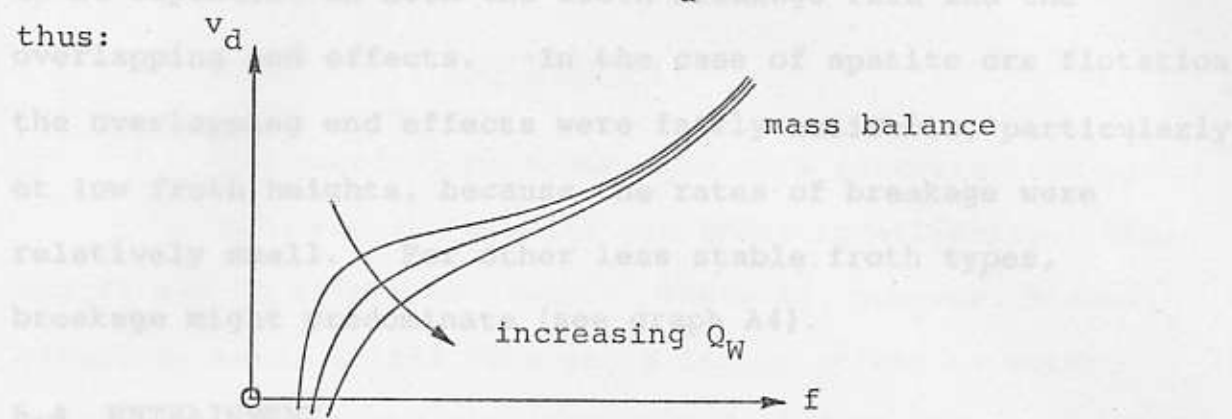
The electrical conductivity provided a very convenient way to study froth behaviour. The experimental results were much as the theory of froth behaviour had predicted, although the end effects were ignored as they were difficult to model. The measurements taken provided quantitative results about rates of breakage, and so enabled a comparison to be made between different types of froth.

It is interesting to note that, in graph C4, the drainage velocity relationship line was almost tangential to the mass balance line in the case of the apatite ore froth, but not in the case of the silica slurry froth. In the mass balance equation,

$$v_d = \frac{Q_A}{A(1-f)} - \frac{Q_W}{A \cdot f} \quad \underline{3.2.2.1}$$

the amount/...

the amount of water overflowing, Q_W , would have the effect of moving the convex part of the v_d vs. f curve downwards, thus:



This means that very nearly the maximum amount of water was being carried over the weir during the apatite ore flotation. The amount of bubble breakage on the surface of the froth was thus very little, as this would have led to some of the water draining back into the body of the froth column, thereby reducing Q_W . In contrast to this, the froth on the silica slurry could be seen to be breaking on the surface during the experiment, and in this case, the measured Q_W was below the maximum. It appears from these observations that the behaviour of the froth near the surface can markedly affect the rest of the froth column. Devices for scraping the

the froth behaviour is large. It is unfortunate that this is a particularly difficult variable to monitor as well as being highly dependent on one froth solids in the cell, and the aeration rate. It is suggested that the froth might be a very convenient

The water overflow rate was shown experimentally to be dependent on both the froth breakage rate and the overlapping end effects. In the case of apatite ore flotation, the overlapping end effects were fairly noticeable, particularly at low froth heights, because the rates of breakage were relatively small. For other less stable froth types, breakage might predominate (see graph A4).

6.4 ENTRAINMENT

In the theory, it was proposed that entrainment was caused by particles becoming trapped in the interstitial water in the rising froth. The results of the run done on silica showed that a larger fraction of large particles were coming over with the froth than would be expected, and it was suggested that these might have been floating, or because of their size, have been trapped in the relatively smaller Plateau borders. On the other hand, no sign of entrainment could be detected in apatite ore flotation. This behaviour is probably because the small region directly below the froth-pulp interface, where the solids for entrainment would come from, was relatively free of solids because of settling.

The experimental results thus show that entrainment, although it probably exists, is negligibly small in normal flotation. Both the results from apatite ore flotation and those from the run done on silica slurry indicate this, and it appears to be the general case for mineral flotation. It is, therefore, unnecessary to consider it when modelling flotation.

CHAPTER 7

CONCLUSIONS

The conclusions drawn from this investigation are:

(1) For the apatite ore under investigation, froth height has no effect on grade. There is, however, a small effect on total solids flow and a larger effect on water overflow. The froth can thus be modelled in the context of the existing flotation model by a function $R(h)$ which is linear in h , and describes the fraction of floated material entering the froth which returns to the pulp again.

(2) The optimal froth height for a single cell is zero. This is a consequence of a decrease in recovery without an increase in grade for increasing froth heights. This cannot be generalised to a full flotation plant, because of the effect of feedback streams, and the necessity of maintaining a specified output grade. By varying recovery, froth height could be used as an indirect control action for grade in a plant.

(3) The effects of entrainment are so small that they can easily be neglected in normal flotation.

(4) The froth from an apatite ore slurry is a particularly stable type of froth, compared to other types of flotation froths. The behaviour of the froth is very dependent on surface effects, and devices for scraping froth off the surface of the cell might have large effects on the processes occurring within the froth body. It is furthermore possible to obtain information, such as bubble size, from a

monitoring/...

monitoring of the froth which may be of use in studying the flotation process itself.

EFFECT OF FROTH HEIGHT ON GRADE, WEIGHT PERCENT SOLIDS,
SOLIDS FLOW, AND WATER FLOW.

In this section, the results from the runs done on apatite ore are presented. This comprises runs A, B, C, D, E, F, G and H. The effects of froth height on grade, wt. % solids, solids flow and water flow are compared for the different runs on graphs A1, A2, A3 and A4 respectively. (The analyses for grade were performed by the Analytical Laboratory of the National Institute for Metallurgy.)

Test run on well. Batch mixing of slurry. Three different feed rates used.

APPENDIX A

Data: Apatite ore 143 kg approx. Water 23.5 ml., Na₂O 147 kg, H₂SiO₃ 72.5 ml., Unitol 58.6 ml., pH 10.2, Temperature approx. 30°C, Air flow 5.8-10⁻⁴ m³/s throughout.

EFFECT OF FROTH HEIGHT ON GRADE, WEIGHT PERCENT SOLIDS,

| Sample Number | Feed setting m ³ /s.10 ⁴ | SOLIDS FLOW, AND WATER FLOW. | | | | Solids conc. wt. % | Grade % |
|---|---|------------------------------|-------------------|----------------------|-----------------------------------|-----------------------|------------|
| | | Sample | m.10 ³ | kg/s.10 ³ | m ³ /s.10 ⁴ | | |
| <p>In this section, the results from the runs done on apatite ore are presented. This comprises runs A, B, C, D, E, F, G and K. The effects of froth height on grade, wt. % solids, solids flow and water flow are compared for the different runs on graphs A1, A2, A3 and A4 respectively. (The analyses for grade were performed by the Analytical Laboratory of the National Institute for Metallurgy.)</p> | | | | | | | |
| 1 | 4.1 | Froth | 13.5 | 8.2 | 26.3 | 23.8 | 14.0 |
| 2 | | Tails | 4 | 4.1 | 133 | 2.97 | 5.24 |
| 3 | | Froth | 13.5 | 8.2 | 26.3 | 23.8 | 14.0 |
| 4 | | Tails | 4 | 4.1 | 133 | 2.97 | 5.24 |
| 5 | 7.0 | Froth | 13 | 12.0 | 37.9 | 24.0 | 14.1 |
| 6 | | Tails | 7 | 23.3 | 504 | 4.41 | 8.44 |
| 7 | | Froth | 13 | 12.0 | 37.9 | 24.0 | 14.1 |
| 8 | | Tails | 7 | 23.3 | 504 | 4.41 | 8.44 |
| 9 | 4.5 | Froth | 30 | 5.5 | 24.2 | 15.5 | 13.3 |
| 10 | | Tails | 23 | 7.9 | 297 | 2.61 | 8.38 |
| 11 | | Froth | 30 | 5.5 | 24.2 | 15.5 | 13.3 |
| 12 | | Tails | 23 | 7.9 | 297 | 2.61 | 8.38 |
| 13 | 4.5 | Froth | 16 | 5.8 | 30.2 | 14.0 | 13.0 |
| 14 | | Tails | 8.5 | 7.9 | 286 | 2.68 | 9.35 |
| 15 | | Froth | 16 | 5.8 | 30.2 | 14.0 | 13.0 |
| 16 | | Tails | 8.5 | 7.9 | 286 | 2.68 | 9.35 |
| 17 | 4.5 | Froth | 8.5 | 6.0 | 41.0 | 12.7 | 12.9 |
| 18 | | Tails | 4.5 | 7.9 | 326 | 2.37 | 10.0 |
| 19 | | Froth | 8.5 | 6.0 | 41.0 | 12.7 | 12.9 |
| 20 | | Tails | 4.5 | 7.9 | 326 | 2.37 | 10.0 |

Test run on cell. Batch mixing of slurry. Three different feed rates used.

Data: Apatite ore 143 kg approx. Berol 23.5 ml., Na_2S 0.147 kg, NaSilicate 72.5 ml., Unitol 58.6 ml., pH 10.2, Temperature approx. 30°C , Air flow $8.8 \times 10^{-4} \text{ m}^3/\text{s}$ throughout.

| Sample Number | Feed setting $\text{m}^3/\text{s} \times 10^4$ | Type of Sample | Froth Height $\text{m} \times 10^2$ | Solids flow $\text{kg}/\text{s} \times 10^3$ | Water flow $\text{m}^3/\text{s} \times 10^6$ | Solids conc. wt. % | Grade $\% \text{P}_2\text{O}_5$ |
|---------------|--|----------------|-------------------------------------|--|--|--------------------|---------------------------------|
| 1 2 | 2.17 | Froth Tails | 19.5 | 9.2 6.0 | 26.3 120 | 25.8 4.76 | 14.0 6.40 |
| 3 4 | | Froth Tails | 15 | 8.2 4.4 | 28.6 104 | 22.3 4.05 | 14.0 7.26 |
| 5 6 | | Froth Tails | 8 | 10.0 5.7 | 31.1 141 | 24.3 3.89 | 14.0 6.72 |
| 7 8 | | Froth Tails | 6 | 8.9 4.1 | 29.5 135 | 23.2 2.97 | 12.5 5.71 |
| 9 10 | 7.0 | Froth Tails | 23.5 | 12.4 4.1 | 36.8 666 | 25.2 5.78 | 13.9 8.63 |
| 11 12 | | Froth Tails | 13 | 12.0 23.3 | 37.9 504 | 24.0 4.41 | 14.3 8.66 |
| 13 14 | | Froth Tails | 7 | 16.7 23.0 | 53.8 - | 23.7 - | 14.5 9.35 |
| 15 16 | | Froth Tails | 5 | 8.8 22.2 | 39.7 575 | 18.1 3.71 | 14.8 9.90 |
| 17 18 | 4.5 | Froth Tails | 30 | 5.5 7.9 | 24.2 297 | 18.5 2.61 | 13.3 9.38 |
| 19 20 | | Froth Tails | ~23 | 6.5 8.5 | 27.6 316 | 19.0 2.62 | 13.0 9.75 |
| 21 22 | | Froth Tails | 16 | 5.8 7.9 | 30.2 286 | 16.0 2.68 | 13.0 9.95 |
| 23 24 | | Froth Tails | 6.5 | 6.0 7.9 | 41.0 326 | 12.7 2.37 | 12.9 10.0 |

RUN B

Similar to run A.

Data: Apatite ore 143 kg. Na_2S 0.147kg, Na Silicate 72.5 ml.Unitol 38.6 ml., Berol 10 ml., Air flow $1.0 \times 10^{-3} \text{ m}^3/\text{s}$.

| Sample No. | Feed setting $\text{m}^3/\text{s} \times 10^4$ | Type of Sample | Froth Height $\text{m} \times 10^2$ | Solids flow $\text{kg}/\text{s} \times 10^3$ | Water flow $\text{m}^3/\text{s} \times 10^6$ | Solids conc. wt. % | Grade $\% \text{P}_2\text{O}_5$ |
|------------|--|----------------|-------------------------------------|--|--|--------------------|---------------------------------|
| 1 2 | 2.17 | Froth Tails | 21 | 4.1 20.4 | 7.4 166 | 35.5 11.0 | 19.2 8.67 |
| 3 4 | | Froth Tails | 7 | 6.0 21.6 | 18.1 153 | 24.7 12.3 | 17.6 7.61 |
| 5 6 | | Froth Tails | 3 | 5.8 10.7 | 25.6 122 | 18.4 8.12 | 16.2 6.69 |
| 7 | | Feed | | | | 7.2 | 9.79 |
| 8 9 | 5.8 | Froth Tails | 21 | 7.8 30.5 | 18.5 425 | 29.5 6.7 | 18.5 9.31 |
| 10 11 | | Froth Tails | 7 | 3.9 53.9 | 14.2 723 | 21.6 6.93 | 19.4 11.2 |
| 12 | | Feed | | | | 5.26 | 12.4 |

RUN C

Batch mixing run, feed sample taken with each froth-tailings pair, to check drift in mixing tanks.

Data: Apatite 143kg. Na_2S 0.147 kg, Na Silicate 72.5 ml.,
Unitol 38.6 ml., Berol 10 ml., pH 10.2, Air flow $9.7 \times 10^{-4} \text{ m}^3/\text{s}$.

| Sample Number | Feed setting $\text{m}^3/\text{s} \times 10^4$ | Type of Sample | Froth Height $\text{m} \times 10^2$ | Solids flow $\text{kg}/\text{s} \times 10^3$ | Water flow $\text{m}^3/\text{s} \times 10^6$ | Solids conc. wt. % | Grade $\% \text{P}_2\text{O}_5$ |
|----------------|---|------------------------|--|---|---|-----------------------|------------------------------------|
| 1 2 3 | 1.5 | Feed Froth Tails | 4.5 | 4.36 16.4 | 17.8 108 | 12.7 19.7 13.1 | 11.1 19.0 9.20 |
| 4 5 6 | 1.5 | Feed Froth Tails | 9.5 | 1.6 15.5 | 14.0 120 | 10.6 10.3 8.15 | 10.5 18.8 8.84 |
| 7 8 9 | 1.5 | Feed Froth Tails | 14 | 2.53 10.6 | 8.6 114 | 8.4 22.7 8.5 | 10.2 18.2 8.48 |
| 10 11 12 | 1.5 | Feed Froth Tails | 19.5 | 2.65 10.8 | 8.5 122 | 7.2 23.7 8.1 | 10.4 18.1 8.72 |
| 13 14 15 | 1.5 | Feed Froth Tails | 26 | 2.38 7.6 | 7.7 118 | 6.8 23.6 6.1 | 10.9 18.3 9.45 |
| 16 17 18 | 4.5 | Feed Froth Tails | 3 | 4.36 15.7 | 27.5 344 | 5.6 13.7 4.4 | 12.0 16.5 8.13 |

Batch mixing run, but intermittently recirculated between tanks. Tank samples taken from contents of cell to compare with tails. Data: Apatite ore 143kg., Na_2S 0.147kg., Na Silicate 72.5 ml., Unitol 38.6 ml., Berol 10 ml., pH 10.2, Air flow $9.7 \times 10^{-4} \text{ m}^3/\text{s}$
Feed setting = $2.67 \times 10^{-4} \text{ m}^3/\text{s}$.

| Sample Number | Type of Sample | Froth Height $\text{m} \times 10^2$ | Solids flow $\text{kg/s} \times 10^3$ | Water flow $\text{m}^3/\text{s} \times 10^6$ | Solids conc. wt. % | Grade % P_2O_5 |
|----------------|------------------------|-------------------------------------|---------------------------------------|--|----------------------|--------------------------------|
| 1 2 3 | Froth Tails Tank | 26 | 2.71 31.0 | 5.78 197 | 31.9 13.6 10.4 | 22.2 9.7 9.1 |
| 4 | Feed | | | | 11.0 | 10.6 |
| 5 6 7 | Froth Tails Tank | 19 | 3.38 25.8 | 10.8 209 | 23.8 11.0 9.25 | 20.6 9.3 10.7 |
| 8 9 10 | Froth Tails Tank | 10.5 | 3.86 14.0 | 15.7 142 | 19.7 8.3 7.3 | 19.7 9.0 8.8 |
| 11 | Feed | | | | 7.7 | 11.6 |
| 12 13 14 | Froth Tails Tank | 2.5 | 4.07 11.5 | 23.1 175 | 15.0 6.2 5.4 | 18.6 8.8 8.4 |

== Spoiled sample

RUN E

Continuous mixing of slurry. Tank samples taken as in Run D.

Data : Solids (apatite ore) feed rate = 0.083 kg/s approx., Unitol 0.083 ml/s., (No other additives) pH 10.2, Air rate 8.3×10^{-4} m³/s, Feed setting 5.8×10^{-4} m³/s.

| Sample Number | Type of Sample | Froth Height m $\times 10^2$ | Solids flow kg/s $\times 10^3$ | Water flow m ³ /s $\times 10^6$ | Solids conc. wt. % | Grade %P ₂ O ₅ |
|-----------------|------------------------|---------------------------------|-----------------------------------|---|-----------------------|---|
| 1 2 3 | Froth Tails Tank | 2 | 27.8 57.6 | 67.5 364 | 29.1 13.7 12.3 | 20.1 7.03 7.27 |
| 4 | Feed | | | | 16.0 | 10.87 |
| 5 6 7 | Froth Tails Tank | 4.5 | 26.6 67.8 | 58.4 396 | 31.3 14.6 12.1 | 21.2 7.02 7.83 |
| 8 9 10 | Froth Tails Tank | 9 | 23.3 74.2 | 46.7 403 | 33.3 15.5 13.2 | 21.60 8.22 8.32 |
| 11 12 13 | Froth Tails Tank | 16 | 18.7 73.5 | 34.4 416 | 35.2 15.0 12.5 | 22.9 8.52 9.33 |
| 14 | Feed | | | | 15.9 | 11.5 |
| 15* 16 17 | Froth Tails Tank | 24 | - 82.8 | - 447 | - 15.6 12.0 | 24.8 8.86 10.9 |

*= Spoiled sample

* = Spoiled sample - data not used in graphs.

RUN F

Continuous mixing of slurry with temperature control.
Random selection of froth heights.

Data : Solids approx. 0.061 kg/s, Unitol 0.042 ml./s

Air rate 11.8×10^{-4} m³/s, Temperature approx. 35°C,

Slurry feed setting 4.5×10^{-4} m³/s.

| Sample Number | Type of Sample | Froth Height m $\times 10^2$ | Solids flow kg/s $\times 10^3$ | Water flow m ³ /s $\times 10^6$ | Solids conc. wt. % | Grade %P ₂ O ₅ |
|---------------|----------------|------------------------------|--------------------------------|--|--------------------|--------------------------------------|
| 1* 21 | Froth Tank | 2 | (7.75) | (4.52) | (63.1) 16.4 | (22.0) 10.6 |
| 2 22 | Froth Tank | 23 | 4.08 | 9.15 | 30.9 15.7 | 24.9 10.6 |
| 3 23 | Froth Tank | 4.5 | 5.55 | 19.5 | 22.1 15.9 | 24.0 10.5 |
| 4 24 | Froth Tank | 10.5 | 5.15 | 15.6 | 24.8 16.0 | 24.2 9.7 |
| F1 | Feed | | | | 19.0 | 10.6 |
| 5 25 | Froth Tank | 17.5 | 5.52 | 16.2 | 25.4 15.7 | 25.1 10.1 |
| 6 26 | Froth Tank | 23 | 6.15 | 14.6 | 29.6 17.6 | 26.0 9.6 |
| 7 27 | Froth Tank | 4.5 | 10.18 | 27.2 | 27.2 17.9 | 25.4 9.9 |
| F2 | Feed | | | | 20.9 | 11.0 |
| 8 28 | Froth Tank | 19 | 8.72 | 19.7 | 30.7 18.0 | 26.0 10.1 |
| 9 29 | Froth Tank | 22.5 | 7.79 | 18.2 | 29.9 17.9 | 26.2 10.5 |

* = Spoiled sample - data not used in graphs.

Continuous mixing of apatite ore slurry (New, coarser, solids used),
Controlled temperature of 36°C.

Data : Solids approx. 0.11 kg/s, Unitol 0.072 ml/s, Air rate 8.7×10^{-4} m³/s, Slurry feed setting 7.0×10^{-4} m³/s.

| Sample Number | Type of Sample | Froth Height, m $\times 10^2$ | Solids flow kg/s $\times 10^3$ | Water flow m ³ /s $\times 10^6$ | Solids conc. wt. % | Grade %P ₂ O ₅ |
|---------------|----------------|-------------------------------|--------------------------------|--|--------------------|--------------------------------------|
| 1 11 | Froth Tank | 11.5 | 8.52 | 30.0 | 22.1 8.22 | 13.8 7.3 |
| 2 12 | Froth Tank | 3.5 | 11.06 | 39.9 | 21.7 7.86 | 14.5 7.0 |
| 3 13 | Froth Tank | 17.5 | 6.44 | 25.0 | 20.6 7.16 | 14.0 7.1 |
| 4 14 | Froth Tank | 24.5 | 5.80 | 20.8 | 21.8 8.53 | 13.6 7.3 |
| 5 15 | Froth Tank | 12 | 7.40 | 30.0 | 19.8 8.06 | 13.8 7.1 |
| 6 16 | Froth Tank | 2 | 7.96 | 69.0 | 10.3 7.45 | 12.2 6.3 |
| 7 17 | Froth Tank | 3 | 18.02 | 56.8 | 24.1 7.25 | 11.9 6.4 |
| 8 18 | Froth Tank | 15 | 15.06 | 43.2 | 25.8 8.10 | 12.3 6.2 |
| 9 19 | Froth Tank | 25 | 14.28 | 37.8 | 27.4 9.60 | 12.7 6.9 |
| 10 20 | Froth Tank | 4 | 17.42 | 50.6 | 25.6 9.45 | 12.5 6.4 |
| 21 31 | Froth Tank | 18 | 14.90 | 39.5 | 27.4 8.64 | 12.2 6.77 |
| 22 32 | Froth Tank | 7 | 16.26 | 44.3 | 26.8 8.92 | 12.5 12.9 |

RUN G CONTINUED -

Run done with continuous mixing of slurry. Conductivity

| Sample Number | Type of Sample | Froth Height, $m \times 10^2$ | Solids flow $kg/s \times 10^3$ | Water flow $m^3/s \times 10^5$ | Solids conc. wt. % | Grade % P_2O_5 |
|---------------|----------------|-------------------------------|--------------------------------|--------------------------------|--------------------|------------------|
| F1 | Feed | | | | 10.25 | 7.57 |
| F2 | Feed | | | | 11.3 | 6.78 |
| F3 | Feed | | | | 13.3 | 7.38 |

| Sample Number | Type of Sample | Froth Height $m \times 10^2$ | Solids flow $kg/s \times 10^3$ | Water Flow $m^3/s \times 10^5$ | Solids conc. wt. % | Grade % P_2O_5 |
|---------------|----------------|------------------------------|--------------------------------|--------------------------------|--------------------|------------------|
| 1 | Feed | | | | 21.1 | 7.44 |
| 2 | Froth Tank | 25 | 704 | 1550 | 31.3 | 21.0 |
| 3 | | | | | 15.4 | 5.44 |
| 4 | Froth Tank | 20 | 343 | 1133 | 23.2 | 18.8 |
| 5 | | | | | 15.4 | 7.26 |
| 6 | Feed | | | | 19.4 | 8.21 |
| 7 | Froth Tank | 23 | 154 | 967 | 16.9 | 10.1 |
| 8 | | | | | 14.4 | 5.05 |

RUN K

Run done with continuous mixing of slurry. Conductivity of froth also recorded. (see Appendix B).

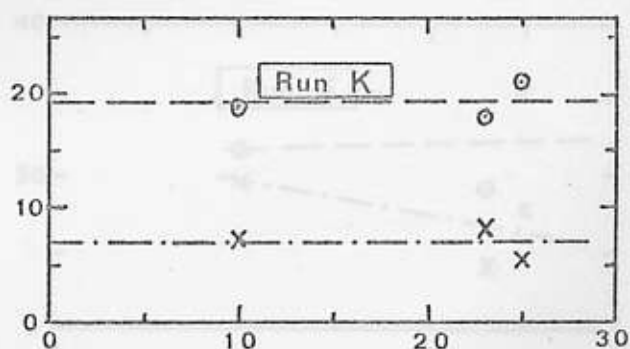
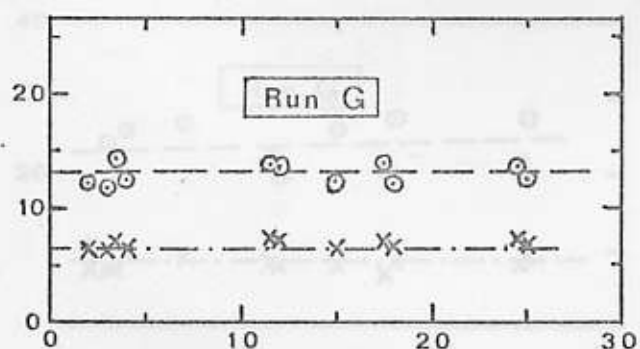
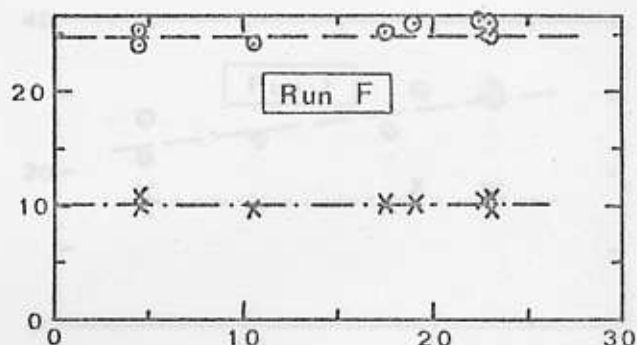
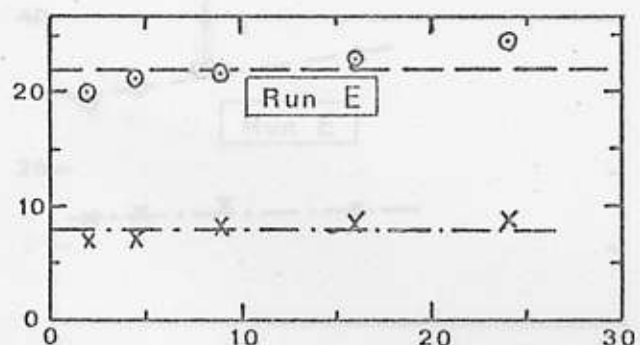
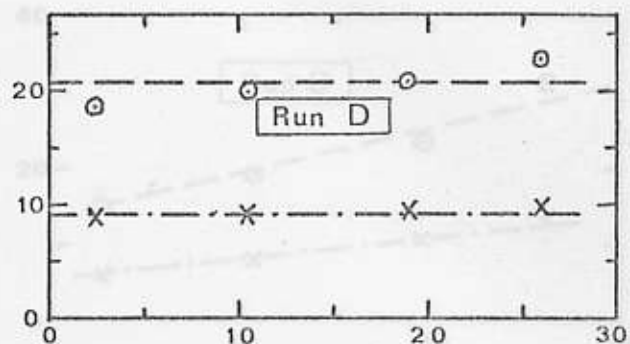
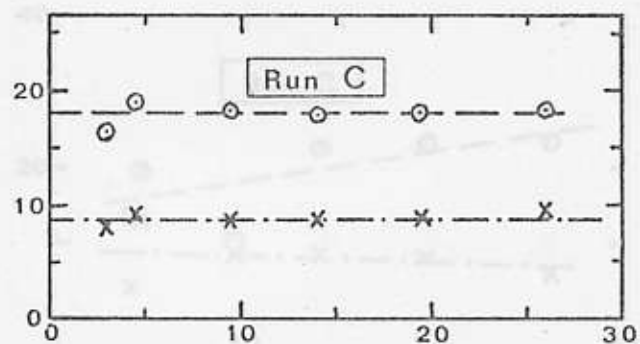
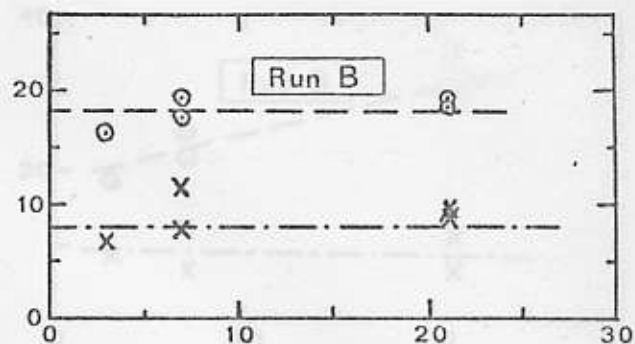
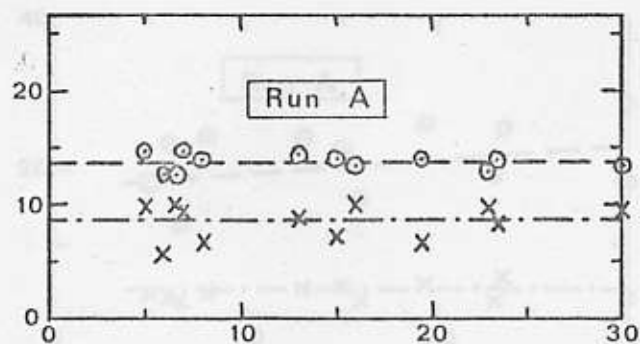
Data : Unitol 0.0208 ml/s, Berol 0.0128 ml/s, Na Silicate 0.18 ml/s, Temperature 35°C, pH 10.2, Slurry feed setting 4.5×10^{-4} m³/s, Air rate 8.3×10^{-4} m³/s.

| Sample Number | Type of Sample | Froth Height m $\times 10^2$ | Solids flow kg/s $\times 10^3$ | Water flow m ³ /s $\times 10^6$ | Solids conc. wt. % | Grade %P ₂ O ₅ |
|---------------|----------------|---------------------------------|-----------------------------------|---|-----------------------|---|
| 1 | Feed | | | | 21.1 | 7.44 |
| 2 3 | Froth Tank | 25 | 704 | 1550 | 31.3 15.4 | 21.0 5.44 |
| 4 5 | Froth Tank | 10 | 343 | 1133 | 23.2 15.6 | 18.8 7.26 |
| 6 | Feed | | | | 19.4 | 8.21 |
| 7 8 | Froth Tank | 23 | 196 | 967 | 16.9 14.4 | 18.1 8.05 |

VERTICAL AXIS - GRADE, % P₂O₅HORIZONTAL AXIS - FROTH HEIGHT, m $\times 10^2$

CONTENTS OF CHL - X FROTH - O

GRAPH A1. GRADE vs FROTH HEIGHT FOR EACH RUN.

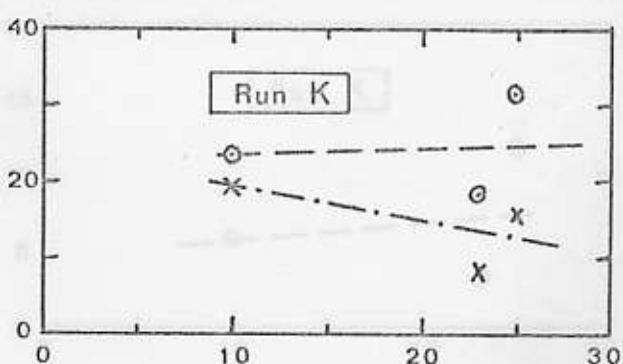
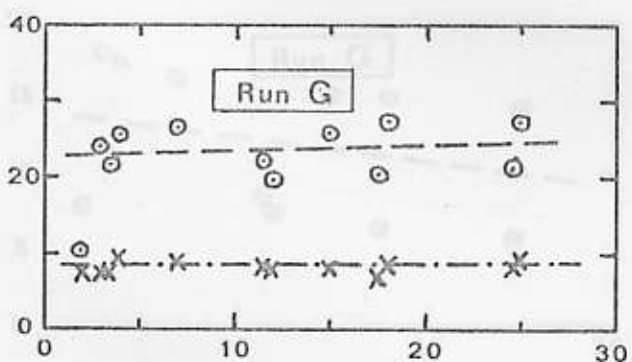
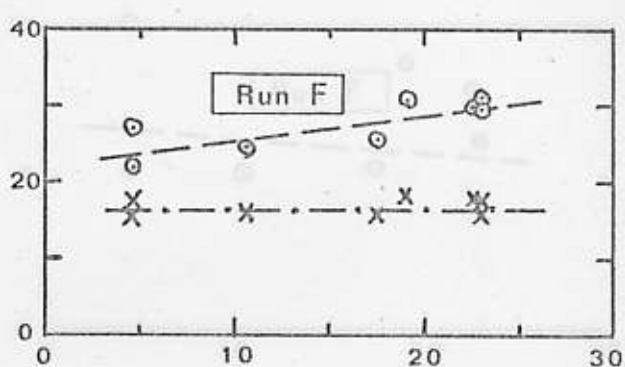
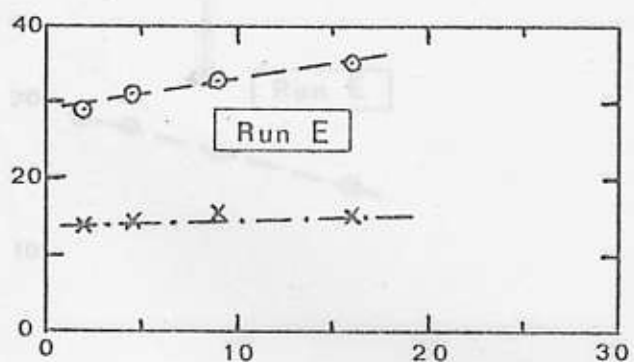
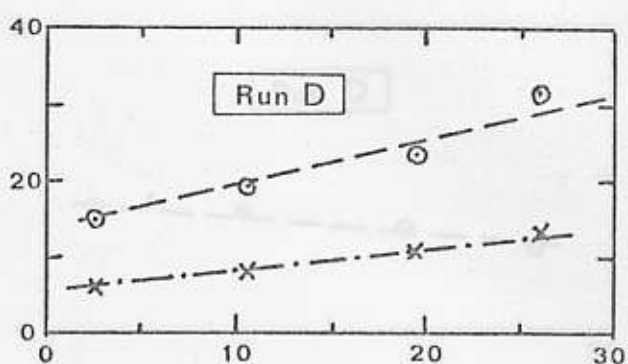
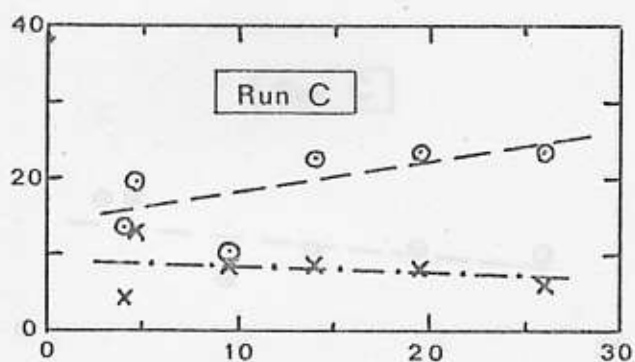
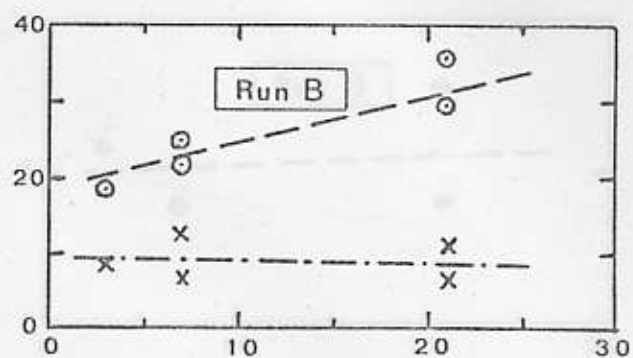
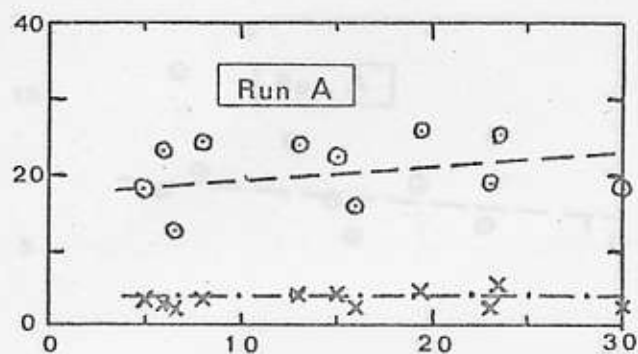


VERTICAL AXES — GRADE, % P₂O₅

HORIZONTAL AXES — FROTH HEIGHT, m x 10²

CONTENTS OF CELL — X FROTH — O

GRAPH A1. GRADE vs FROTH HEIGHT FOR EACH RUN.



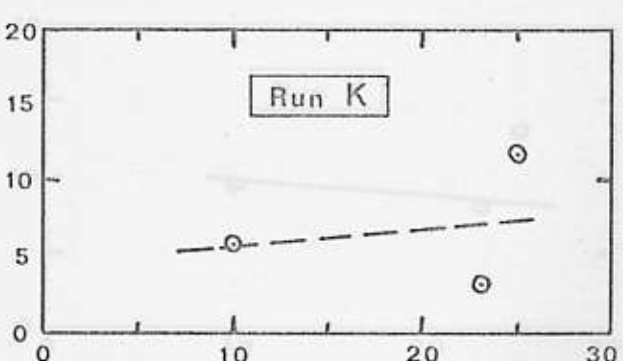
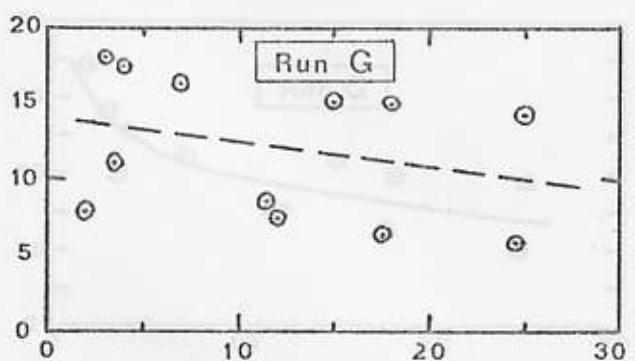
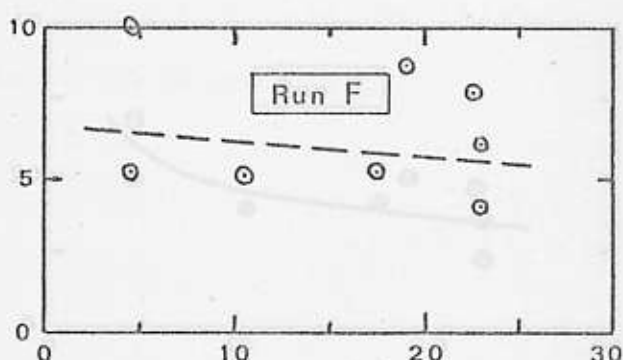
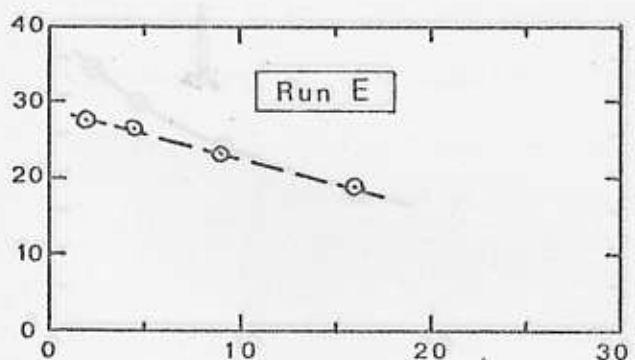
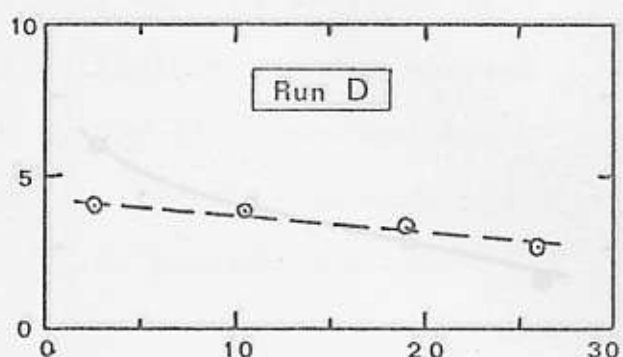
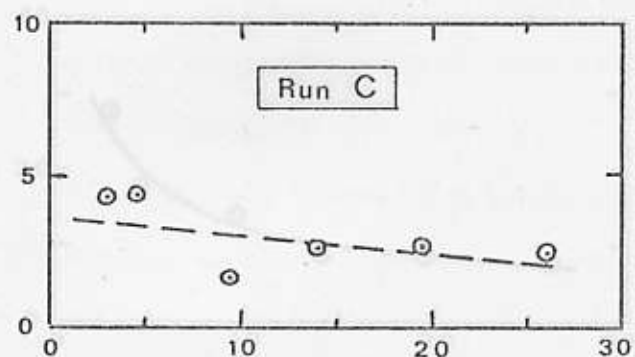
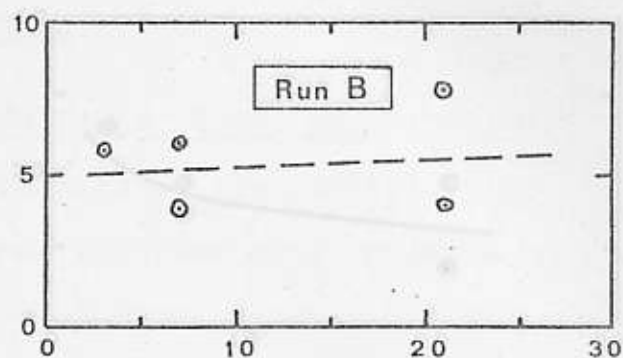
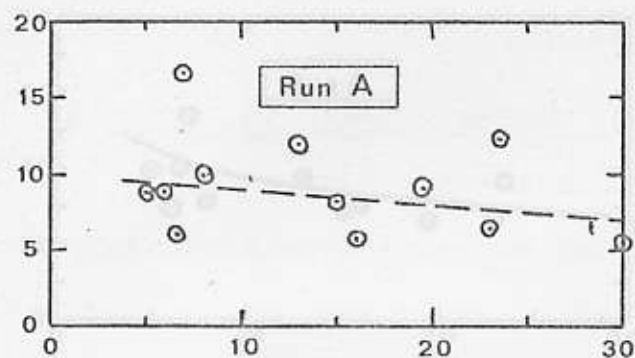
VERTICAL AXES — WEIGHT PERCENT OF SOLIDS

HORIZONTAL AXES — FROTH HEIGHT, $m \times 10^2$

CONTENTS OF CELL — X

FROTH — O

GRAPH A2. WEIGHT PERCENT SOLIDS vs FROTH HEIGHT.



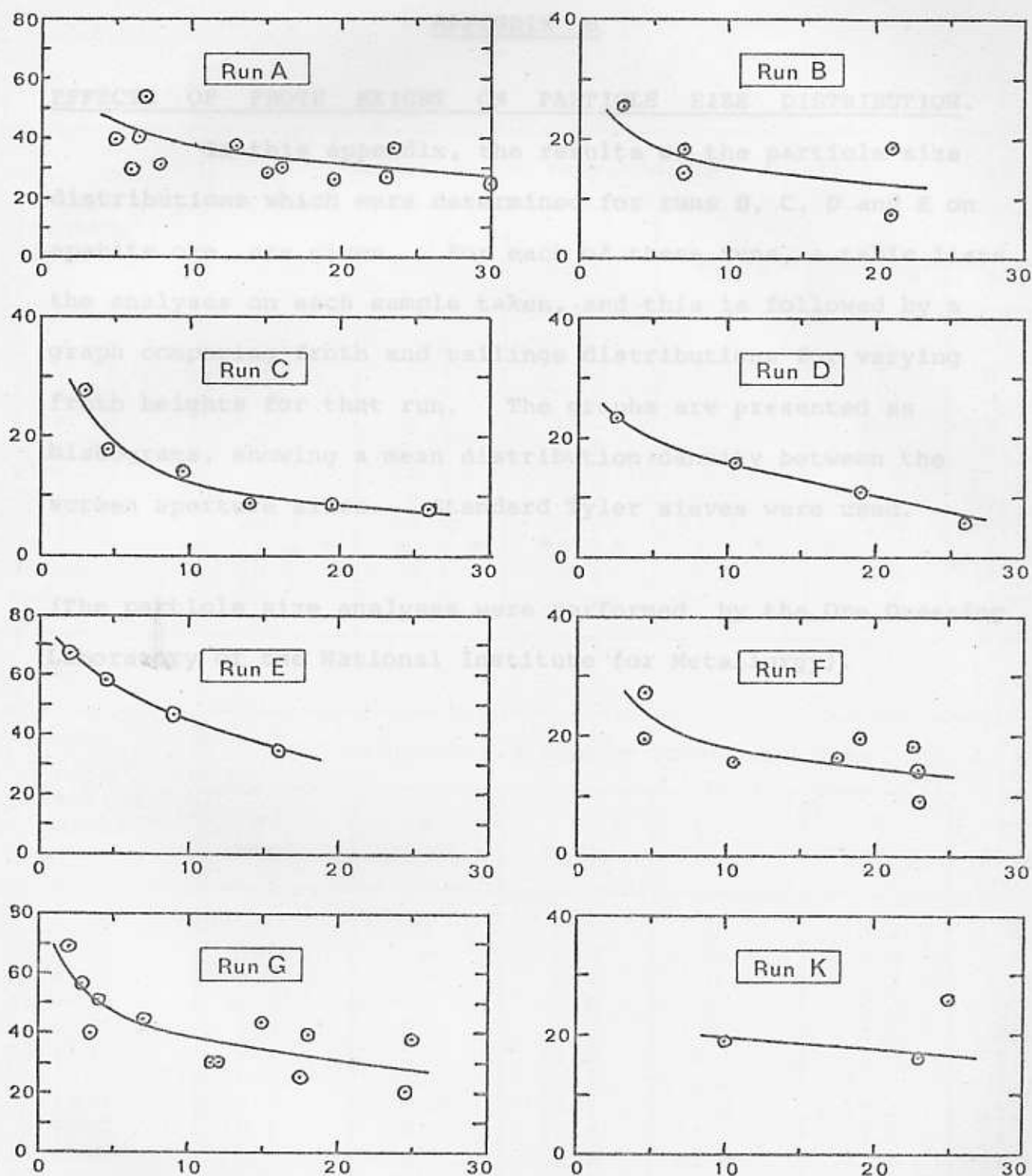
VERTICAL AXIS — LIQUID OUTFLOW, $m^3/s \times 10^3$ (NOTE CHANGES OF SCALE)

VERTICAL AXES — SOLIDS FLOW, $kg/s \times 10^3$ (NOTE CHANGES OF SCALE)

HORIZONTAL AXIS — FROTH HEIGHT, $m \times 10^2$

HORIZONTAL AXES — FROTH HEIGHT, $m \times 10^2$.

GRAPH A3. SOLIDS OVERFLOW vs FROTH HEIGHT.



VERTICAL AXES: LIQUID OVERFLOW $\text{m}^3/\text{s} \times 10^6$ (NOTE CHANGES OF SCALE)

HORIZONTAL AXES: FROTH HEIGHT $\text{m} \times 10^2$

GRAPH A4. WATER OVERFLOW vs FROTH HEIGHT.

RUN B. PARTICLE SIZE D. APPENDIX B

EFFECTS OF FROTH HEIGHT ON PARTICLE SIZE DISTRIBUTION.

In this appendix, the results of the particle size distributions which were determined for runs B, C, D and E on apatite ore, are given. For each of these runs, a table lists the analyses on each sample taken, and this is followed by a graph comparing froth and tailings distributions for varying froth heights for that run. The graphs are presented as histograms, showing a mean distribution density between the screen aperture sizes. Standard Tyler sieves were used.

(The particle size analyses were performed by the Ore Dressing Laboratory of the National Institute for Metallurgy).

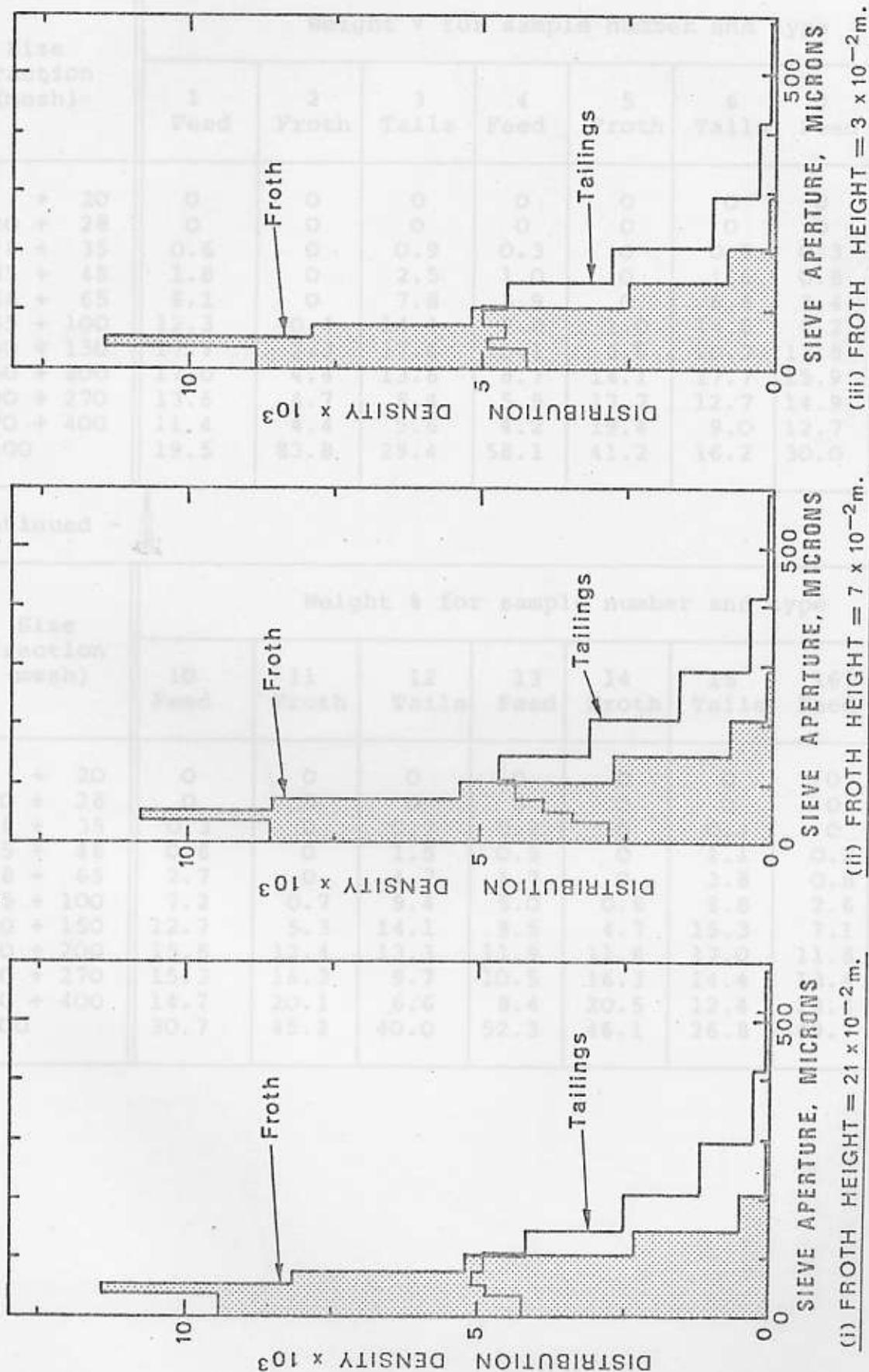
| Size fraction (mesh) | Weight % for sample number and type | | | | | |
|----------------------------|-------------------------------------|------------|------------|-------------|-------------|------------|
| | 7 Feed | 8 Froth | 9 Tails | 10 Froth | 11 Tails | 12 Feed |
| + 20 | 0 | 0 | 0.1 | 0 | 0.2 | 0 |
| - 20 + 24 | 0.1 | 0 | 0.3 | 0 | 0.5 | 0 |
| - 24 + 28 | 0.3 | 0 | 0.8 | 0 | 1.2 | 0.1 |
| - 28 + 35 | 0.1 | 0 | 2.6 | 0 | 2.0 | 0.2 |
| - 35 + 48 | 4.5 | 0.1 | 6.6 | 0 | 4.4 | 0.4 |
| - 48 + 65 | 9.2 | 1.6 | 11.8 | 0.3 | 6.7 | 2.0 |
| - 65 + 100 | 14.4 | 1.9 | 15.4 | 1.1 | 10.1 | 6.1 |
| - 100 + 150 | 18.8 | 11.0 | 15.2 | 8.8 | 13.1 | 11.9 |
| - 150 + 200 | 13.7 | 16.8 | 12.6 | 14.3 | 13.1 | 14.4 |
| - 200 + 270 | 12.7 | 21.1 | 10.9 | 21.3 | 15.6 | 16.4 |
| - 270 + 400 | 29.0 | 40.5 | 21.7 | 32.0 | 38.1 | 45.1 |

RUN B. PARTICLE SIZE DISTRIBUTIONS.

| Size fraction (mesh) | Weight % for sample number and type | | | | | |
|----------------------------|-------------------------------------|------------|------------|------------|------------|------------|
| | 1 Froth | 2 Tails | 3 Froth | 4 Tails | 5 Froth | 6 Tails |
| + 20 | 0 | 0.1 | 0 | 0 | 0 | 0 |
| - 20 + 28 | 0 | 0.4 | 0 | 0.5 | 0 | 0.1 |
| - 28 + 35 | 0 | 1.5 | 0 | 1.8 | 0 | 0.8 |
| - 35 + 48 | 0 | 4.8 | 0.1 | 5.8 | 0.1 | 3.3 |
| - 48 + 65 | 0.3 | 10.3 | 0.4 | 14.3 | 0.6 | 9.9 |
| - 65 +100 | 3.2 | 15.6 | 4.0 | 19.4 | 4.6 | 17.2 |
| -100 +150 | 10.4 | 18.7 | 12.2 | 20.3 | 11.6 | 20.1 |
| -150 +200 | 16.6 | 14.8 | 16.7 | 13.7 | 15.6 | 15.5 |
| -200 +270 | 17.0 | 10.3 | 17.5 | 8.1 | 16.2 | 9.7 |
| -270 +400 | 17.1 | 7.4 | 16.3 | 5.2 | 17.4 | 7.5 |
| - 400 | 35.4 | 16.1 | 32.8 | 10.9 | 33.9 | 15.9 |

continued -

| Size fraction (mesh) | Weight % for sample number and type | | | | | |
|----------------------------|-------------------------------------|------------|------------|-------------|-------------|------------|
| | 7 Feed | 8 Froth | 9 Tails | 10 Froth | 11 Tails | 12 Feed |
| + 20 | 0 | 0 | 0.1 | 0 | 0.2 | 0 |
| - 20 + 28 | 0.1 | 0 | 0.3 | 0 | 0.5 | 0 |
| - 28 + 35 | 0.3 | 0 | 0.8 | 0 | 1.2 | 0.1 |
| - 35 + 48 | 0.3 | 0 | 2.6 | 0 | 2.0 | 0.2 |
| - 48 + 65 | 4.5 | 0.1 | 6.6 | 0 | 4.4 | 0.4 |
| - 65 +100 | 9.2 | 1.6 | 11.8 | 0.3 | 6.7 | 2.0 |
| -100 +150 | 14.6 | 6.9 | 15.4 | 3.1 | 10.1 | 6.1 |
| -150 +200 | 15.6 | 13.0 | 15.2 | 8.8 | 13.1 | 11.9 |
| -200 +270 | 13.7 | 16.8 | 12.6 | 14.3 | 13.1 | 14.4 |
| -270 +400 | 12.7 | 21.1 | 10.9 | 21.5 | 13.6 | 16.8 |
| - 400 | 29.0 | 40.5 | 23.7 | 52.0 | 35.1 | 48.1 |



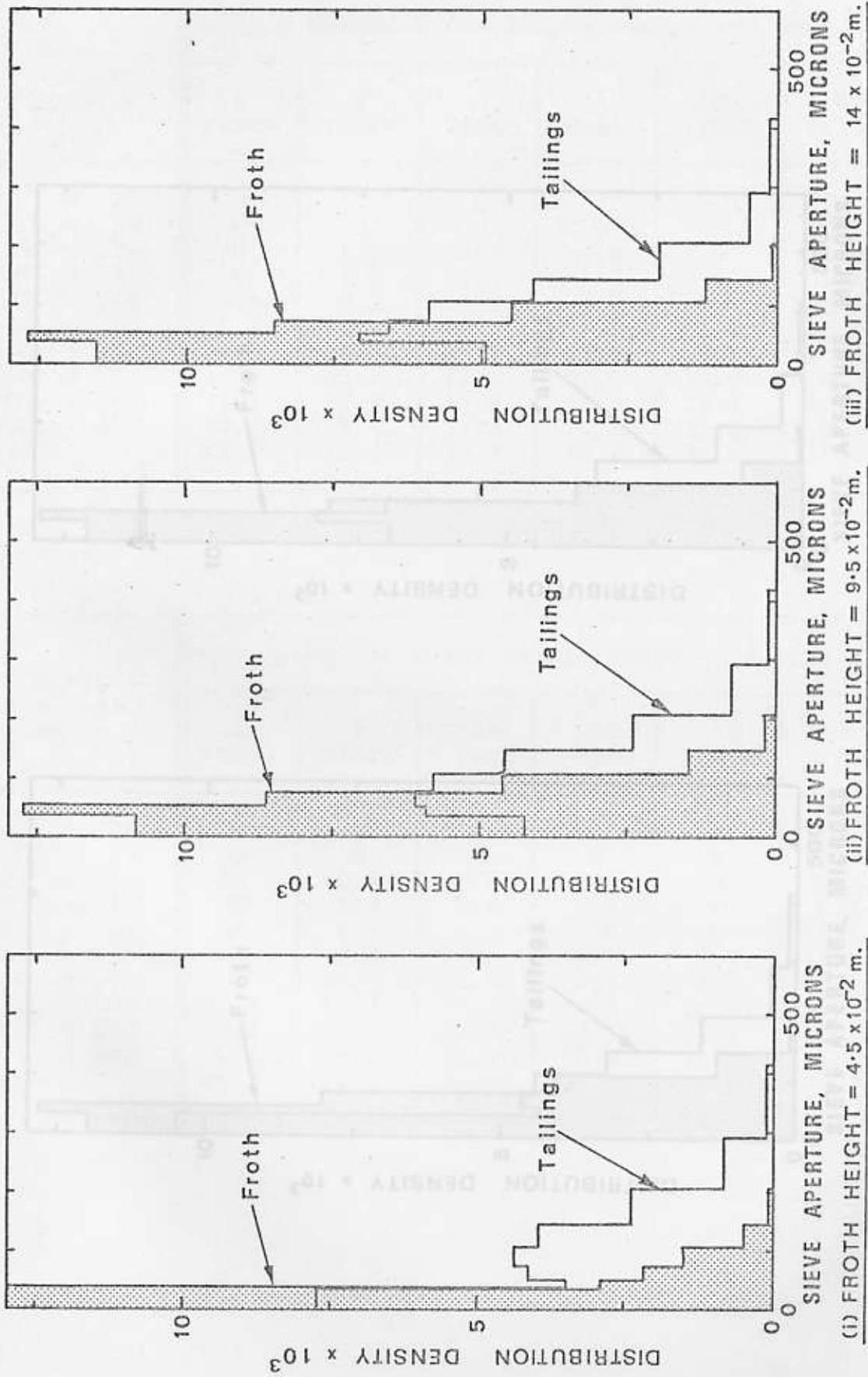
GRAPH B1. COMPARISON OF PARTICLE SIZE DISTRIBUTIONS FOR VARYING FROTH HEIGHTS. (RUN B)

RUN C. PARTICLE SIZE DISTRIBUTIONS.

| Size fraction (mesh) | Weight % for sample number and type | | | | | | | | |
|----------------------|-------------------------------------|---------|---------|--------|---------|---------|--------|---------|---------|
| | 1 Feed | 2 Froth | 3 Tails | 4 Feed | 5 Froth | 6 Tails | 7 Feed | 8 Froth | 9 Tails |
| + 20 | 0 | 0 | 0 | 0 | 0 | 0 | 0 | 0 | 0 |
| - 20 + 28 | 0 | 0 | 0 | 0 | 0 | 0 | 0 | 0 | 0 |
| - 28 + 35 | 0.6 | 0 | 0.9 | 0.3 | 0 | 0.7 | 0.3 | 0 | 0.7 |
| - 35 + 48 | 1.8 | 0 | 2.5 | 1.0 | 0 | 1.6 | 0.8 | 0 | 2.3 |
| - 48 + 65 | 6.1 | 0 | 7.8 | 3.9 | 0 | 6.6 | 3.4 | 0 | 4.9 |
| - 65 + 100 | 12.3 | 0.4 | 14.4 | 7.8 | 1.0 | 14.8 | 8.2 | 0.8 | 12.1 |
| - 100 + 150 | 17.7 | 2.3 | 17.6 | 10.1 | 6.6 | 20.7 | 13.8 | 5.6 | 18.6 |
| - 150 + 200 | 17.0 | 4.4 | 13.6 | 8.7 | 14.1 | 17.7 | 15.9 | 13.6 | 17.9 |
| - 200 + 270 | 13.6 | 4.7 | 8.4 | 5.9 | 17.7 | 12.7 | 14.9 | 17.6 | 13.7 |
| - 270 + 400 | 11.4 | 4.4 | 5.6 | 4.2 | 19.4 | 9.0 | 12.7 | 19.5 | 10.8 |
| - 400 | 19.5 | 83.8 | 29.4 | 58.1 | 41.2 | 16.2 | 30.0 | 43.5 | 19.0 |

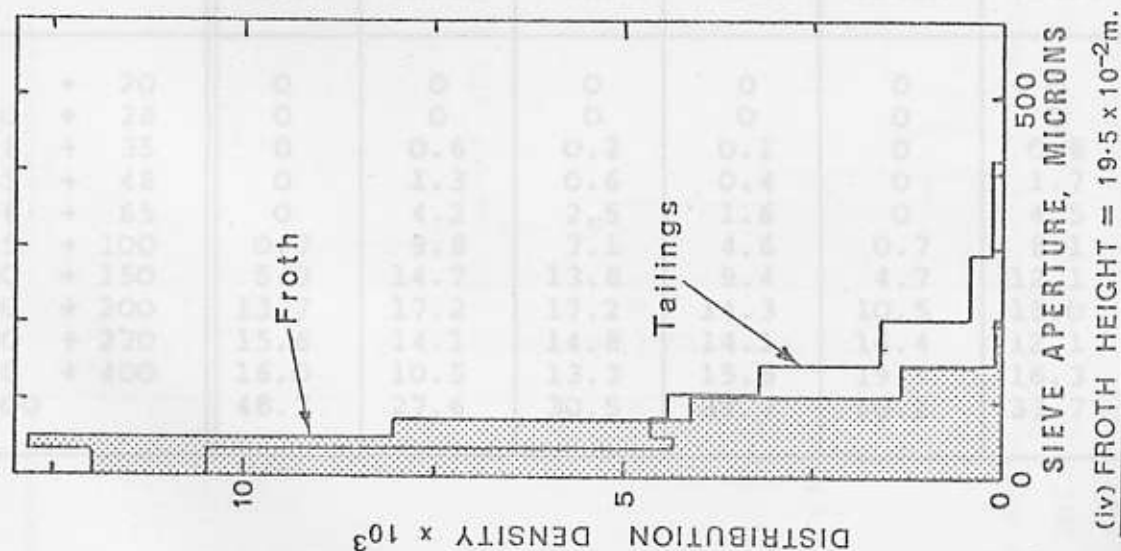
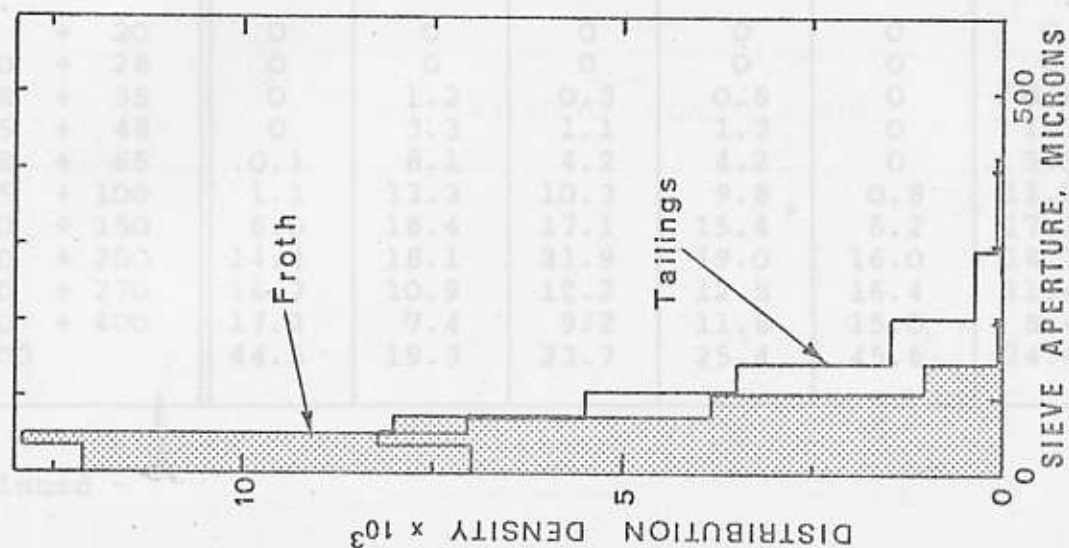
continued -

| Size fraction (mesh) | Weight % for sample number and type | | | | | | | | |
|----------------------|-------------------------------------|----------|----------|---------|----------|----------|---------|----------|----------|
| | 10 Feed | 11 Froth | 12 Tails | 13 Feed | 14 Froth | 15 Tails | 16 Feed | 17 Froth | 18 Tails |
| + 20 | 0 | 0 | 0 | 0 | 0 | 0 | 0 | 0 | 0 |
| - 20 + 28 | 0 | 0 | 0 | 0 | 0 | 0 | 0 | 0 | 0 |
| - 28 + 35 | 0.3 | 0 | 0.7 | 0.2 | 0 | 0.4 | 0 | 0 | 0.5 |
| - 35 + 48 | 0.6 | 0 | 1.5 | 0.5 | 0 | 1.1 | 0.2 | 0 | 1.9 |
| - 48 + 65 | 2.7 | 0 | 4.7 | 1.7 | 0 | 3.8 | 0.8 | 0 | 4.8 |
| - 65 + 100 | 7.2 | 0.7 | 9.4 | 5.0 | 0.6 | 8.8 | 2.6 | 0.9 | 8.1 |
| - 100 + 150 | 12.7 | 5.3 | 14.1 | 9.5 | 4.7 | 15.3 | 7.1 | 4.3 | 12.2 |
| - 150 + 200 | 15.8 | 12.4 | 13.3 | 11.9 | 11.8 | 17.0 | 11.8 | 9.4 | 13.9 |
| - 200 + 270 | 15.3 | 16.3 | 9.7 | 10.5 | 16.3 | 14.4 | 13.4 | 13.8 | 12.8 |
| - 270 + 400 | 14.7 | 20.1 | 6.6 | 8.4 | 20.5 | 12.4 | 14.4 | 19.9 | 11.8 |
| - 400 | 30.7 | 45.2 | 40.0 | 52.3 | 46.1 | 26.8 | 49.7 | 51.7 | 34.0 |



GRAPH B2. COMPARISON OF PARTICLE SIZE DISTRIBUTIONS FOR VARYING FROTH HEIGHTS. (RUN C) / Continued over...

FIG. 9. PARTICLE SIZE DISTRIBUTIONS.



GRAPH B2 Continued. COMPARISON OF PARTICLE SIZE DISTRIBUTIONS FOR VARYING

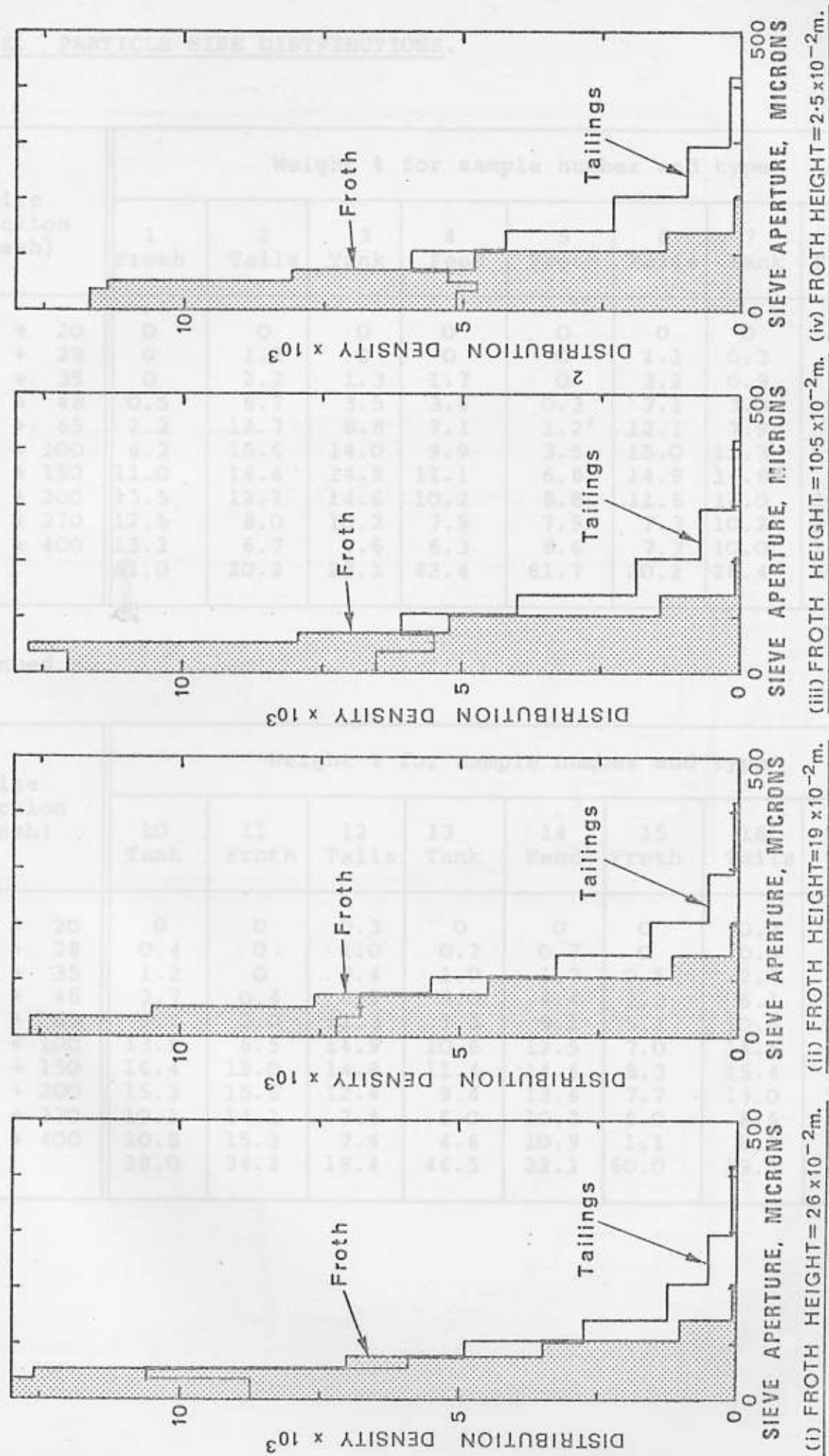
FROTH HEIGHTS. (RUN C)

RUN D. PARTICLE SIZE DISTRIBUTIONS.

| Size fraction (mesh) | Weight % for sample number and type | | | | | | |
|----------------------|-------------------------------------|---------|--------|--------|---------|---------|--------|
| | 1 Froth | 2 Tails | 3 Tank | 4 Feed | 5 Froth | 6 Tails | 7 Tank |
| + 20 | 0 | 0 | 0 | 0 | 0 | 0 | 0 |
| - 20 + 28 | 0 | 0 | 0 | 0 | 0 | 0 | 0 |
| - 28 + 35 | 0 | 1.2 | 0.3 | 0.6 | 0 | 0.8 | 0.2 |
| - 35 + 48 | 0 | 3.3 | 1.1 | 1.3 | 0 | 1.7 | 0.9 |
| - 48 + 65 | 0.1 | 8.1 | 4.2 | 4.2 | 0 | 5.5 | 3.8 |
| - 65 + 100 | 1.1 | 13.3 | 10.3 | 9.8 | 0.8 | 11.7 | 10.0 |
| -100 + 150 | 6.0 | 18.4 | 17.1 | 15.4 | 6.2 | 17.2 | 16.7 |
| -150 + 200 | 14.4 | 18.1 | 21.9 | 19.0 | 16.0 | 18.7 | 19.4 |
| -200 + 270 | 16.7 | 10.9 | 12.2 | 12.5 | 16.4 | 11.4 | 13.9 |
| -270 + 400 | 17.2 | 7.4 | 9.2 | 11.8 | 15.0 | 8.4 | 10.9 |
| - 400 | 44.5 | 19.3 | 23.7 | 25.4 | 45.6 | 24.6 | 24.2 |

continued -

| Size fraction (mesh) | Weight % for sample number and type | | | | | | |
|----------------------|-------------------------------------|---------|---------|---------|----------|----------|---------|
| | 8 Froth | 9 Tails | 10 Tank | 11 Feed | 12 Froth | 13 Tails | 14 Tank |
| + 20 | 0 | 0 | 0 | 0 | 0 | 0 | 0 |
| - 20 + 28 | 0 | 0 | 0 | 0 | 0 | 0 | 0 |
| - 28 + 35 | 0 | 0.6 | 0.2 | 0.1 | 0 | 0.8 | 0.3 |
| - 35 + 48 | 0 | 1.3 | 0.6 | 0.4 | 0 | 1.7 | 0.5 |
| - 48 + 65 | 0 | 4.2 | 2.5 | 1.6 | 0 | 4.5 | 2.1 |
| - 65 + 100 | 0.7 | 9.8 | 7.1 | 4.6 | 0.7 | 8.1 | 5.7 |
| -100 + 150 | 5.3 | 14.7 | 13.8 | 9.4 | 4.7 | 12.1 | 10.8 |
| -150 + 200 | 13.7 | 17.2 | 17.2 | 14.3 | 10.5 | 15.0 | 14.9 |
| -200 + 270 | 15.6 | 14.1 | 14.8 | 14.1 | 14.4 | 12.1 | 14.4 |
| -270 + 400 | 16.0 | 10.5 | 13.3 | 15.8 | 19.5 | 16.3 | 12.9 |
| - 400 | 48.7 | 27.6 | 30.5 | 39.7 | 50.2 | 33.7 | 37.1 |



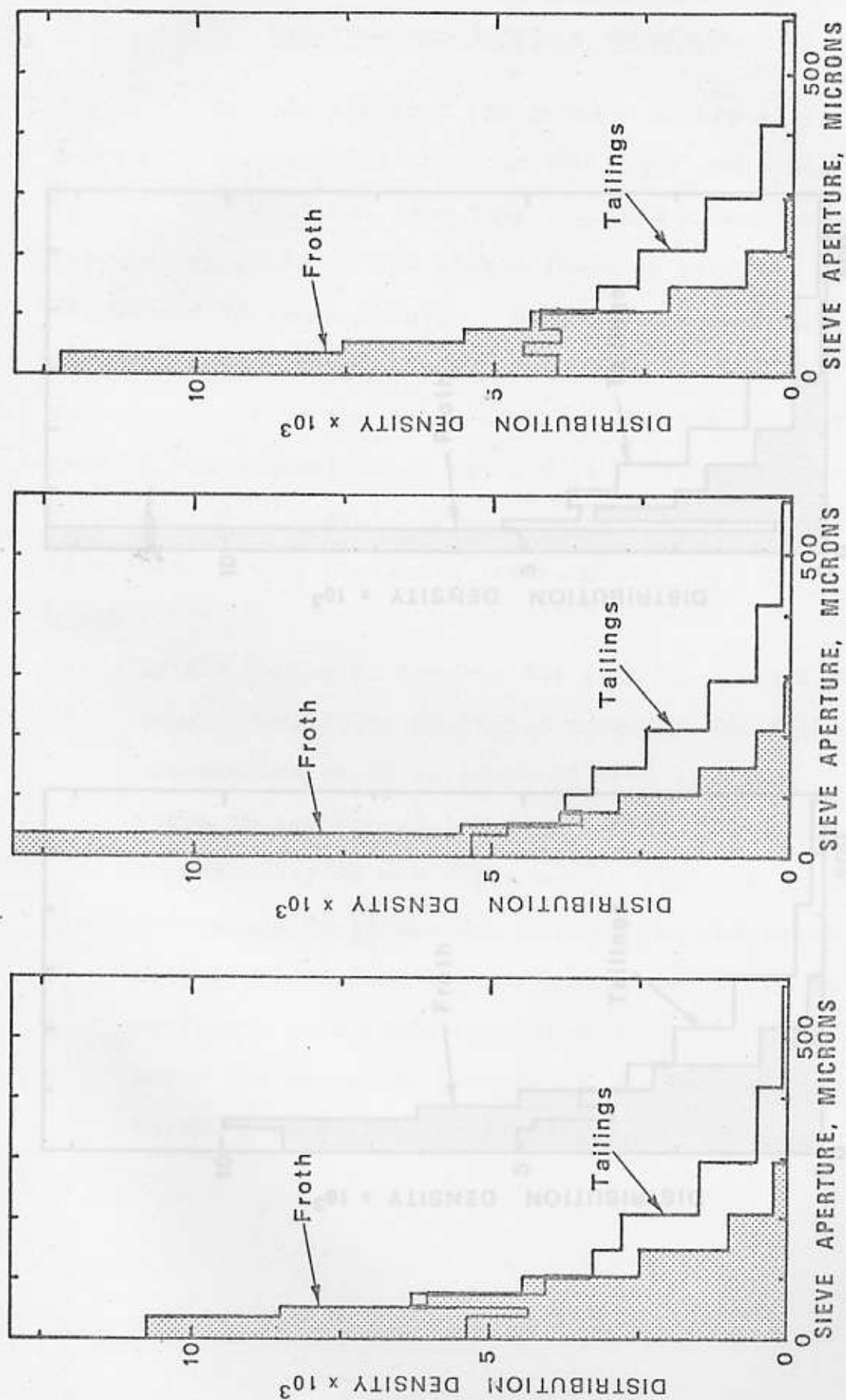
GRAPH B3. COMPARISON OF PARTICLE SIZE DISTRIBUTIONS FOR VARYING FROTH HEIGHTS. (RUN D)

RUN E. PARTICLE SIZE DISTRIBUTIONS.

| Size fraction (mesh) | Weight % for sample number and type | | | | | | | | |
|----------------------|-------------------------------------|---------|--------|--------|---------|---------|--------|---------|---------|
| | 1 Froth | 2 Tails | 3 Tank | 4 Feed | 5 Froth | 6 Tails | 7 Tank | 8 Froth | 9 Tails |
| + 20 | 0 | 0 | 0 | 0 | 0 | 0 | 0 | 0 | 0.4 |
| - 20 + 28 | 0 | 1.2 | 0 | 0 | 0 | 1.1 | 0.3 | 0 | 1.2 |
| - 28 + 35 | 0 | 2.2 | 1.3 | 1.7 | 0 | 3.2 | 0.9 | 0 | 3.8 |
| - 35 + 48 | 0.5 | 6.7 | 3.5 | 3.4 | 0.3 | 7.1 | 3.2 | 0.3 | 7.3 |
| - 48 + 65 | 2.2 | 12.7 | 8.8 | 7.1 | 1.2 | 12.1 | 7.9 | 1.5 | 13.3 |
| - 65 + 100 | 6.2 | 15.6 | 14.0 | 9.9 | 3.5 | 15.0 | 12.3 | 4.7 | 15.9 |
| -100 + 150 | 11.0 | 14.6 | 14.9 | 11.1 | 6.8 | 14.9 | 14.8 | 9.4 | 15.1 |
| -150 + 200 | 13.5 | 12.1 | 14.6 | 10.2 | 8.8 | 11.8 | 14.0 | 13.1 | 12.9 |
| -200 + 270 | 12.5 | 8.0 | 10.2 | 7.9 | 7.9 | 7.3 | 10.2 | 11.4 | 8.2 |
| -270 + 400 | 13.1 | 6.7 | 9.6 | 6.3 | 8.6 | 7.3 | 10.0 | 12.8 | 6.9 |
| - 400 | 41.0 | 20.2 | 23.1 | 42.4 | 61.7 | 20.2 | 26.4 | 46.8 | 15.0 |

continued -

| Size fraction (mesh) | Weight % for sample number and type | | | | | | | |
|----------------------|-------------------------------------|----------|----------|---------|---------|----------|----------|---------|
| | 10 Tank | 11 Froth | 12 Tails | 13 Tank | 14 Feed | 15 Froth | 16 Tails | 17 Tank |
| + 20 | 0 | 0 | 0.3 | 0 | 0 | 0 | 0.3 | 0 |
| - 20 + 28 | 0.4 | 0 | 1.0 | 0.2 | 0.7 | 0 | 0.9 | 0.1 |
| - 28 + 35 | 1.2 | 0 | 3.4 | 1.0 | 1.7 | 0.5 | 2.7 | 0.5 |
| - 35 + 48 | 3.7 | 0.4 | 6.7 | 3.0 | 4.4 | 2.3 | 6.1 | 1.6 |
| - 48 + 65 | 9.2 | 2.0 | 12.3 | 7.3 | 9.1 | 5.1 | 10.6 | 5.5 |
| - 65 + 100 | 13.9 | 6.5 | 14.9 | 10.6 | 12.5 | 7.0 | 14.5 | 11.4 |
| -100 + 150 | 16.4 | 12.0 | 14.8 | 11.4 | 14.6 | 8.3 | 15.4 | 15.9 |
| -150 + 200 | 15.3 | 15.5 | 12.4 | 9.4 | 13.6 | 7.7 | 13.0 | 14.9 |
| -200 + 270 | 10.1 | 14.1 | 7.4 | 6.0 | 10.3 | 8.0 | 8.6 | 10.5 |
| -270 + 400 | 10.8 | 15.3 | 7.4 | 4.6 | 10.9 | 1.1 | 8.0 | 10.6 |
| - 400 | 19.0 | 34.2 | 19.4 | 46.5 | 22.2 | 60.0 | 19.1 | 29.0 |

(i) FROTH HEIGHT = $2 \times 10^{-2} \text{ m}$.(ii) FROTH HEIGHT = $4.5 \times 10^{-2} \text{ m}$.(iii) FROTH HEIGHT = $9 \times 10^{-2} \text{ m}$.

GRAPH B4 COMPARISON OF PARTICLE SIZE DISTRIBUTIONS FOR VARYING

FROTH HEIGHTS (RUN E)

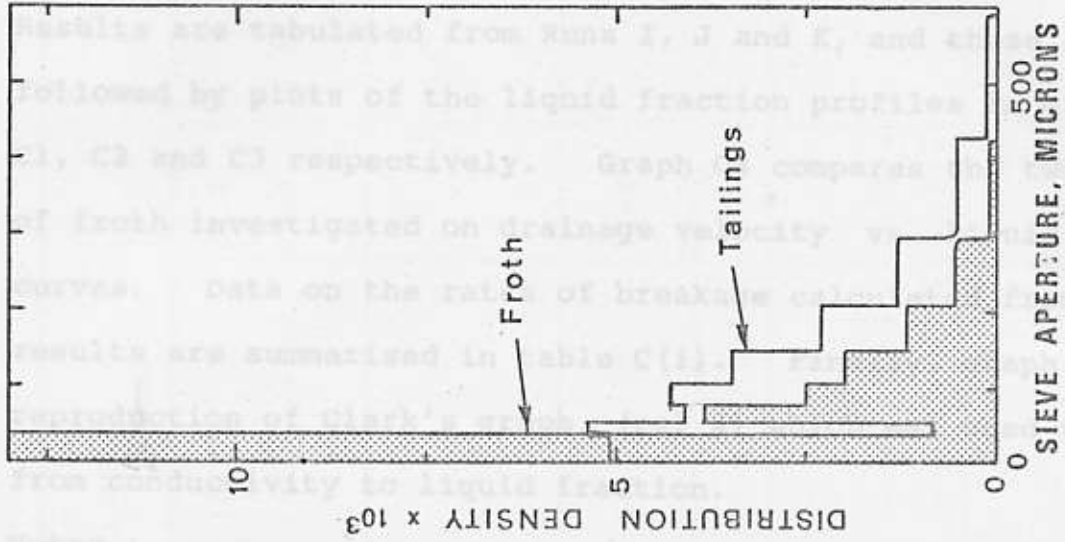
/Continued over...

APPENDIX C

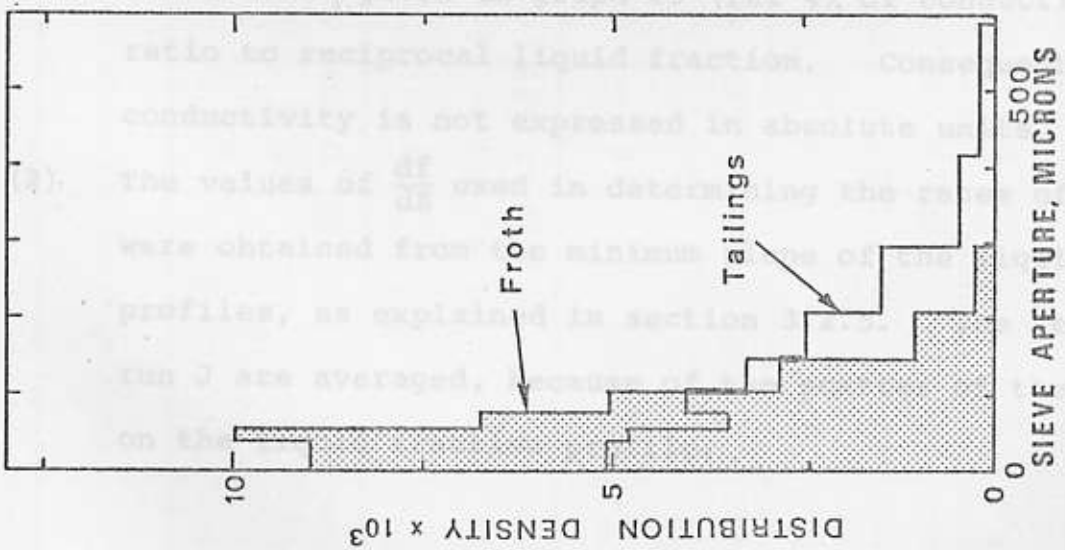
RESULTS OF CONDUCTIVITY MEASUREMENTS ON FROTH : LIQUID FRACTION

PROFILES AND RATES OF BREAKAGE.

In this section, the results of the electrical conductivity measurements taken on the froth are presented.



(v) FROTH HEIGHT = $24 \times 10^{-2} \text{ m}$.



(iv) FROTH HEIGHT = $16 \times 10^{-2} \text{ m}$.

GRAPH B4 Continued. COMPARISON OF PARTICLE SIZE DISTRIBUTIONS FOR VARYING FROTH HEIGHTS. (RUN E)

APPENDIX CRESULTS OF CONDUCTIVITY MEASUREMENTS ON FROTH : LIQUID FRACTION
PROFILES AND RATES OF BREAKAGE.

In this section, the results of the electrical conductivity measurements taken on the froth are presented. Results are tabulated from Runs I, J and K, and these are followed by plots of the liquid fraction profiles in graphs C1, C2 and C3 respectively. Graph C4 compares the two types of froth investigated on drainage velocity vs. liquid fraction curves. Data on the rates of breakage calculated from these results are summarised in table C(i). Finally, graph C5 is a reproduction of Clark's graph, (ref 4) which was used to convert from conductivity to liquid fraction.

Notes :

- (1) In the tables of results for runs I, J and K, the conversion from conductivity to liquid fraction was done via Clark's correlation, given in graph C5 (ref 4), of conductivity ratio to reciprocal liquid fraction. Consequently the conductivity is not expressed in absolute units.
- (2) The values of $\frac{df}{dz}$ used in determining the rates of breakage were obtained from the minimum slope of the liquid fraction profiles, as explained in section 3.2.5. The results for run J are averaged, because of the scatter of the points on the liquid fraction profile.

Run done on depressed silica slurry, using Dowfroth 250 as frother
Additives: 30 mls HF (to depress silica), 25 mls Dowfroth 250.

| Conductivity of bulk solution = 250 units | | | | | | | | | | | Total froth height $m \times 10^2$ | Q_A/A $m/s \times 10^2$ | Q_W/A $m/s \times 10^2$ |
|---|-------|-------|-------|-------|-------|-------|-------|-------|-------|------|---|------------------------------|------------------------------|
| 1. Depth below weir $metres \times 10^2$ | 0 | 2.5 | 5 | 7.5 | 10 | 12.5 | 15 | 17.5 | 20 | 23.5 | 1.10 | 0.01155 | |
| Mean conductivity | 15.1 | 19.3 | 20.0 | 21.2 | 22.7 | 24.3 | 26.0 | 28.0 | 29.8 | | | | |
| f, liquid fraction | 0.122 | 0.149 | 0.152 | 0.159 | 0.167 | 0.175 | 0.185 | 0.196 | 0.204 | | | | |
| 2. Depth below weir $metres \times 10^2$ | 0 | 1 | 2 | 3 | 4 | 5 | | | | 7.0 | 1.10 | 0.0344 | |
| Mean conductivity | 17.2 | 21.8 | 24.3 | 26.2 | 27.3 | 29.2 | | | | | | | |
| f, liquid fraction | 0.137 | 0.159 | 0.175 | 0.185 | 0.192 | 0.204 | | | | | | | |
| 3. Depth below weir $metres \times 10^2$ | 0 | 2.5 | 5 | 7.5 | 10 | 12.5 | 15 | 17.5 | | 21.5 | 1.80 | 0.0210 | |
| Mean conductivity | 16.2 | 20.8 | 22.1 | 23.1 | 24.2 | 25.0 | 27.3 | 29.9 | | | | | |
| f, liquid fraction | 0.128 | 0.156 | 0.161 | 0.172 | 0.175 | 0.179 | 0.189 | 0.204 | | | | | |
| 4. Depth below weir $metres \times 10^2$ | 0 | 1 | 2 | 3 | 4 | 5 | 6 | 7 | | 10.0 | 1.80 | 0.0427 | |
| Mean conductivity | 17.2 | 19.7 | 21.4 | 23.3 | 23.9 | 24.5 | 25.9 | 28.0 | | | | | |
| f, liquid fraction | 0.135 | 0.149 | 0.159 | 0.172 | 0.175 | 0.179 | 0.181 | 0.196 | | | | | |
| 5. Depth below weir $metres \times 10^2$ | 0 | 1 | 2 | 3 | | | | | | 5.0 | 1.80 | 0.0554 | |
| Mean conductivity | 18.6 | 23.6 | 27.7 | 29.7 | | | | | | | | | |
| f, liquid fraction | 0.143 | 0.172 | 0.192 | 0.204 | | | | | | | | | |

Run done on apatite ore, but only one froth level used. The three sets of measurements were taken at different times. Continuous mixing of slurry.

Data: Temperature controlled 34°C, Unitol feed 0.104 ml/sec., Na Silicate 0.161 ml/sec., Slurry feed setting 4.5×10^{-4} m³/sec., air rate 1.08×10^{-3} m³/sec., $Q_A/A = 0.0175$ m/sec., froth height = 0.24 m to weir, Conductivity of bulk solution = 1040 units.

| Sample Number | Sample Type | Solids flow Kg/sec $\times 10^3$ | Water flow m ³ /sec $\times 10^6$ | Solids conc. Wt. % | Grade % P ₂ O ₅ | Q _w /A m/sec $\times 10^4$ |
|---------------|-------------|----------------------------------|--|--------------------|---------------------------------------|---------------------------------------|
| 1 | Froth Tank | 10.9 | 37.2 | 22.6 | 14.2 | 6.03 |
| 2 | Froth | 12.7 | 38.7 | 14.3 | 6.25 | 6.26 |
| 3 | Froth | 17.3 | 46.5 | 24.6 | 14.4 | 7.50 |
| | | | | 27.1 | 15.4 | |

| Depth below weir m $\times 10^2$ | 0 | 1 | 2.5 | 5 | 7.5 | 10 | 12.5 | 15 | 17.5 | 20 | 22.5 |
|----------------------------------|--------|--------|--------|--------|-------|--------|--------|--------|--------|-------|--------|
| 1. Conductivity units | 32 | 38 | 37 | 47 | 49 | 51 | 53 | 50 | 54 | 59 | 61 |
| f=liquid fraction | 0.0695 | 0.0800 | 0.0787 | 0.0862 | 0.099 | 0.103 | 0.1065 | 0.102 | 0.1075 | 0.116 | 0.119 |
| 2. Conductivity units | 40 | 48 | 50 | 46 | 53 | 54 | 55 | 55 | 55 | 56 | 61 |
| f=liquid fraction | 0.0834 | 0.098 | 0.102 | 0.094 | 0.106 | 0.1075 | 0.110 | 0.110 | 0.110 | 0.111 | 0.118 |
| 3. Conductivity units | 42 | 48 | 56 | 62 | 65 | 64 | 60 | 64 | 66 | 68 | 66 |
| f=liquid fraction | 0.0878 | 0.098 | 0.111 | 0.1205 | 0.127 | 0.1235 | 0.1165 | 0.1235 | 0.1265 | 0.128 | 0.1265 |

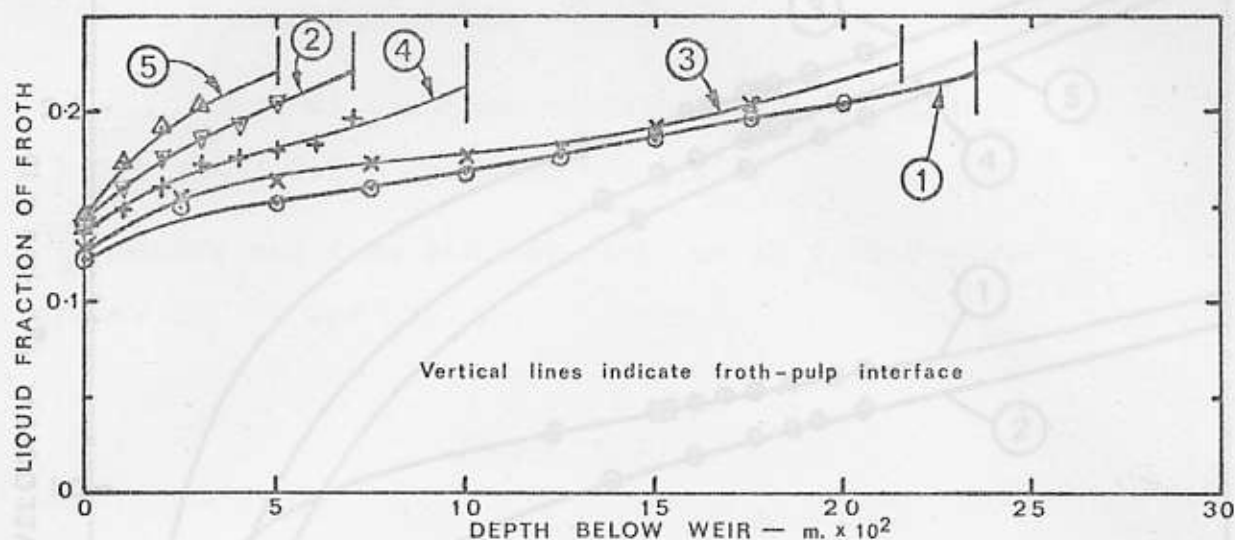
RUN K

Run done on apatite ore (see results in appendix A for further data).

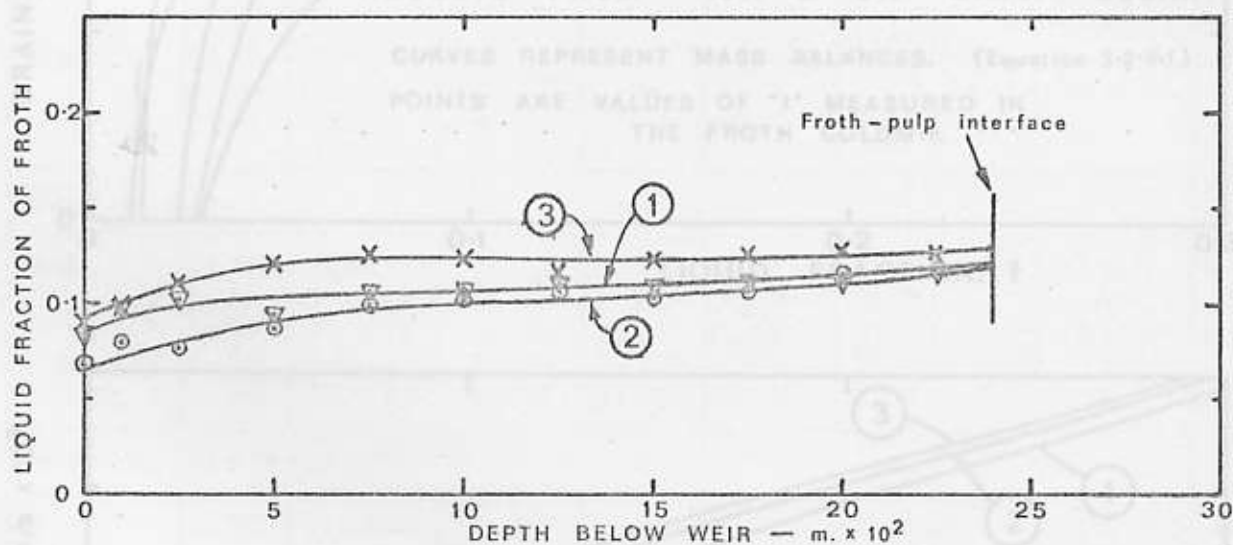
Data: $Q_A/A = 0.0134$ m/sec. Conductivity of bulk solution = 1260 units.

| Number | Froth Height $m \times 10^2$ | Q_w/A m/sec $\times 10^4$ | Corresponding sample nos. in appendix A |
|--------|---------------------------------|--------------------------------|--|
| 1 | 25 | 4.15 | 2, 3 |
| 2 | 10 | 3.05 | 4, 5 |
| 3 | 23 | 2.60 | 7, 8 |

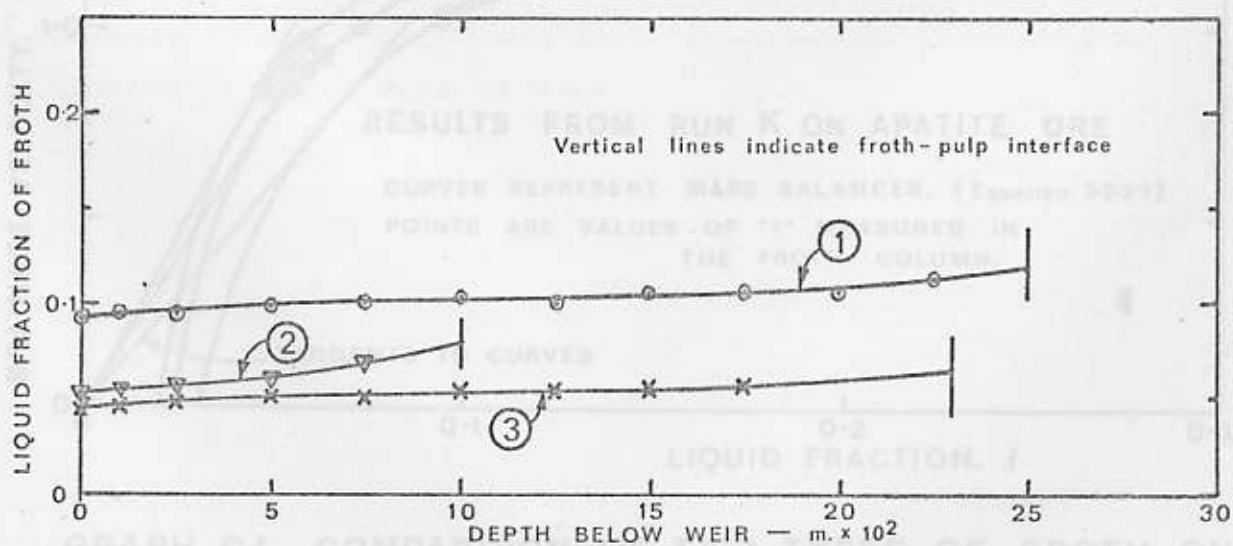
| Depth below weir, $m \times 10^{2+}$ | 0 | 1 | 2.5 | 5 | 7.5 | 10 | 12.5 | 15 | 17.5 | 20 | 22.5 |
|--|----------------|----------------|----------------|----------------|--------------|--------------|--------------|--------------|----------------|--------------|-------------|
| 1. Mean conductivity f, liquid fraction | 55 0.0935 | 57 0.0960 | 57 0.0960 | 60 0.100 | 61 0.102 | 62 0.104 | 61 0.102 | 64 0.1065 | 65 0.1075 | 65 0.1075 | 70 0.114 |
| 2. Mean conductivity f, liquid fraction | 27.5 0.0535 | 28.5 0.0546 | 31 0.0581 | 34 0.0625 | 40 0.0715 | | | | | | |
| 3. Mean conductivity f, liquid fraction | 22 0.0454 | 23.5 0.0476 | 24.5 0.0493 | 27.5 0.0532 | 27 0.0524 | 29 0.0552 | 29 0.0552 | 29 0.0552 | 29.5 0.0562 | 30 0.0568 | |



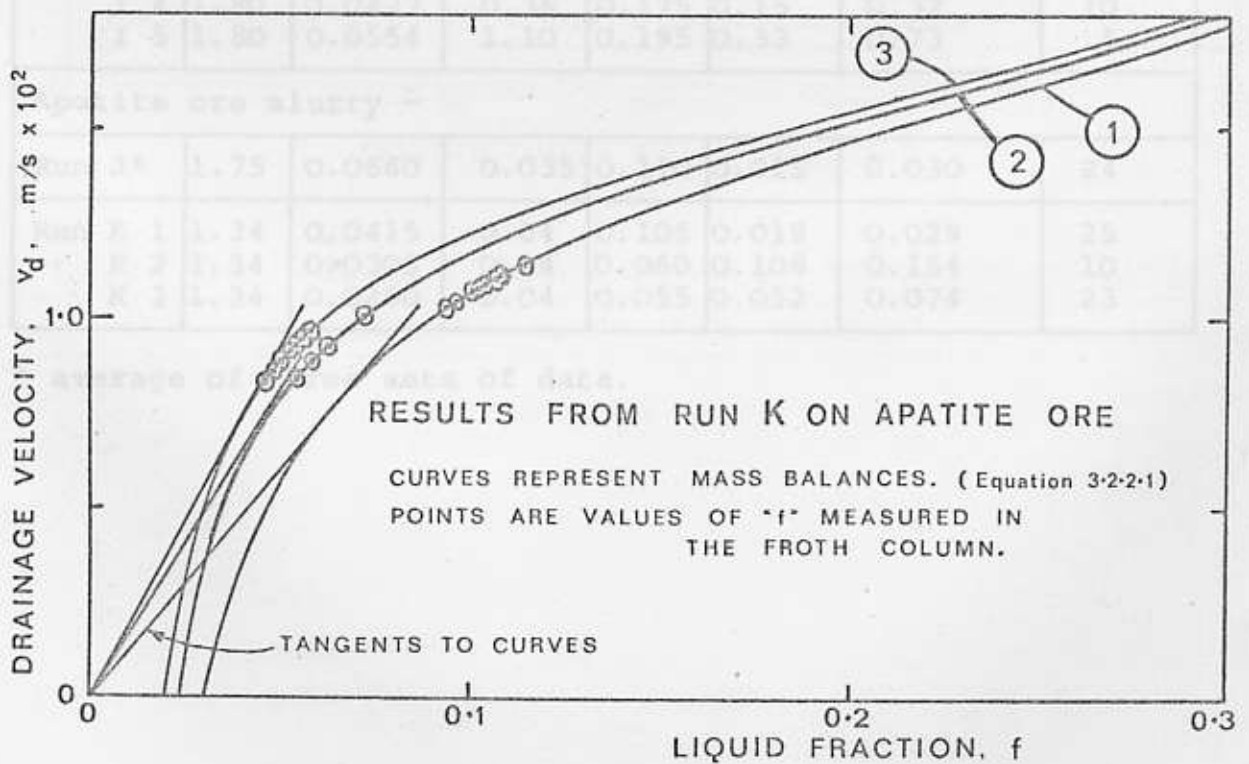
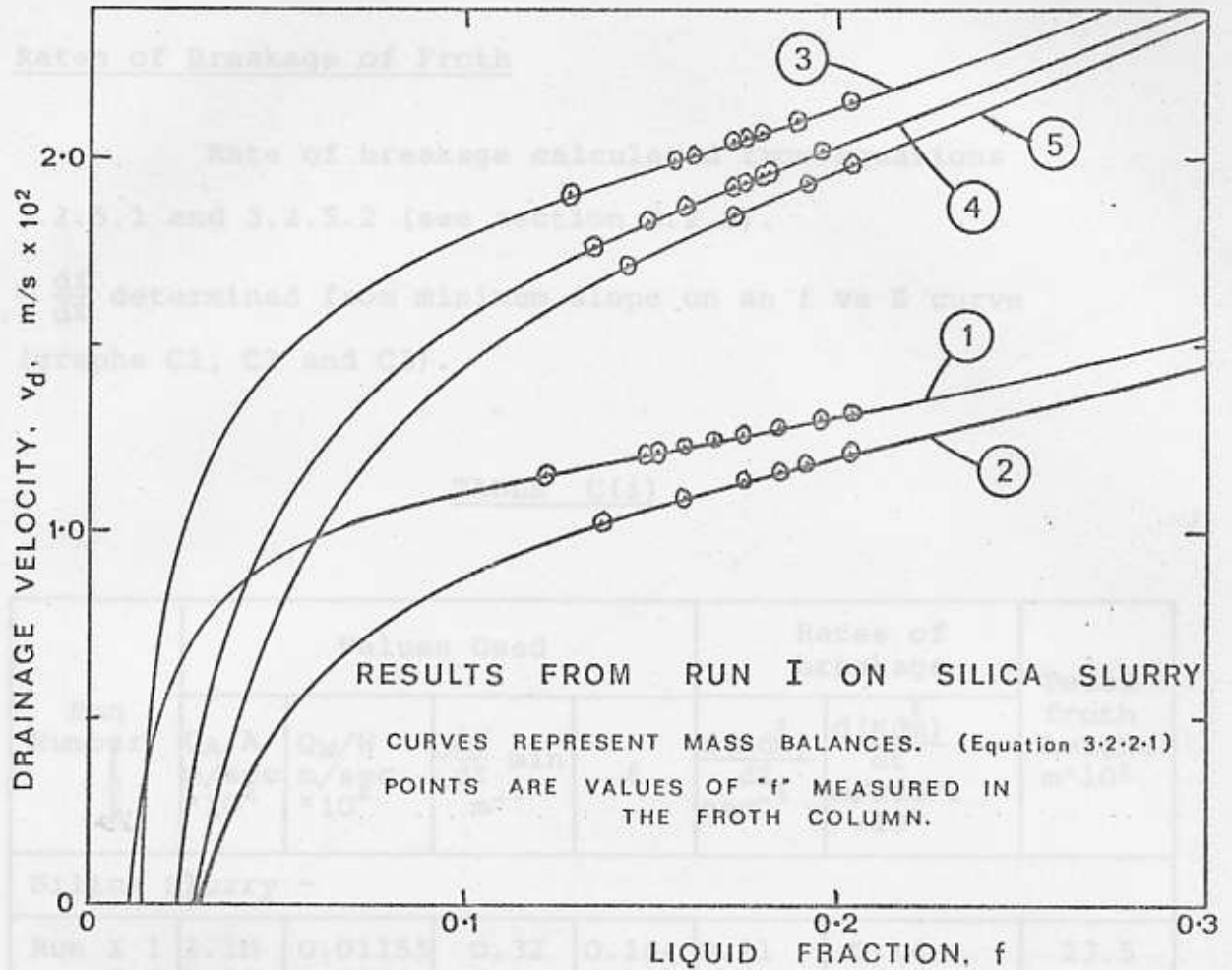
GRAPH C1. LIQUID FRACTION PROFILES FOR RUN I
(Silica Slurry)



GRAPH C2. LIQUID FRACTION PROFILES FOR RUN J
(Apatite Ore Slurry)



GRAPH C3. LIQUID FRACTION PROFILES FOR RUN K
(Apatite Ore Slurry)



GRAPH C4. COMPARISON OF TWO TYPES OF FROTH ON
A v_d vs f PLOT.

Rates of Breakage of Froth

Rate of breakage calculated from equations
3.2.5.1 and 3.2.5.2 (see section 3.2.5).

- $\frac{df}{dz}$ determined from minimum slope on an f vs Z curve
(graphs C1, C2 and C3).

TABLE C(i)

| Run Number | Values Used | | | | Rates of breakage | | Total froth height $m \times 10^2$ |
|----------------------|--------------------------------|--------------------------------|------------------------------------|-------|--------------------------------------|--|---------------------------------------|
| | Q_A/A $m/sec \times 10^2$ | Q_W/W $m/sec \times 10^2$ | $\frac{df}{dz} \frac{min}{m^{-1}}$ | f | $\frac{d(Kd_m^2)}{dz}$ sec^{-1} | $\frac{d(Kd_m^2)}{dt}$ $m/sec^{-2} \times 10^2$ | |
| Silica Slurry - | | | | | | | |
| Run I 1 | 1.10 | 0.01155 | 0.32 | 0.164 | 0.11 | 0.14 | 23.5 |
| I 2 | 1.10 | 0.0344 | 0.90 | 0.19 | 0.17 | 0.23 | 7 |
| I 3 | 1.80 | 0.0210 | 0.20 | 0.17 | 0.10 | 0.22 | 21.5 |
| I 4 | 1.80 | 0.0427 | 0.36 | 0.175 | 0.15 | 0.32 | 10 |
| I 5 | 1.80 | 0.0554 | 1.10 | 0.195 | 0.33 | 0.73 | 5 |
| Apatite ore slurry - | | | | | | | |
| Run J* | 1.75 | 0.0660 | 0.035 | 0.110 | 0.015 | 0.030 | 24 |
| Run K 1 | 1.34 | 0.0415 | 0.04 | 0.105 | 0.019 | 0.029 | 25 |
| K 2 | 1.34 | 0.0305 | 0.14 | 0.060 | 0.108 | 0.154 | 10 |
| K 3 | 1.34 | 0.0260 | 0.04 | 0.055 | 0.052 | 0.074 | 23 |

* average of three sets of data.

APPENDIX D

| SAMPLE NO. | FROTH HEIGHT IN. x 10 ² |
|------------|------------------------------------|
| 2 | 25 |
| 3 | 4.5 |
| 4 | 10.5 |
| 5 | 11 |
| 6 | 23 |
| 7 | 25 |
| 8 | 25 |

ENTRAINMENT STUDY

This appendix presents the results of the work done to investigate entrainment of solids by the froth.

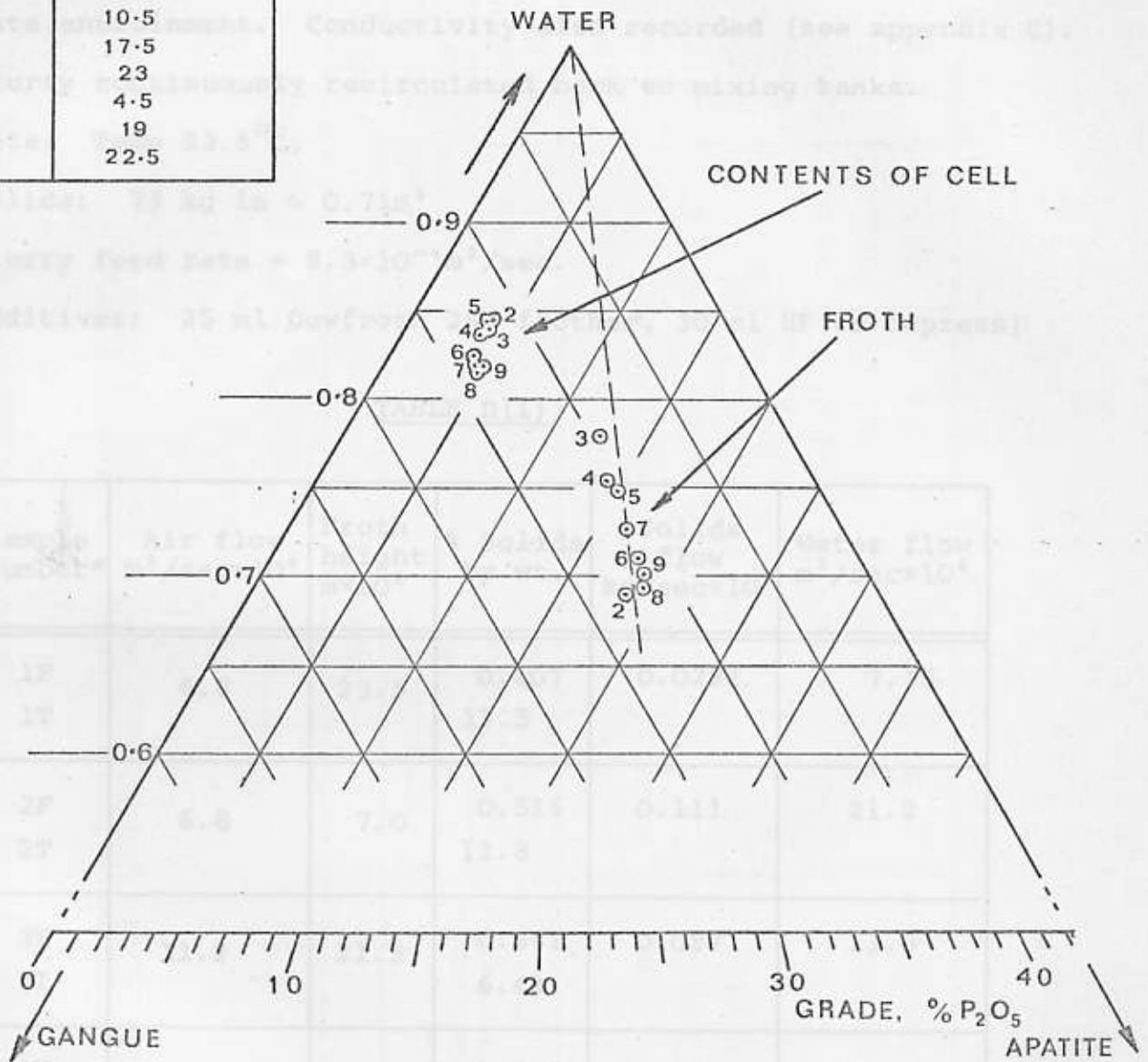
Graph D1 shows the results from run F (data from appendix A) plotted on a triangular diagram of water-gangue-apatite, to determine whether entrainment was a noticeable effect of froth height.

The results of one run, Run I, done specifically to investigate entrainment, are also presented. This run used a silica slurry depressed with hydrofluoric acid, so that flotation effects would be minimal. In graph D2, the entrainment fraction (see section 3.3.2) determined experimentally is compared with the theoretical curve on a plot against particle size.



GRAPH D1. RESULTS FROM RUN F PLOTTED ON A
TRIANGULAR DIAGRAM.

| SAMPLE NO | FROTH HEIGHT m. x 10 ² |
|-----------|--------------------------------------|
| 2 | 23 |
| 3 | 4.5 |
| 4 | 10.5 |
| 5 | 17.5 |
| 6 | 23 |
| 7 | 4.5 |
| 8 | 19 |
| 9 | 22.5 |



GRAPH D1. RESULTS FROM RUN F PLOTTED ON A
TRIANGULAR DIAGRAM.

RUN I

Experiment using depressed silica slurry to investigate entrainment. Conductivity also recorded (see appendix C). Slurry continuously recirculated back to mixing tanks.

Data: Temp 23.5°C,

Solids: 73 kg in ~ 0.71m³

Slurry feed rate = 8.3×10^{-4} m³/sec.

Additives: 25 ml Dowfroth 250 frother, 30 ml HF (to depress)

TABLE D(i)

| Sample number* | Air flow m ³ /sec × 10 ⁴ | Froth height m × 10 ² | % Solids by wt. | Solids flow kg/sec × 10 ³ | Water flow m ³ /sec × 10 ⁶ |
|----------------|---|-------------------------------------|--------------------|---|---|
| 1F 1T | 6.8 | 23.5 | 0.407 12.5 | 0.0292 | 7.15 |
| 2F 2T | 6.8 | 7.0 | 0.516 11.8 | 0.111 | 21.2 |
| 3F 3T | 11.2 | 21.5 | 0.661 6.42 | 0.087 | 13.0 |
| 4F 4T | 11.2 | 10.0 | 0.709 7.46 | 0.187 | 26.5 |
| 5F 5T | 11.2 | 5.0 | 1.230 8.02 | 0.282 | 34.4 |

* F = froth, T = tank.

Data on particle size distributions and entrainment fractions for samples 3, 4, 5 (i.e. for high air flows) are shown overleaf.

RUN I continued

In the following table, the entrainment fraction for each size range was calculated from:

$$E_D = \frac{\text{Wt. \% in size range in froth solids}}{\text{Wt. \% in size range in tank solids}} \times \frac{\% \text{ solids in froth}}{\% \text{ solids in tank}}$$

TABLE D(ii)

| Size fraction (U.S. Standard Sieves). | Sample 3 | | | Sample 4 | | | Sample 5 | | |
|---------------------------------------|-----------------------------|--------------|----------------------------|-----------------------------|--------------|----------------------------|-----------------------------|--------------|----------------------------|
| | Particle size distributions | | Entrainment fraction E_D | Particle size distributions | | Entrainment fraction E_D | Particle size distributions | | Entrainment fraction E_D |
| | Froth (Wt. %) | Tank (Wt. %) | | Froth (Wt. %) | Tank (Wt. %) | | Froth (Wt. %) | Tank (Wt. %) | |
| + 50 | 0 | 0.83 | 0 | 0 | 0.68 | 0 | 0.8 | 0.5 | |
| - 50+ 70 | 1.54 | 8.03 | 0.0198 | 1.2 | 5.88 | 0.019 | 1.7 | 6.3 | 0.041 |
| - 70+100 | 10.75 | 19.25 | 0.0574 | 4.7 | 17.22 | 0.026 | 4.1 | 17.7 | 0.043 |
| -100+140 | 15.4 | 23.40 | 0.0677 | 9.4 | 23.10 | 0.039 | 7.4 | 23.3 | 0.049 |
| -140+200 | 12.3 | 20.10 | 0.0630 | 14.1 | 20.90 | 0.071 | 10.8 | 21.3 | 0.078 |
| -200+270 | 12.3 | 16.75 | 0.0757 | 18.8 | 15.70 | 0.114 | 24.0 | 16.6 | 0.222 |
| -270+400 | 15.4 | 6.79 | 0.2335 | 17.6 | 8.06 | 0.207 | 22.3 | 7.2 | 0.475 |
| -400 | 32.3 | 4.85 | 0.685 | 34.1 | 8.47 | 0.383 | 29.0 | 7.3 | 0.610 |

RUN I continued

CALCULATION OF THEORETICAL ENTRAINMENT FRACTION

Formulae used: (see section 3.3.2)

$$E_D = \frac{(v_{\max} - u_s)^2}{2(v_{\max} - v_{\min})\bar{v}_i + (u_s - v_{\min})^2}$$

3.3.2.1

Stokes velocity, $u_s = \frac{D^2 g}{18\mu} (\rho_s - \rho_L)$ Where $v_{\max} = \frac{Q_A}{A(1-f)}$

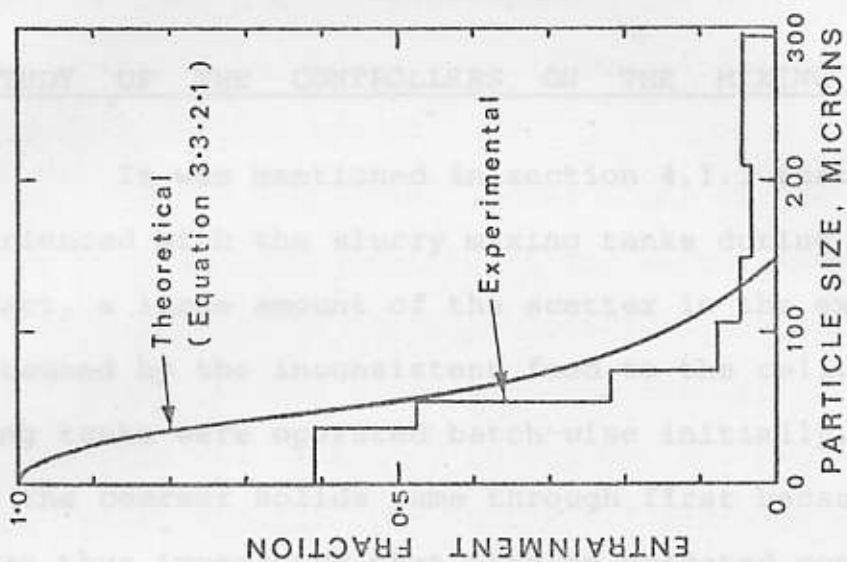
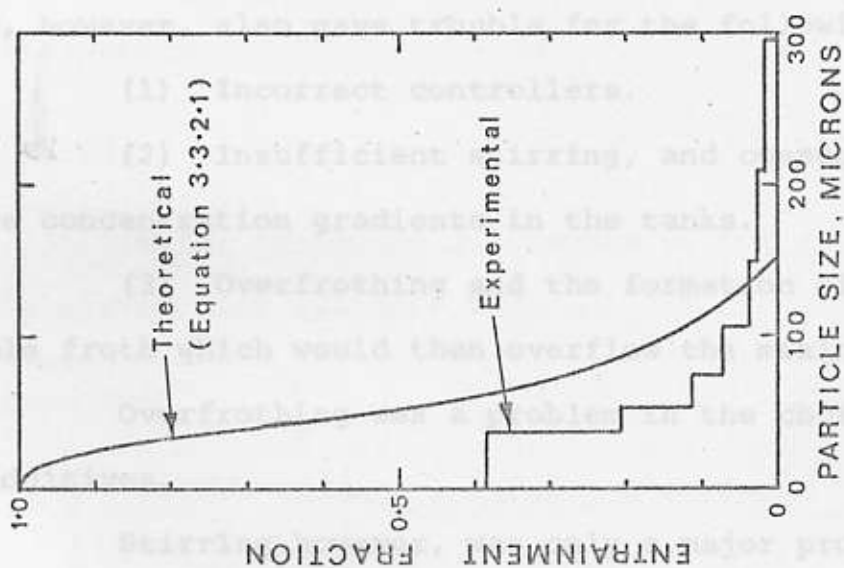
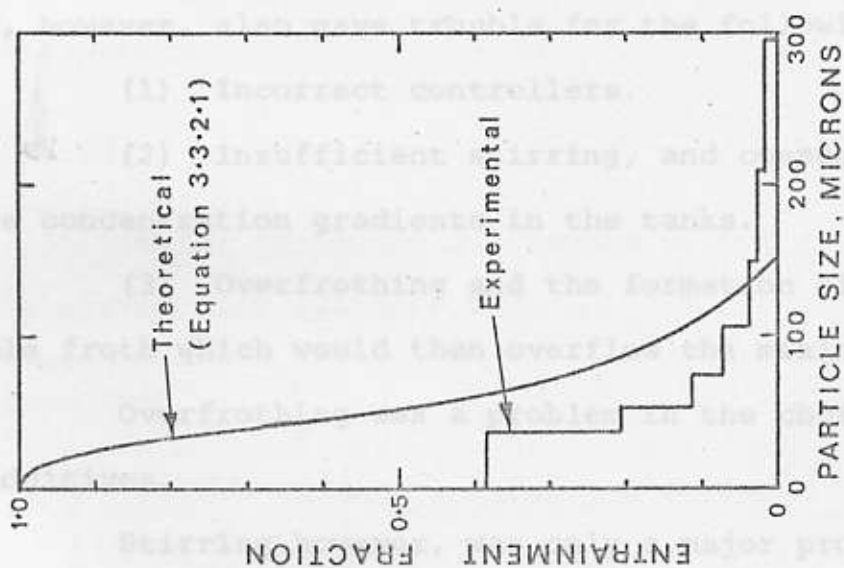
$$\bar{v}_i = \frac{Q_W}{Af}$$

$$v_{\min} = 2\bar{v}_i - v_{\max}$$

Values used:

TABLE D(iii)

| Sample number | Mean f over column | v_{\max} m/sec $\times 10^2$ | \bar{v}_i m/sec $\times 10^2$ | v_{\min} m/sec $\times 10^2$ | D m $\times 10^{-6}$ | u_s m/sec $\times 10^2$ | E_D |
|---------------|--------------------|-----------------------------------|------------------------------------|-----------------------------------|-------------------------|------------------------------|-------|
| 3 | 0.171 | 2.17 | 0.123 | -1.92 | 30 | 0.091 | 0.855 |
| | | | | | 50 | 0.339 | 0.549 |
| | | | | | 100 | 1.01 | 0.140 |
| | | | | | 147 | v_{\max} | 0 |
| 4 | 0.168 | 2.16 | 0.254 | -1.65 | 30 | 0.091 | 0.863 |
| | | | | | 50 | 0.339 | 0.561 |
| | | | | | 100 | 1.01 | 0.146 |
| | | | | | 146 | v_{\max} | 0 |
| 5 | 0.178 | 2.19 | 0.311 | -1.57 | 30 | 0.091 | 0.865 |
| | | | | | 50 | 0.339 | 0.571 |
| | | | | | 100 | 1.01 | 0.155 |
| | | | | | 148 | v_{\max} | 0 |

No.3. FROTH HEIGHT = $21.5 \times 10^2 \text{ m}$ No.4. FROTH HEIGHT = $10 \times 10^2 \text{ m}$ No.5. FROTH HEIGHT = $5 \times 10^2 \text{ m}$

GRAPH D2. ENTRAINMENT FRACTION vs. PARTICLE SIZE. COMPARISON AT VARIOUS

FROTH HEIGHTS. (RUN I.)

APPENDIX ESTUDY OF THE CONTROLLERS ON THE MIXING TANKS

It was mentioned in section 4.1.3 that much difficulty was experienced with the slurry mixing tanks during the experimentation. In fact, a large amount of the scatter in the experimental results was caused by the inconsistent feed to the cell. When the mixing tanks were operated batch-wise initially, it was found that the coarser solids came through first because of poor mixing. It was thus imperative that they be operated continuously. This, however, also gave trouble for the following three reasons:

- (1) Incorrect controllers.
- (2) Insufficient stirring, and consequently fairly large concentration gradients in the tanks.
- (3) Overfrothing and the formation of a rather stable froth which would then overflow the mixing tanks.

Overfrothing was a problem in the choice and quantity of additives.

Stirring however, was only a major problem when the system was not at a steady state. Oscillations (for example, in the level of liquid in the lower tank) caused a variation in the particle size distribution of the slurry leaving the mixing system. Unwanted oscillations are a result of a bad control system. It was noticed, even at the beginning, that the mixing tanks had difficulty in reaching a steady state condition.

Although the job of rebuilding the mixing tanks was a task beyond the scope of this investigation, it was

decided/....

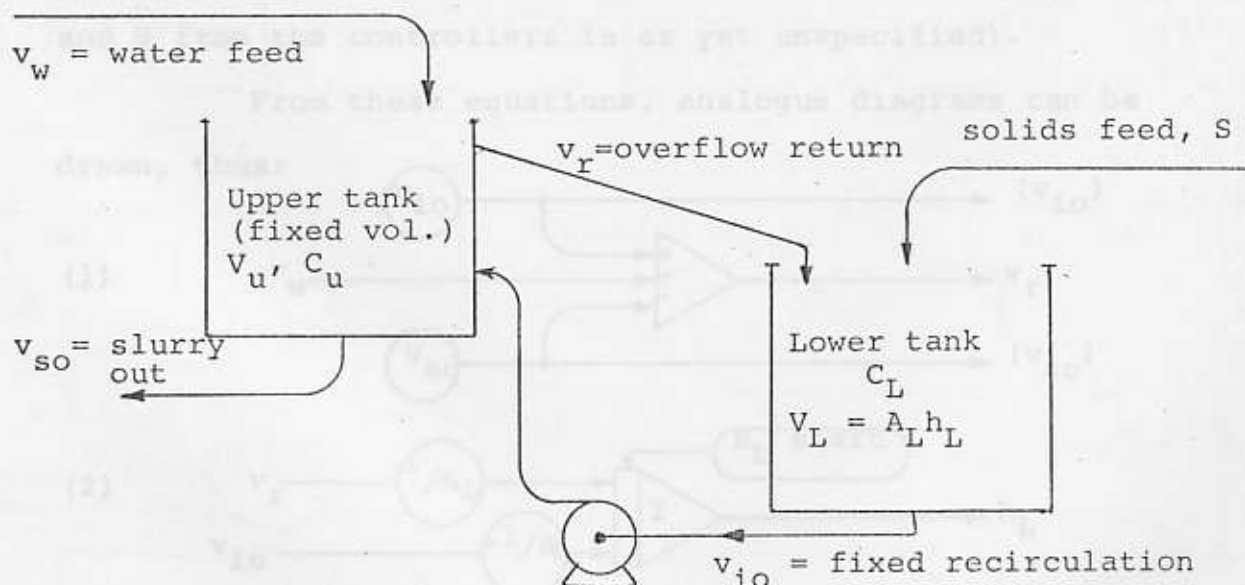
decided to make a short study of the controls to see whether it was possible to reduce some of the experimental scatter. Two approaches were tried:

(1) A simplified linear model of the system was used to give an understanding of the setup, and to form a basis for deciding on suitable modifications for improvement.

(2) A more exact analogue simulation of the system on a computer was then used to try out any predictions made by the linear model. The "C.S.M.P." analogue systems modelling program (reference 11) on the IBM 1130 was used for simulation.

Basic Model

(Refer to figure 3, chapter 4, for a general description of the mixing tank system).



(for nomenclature, see appendix G.)

Four equations, two liquid and two solids mass balances, can be written to describe the basic operation of the mixing tanks:

Liquid/...

Liquid balance over upper tank:

$$v_r = v_{io} + v_w - v_{so} \quad (1)$$

Liquid balance over lower tank:

$$A_L \frac{dh_L}{dt} = v_r - v_{io}$$

or
$$h_L = \frac{1}{A_L} \int (v_r - v_{io}) dt \quad (2)$$

Solids balance over lower tank:

$$S + v_r C_u = v_{io} C_L + \frac{d A_L h_L C_L}{dt}$$

or
$$h_L C_L = \frac{1}{A_L} \int (S + v_r C_u - v_{io} C_L) dt \quad (3)$$

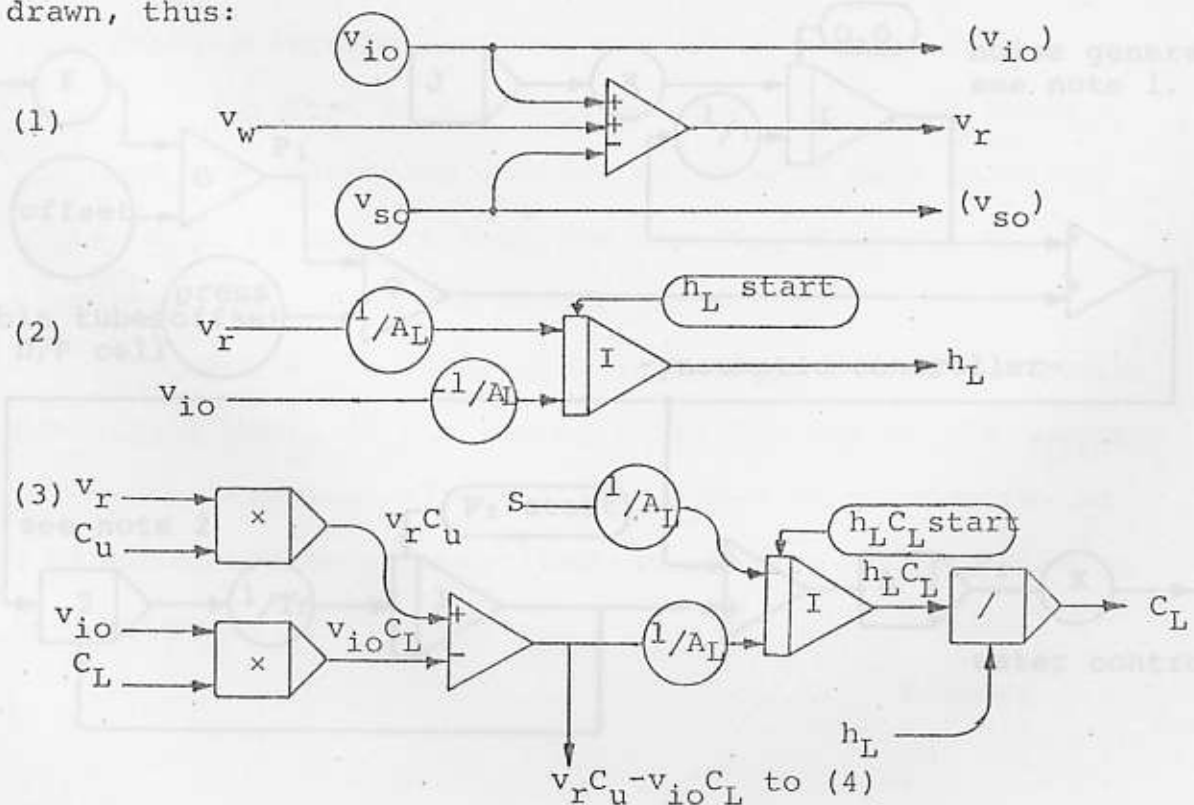
Solids balance over upper tank:

$$v_{io} C_L = (v_r + v_{so}) C_u + v_u \frac{dC_u}{dt}$$

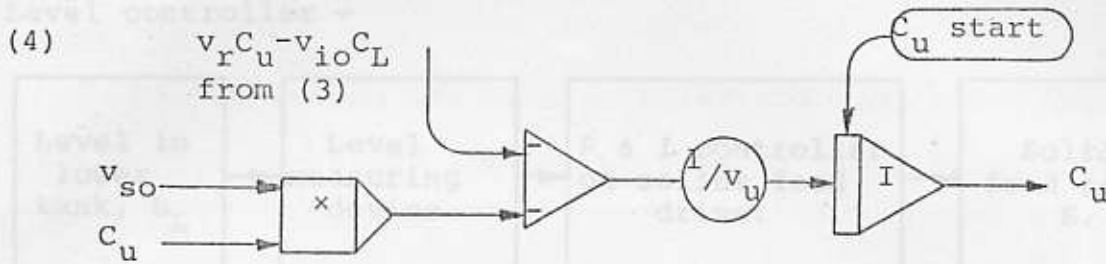
or
$$C_u = \frac{1}{v_u} \int (v_{io} C_L - (v_r + v_{so}) C_u) dt \quad (4)$$

(Note that these equations only model the tanks: they are incomplete in that the behaviour of the input variables v_w and S from the controllers is as yet unspecified).

From these equations, analogue diagrams can be drawn, thus:



(4)/...

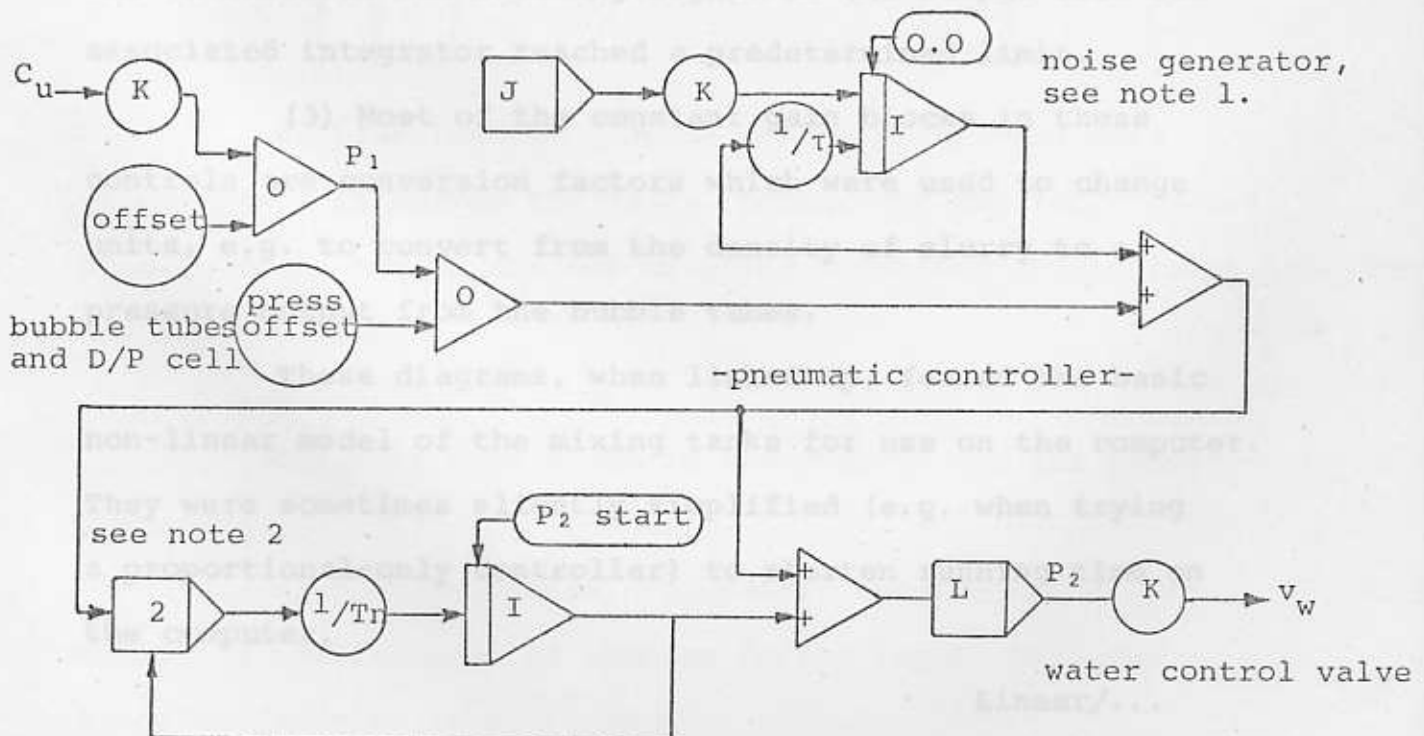
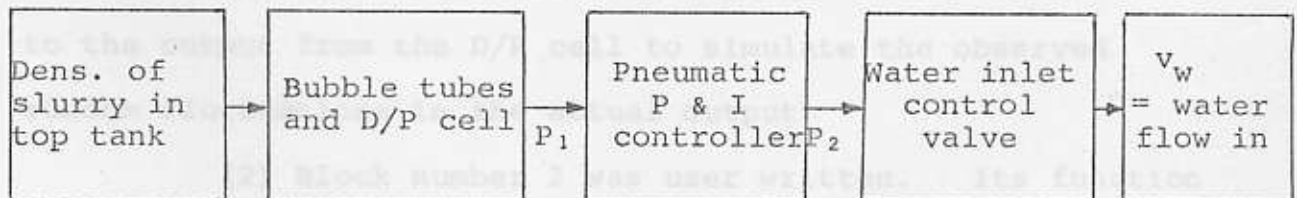


(For meaning of symbols, refer to appendix G page G3).

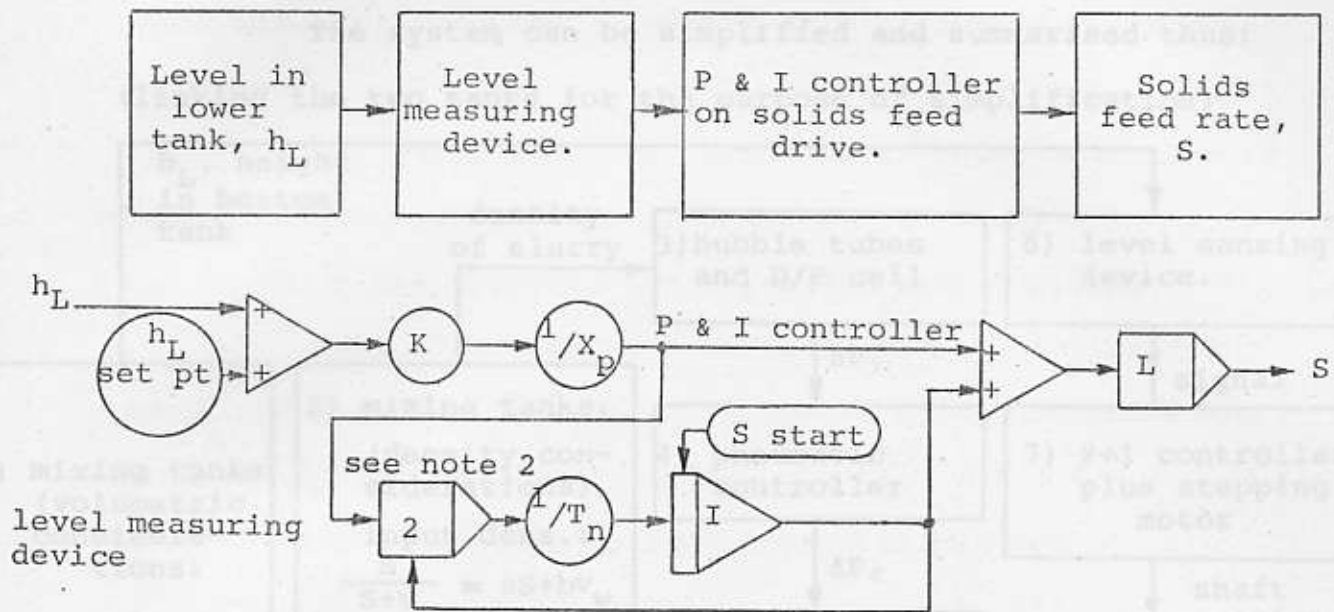
Controls

The existing controls were two proportional plus integral controllers on the solids feed and water feed, controlled by the level in the lower tank and density in the top tank respectively. Block diagrams summarising the setup in each case, and the corresponding model used, are given below.

Density controller -



Level controller -

Notes:

(1) The RC filtered noise generator was added to the output from the D/P cell to simulate the observed random fluctuations in the actual output.

(2) Block number 2 was user written. Its function was to restrict the incoming signal if the output from its associated integrator reached a predetermined limit.

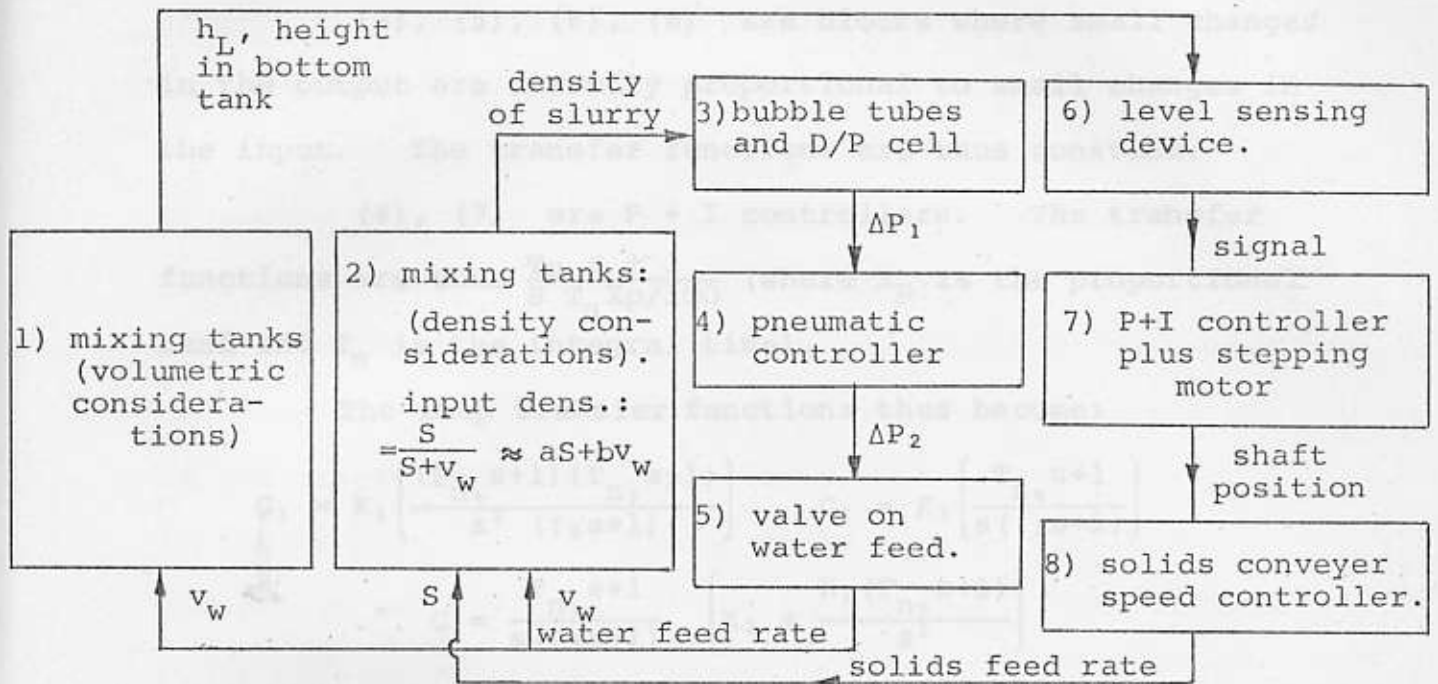
(3) Most of the constant gain blocks in these controls are conversion factors which were used to change units, e.g. to convert from the density of slurry to a pressure output from the bubble tubes.

These diagrams, when linked up, formed the basic non-linear model of the mixing tanks for use on the computer. They were sometimes slightly simplified (e.g. when trying a proportional-only controller) to shorten running time on the computer.

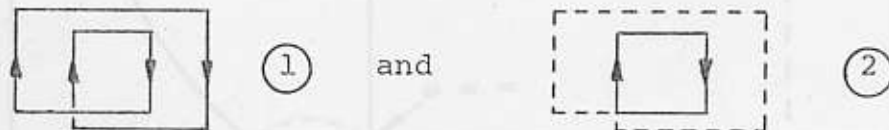
Linear/...

Linear Model

The system can be simplified and summarised thus:
(linking the two tanks for the purpose of simplification)



The system can be divided into two loops:



By breaking the diagram at the water feed rate stream where it leaves the valve block, the two loops become open. If G_1 and G_2 are the transfer functions around loops (1) and (2), then

$$G_{\text{system}} = G_1 + G_2$$

Consider each block in the diagram and its transfer functions:

(1) Mixing tanks, volumetric consideration. The output is the integral of changes in the input, thus the transfer function is (const./S.)

(2) Mixing tanks, density consideration. This

is both/...

6 is both a summer (where the two loops meet) and a C.S.T.R. whose transfer function is $\text{const.}/(\tau_2 s + 1)$ (where τ_2 is the dead time).

(3), (5), (6), (8) are blocks where small changes in the output are directly proportional to small changes in the input. The transfer functions are thus constant.

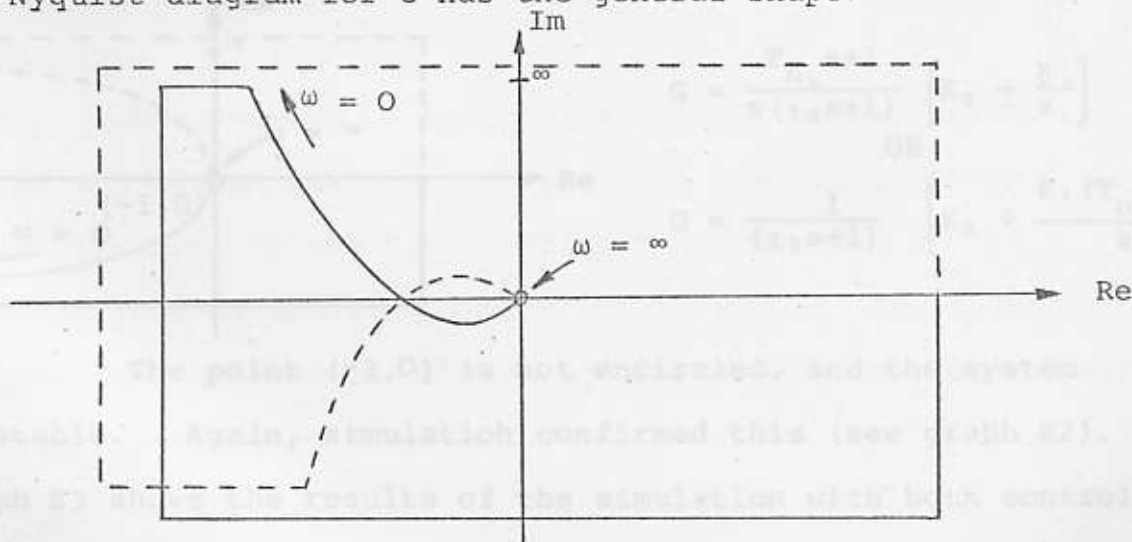
(4), (7) are P + I controllers. The transfer functions are thus $\frac{T_n s + 1}{s T_n X_p / 100}$ (where X_p is the proportional band and T_n is the integral time).

The loop transfer functions thus become:

$$G_1 = K_1 \left[\frac{(T_{n4} s + 1)(T_{n7} s + 1)}{s^3 (\tau_2 s + 1)} \right] \quad G_2 = K_2 \left[\frac{T_{n4} s + 1}{s (\tau_2 s + 1)} \right]$$

$$\therefore G = \frac{T_{n4} s + 1}{s (\tau_2 s + 1)} \left[K_2 + \frac{K_1 (T_{n7} s + 1)}{s^2} \right]$$

The Nyquist diagram for G has the general shape:



Except for the small area near the origin, the entire plane is encircled. For values of $\tau_2 > T_{n4}$, this area is particularly small.

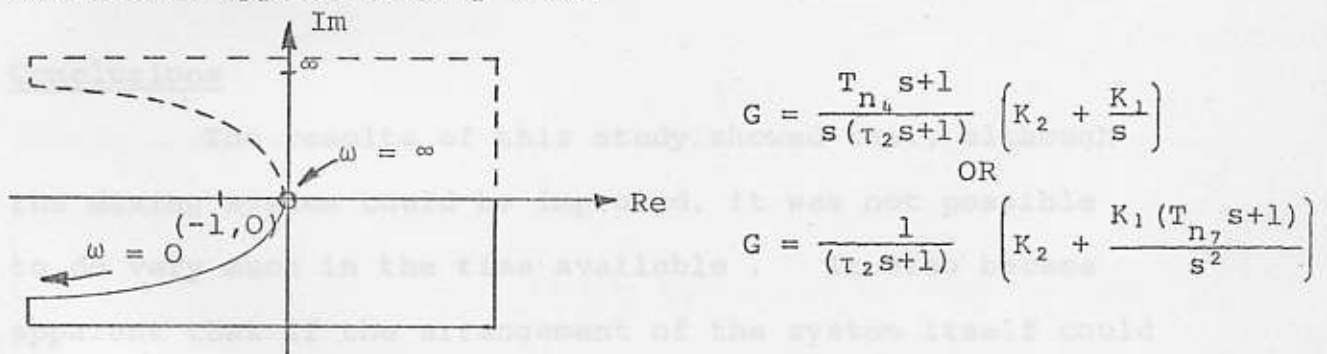
Results of Controller Study

The results of the linear study show that the

mixing/..

mixing tank system as it existed was inherently unstable. This was confirmed by the analogue simulation (see graph E1). Graph C5 shows similar results obtained from the actual plant. In practice, the system required frequent human intervention while operating.

Returning to the Nyquist diagram of the linear model, it should have been possible to obtain settings on the instruments which would have been stable, even though the system would appear underdamped. The fact that this was not possible is probably because of the oversimplification of the linear model, which is itself critical. However, it can be seen that the system could be made stable by removal of one (or more) of the integrators. The diagram would then appear roughly thus:



The point $(-1, 0)$ is not encircled, and the system is stable. Again, simulation confirmed this (see graph E2). Graph E3 shows the results of the simulation with both controllers purely proportional.

The most convenient place to remove one of the integrators was the level control for the solids feed. Even so, to convert either controller to purely proportional action would have taken a fair length of time, as completely

new units/..

new units would have been needed.

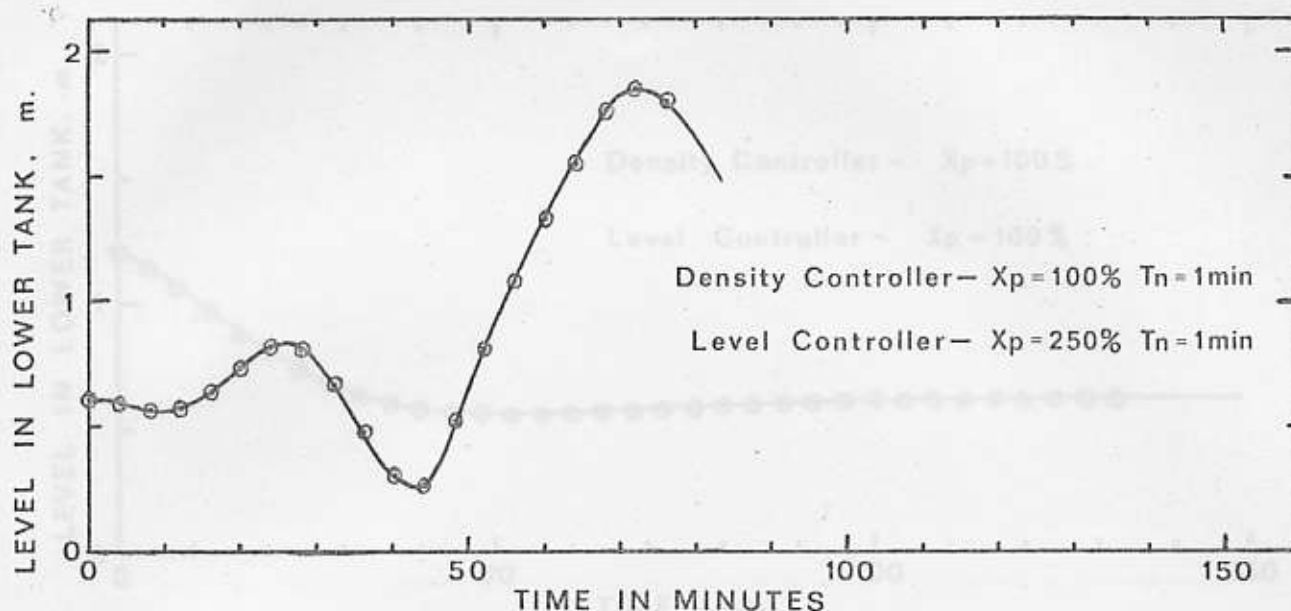
Another alternative was to use the level in the lower tank to control the water feed rate into the system, while the solids feed was held constant. A more detailed linear analysis showed that this was always stable, and that the system could be made asymptotically stable (i.e. no oscillations) by choosing certain matching values for the parameters X_p and T_n .

Graph E4 shows the analogue of this stable system oscillating for large values of X_p and T_n . When this setup was tried out in practice, it was found that the solids feed could not be kept sufficiently constant, so that even though the system was stable, the density of the slurry drifted during the run.

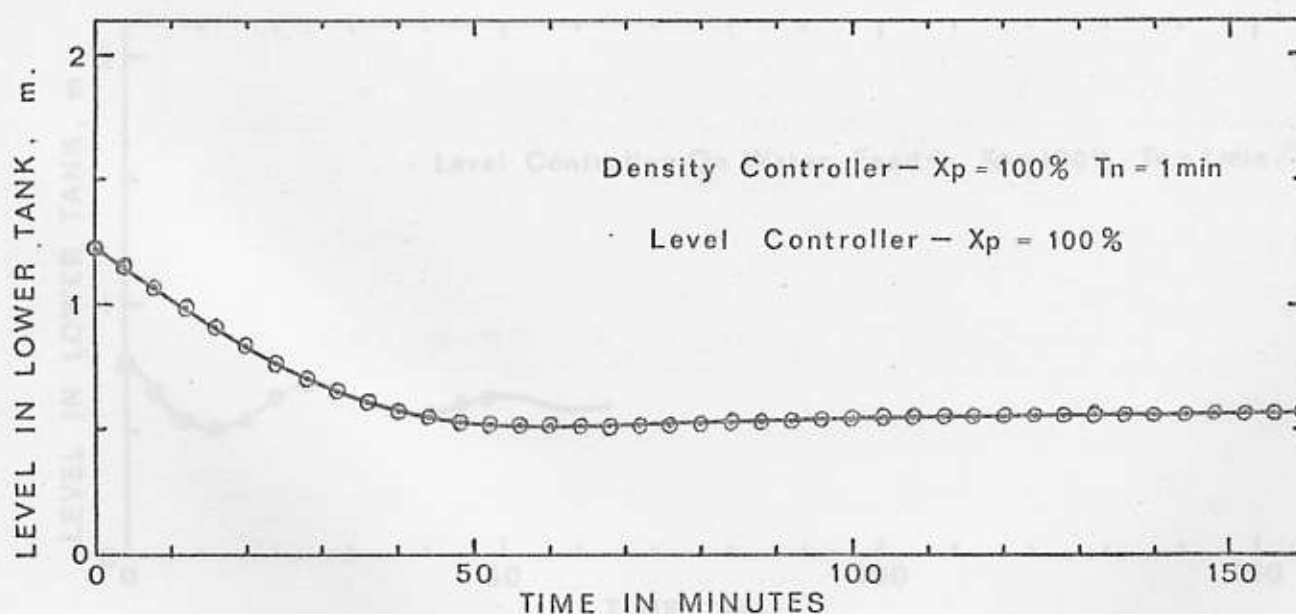
Conclusions

The results of this study showed that, although the mixing system could be improved, it was not possible to do very much in the time available. It also became apparent that if the arrangement of the system itself could be improved, or some other form of control fitted, far better performance could be achieved.

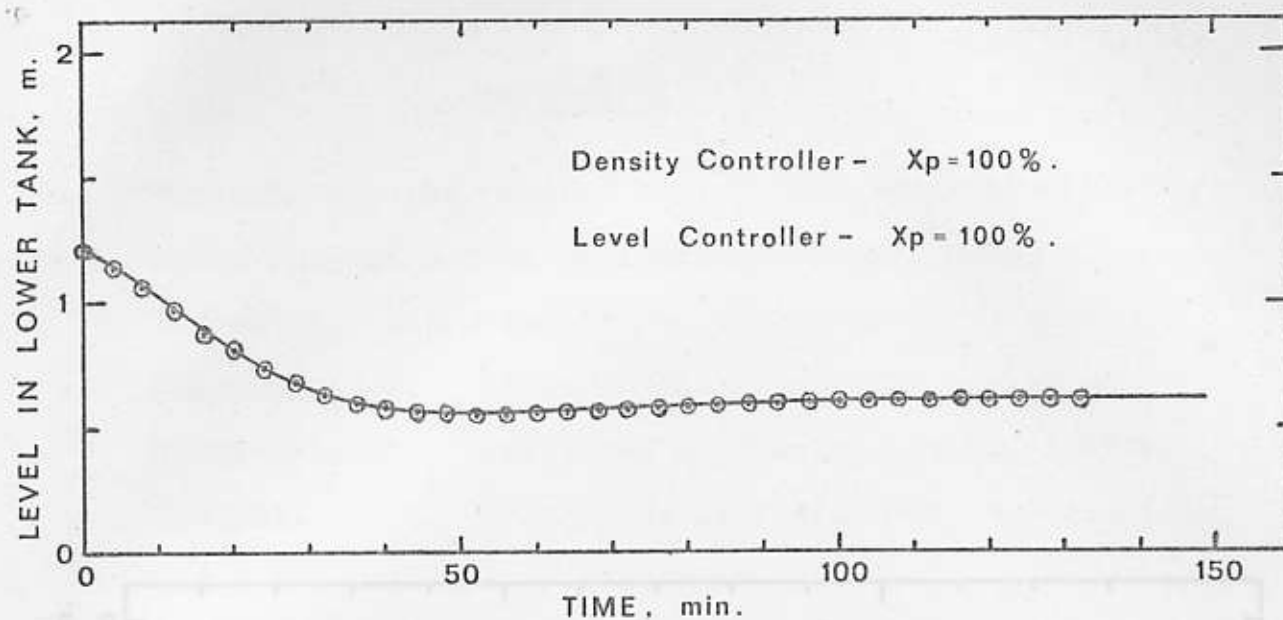
GRAPH E2. RESULTS OF SIMULATION
(Density Controller PI, Level Controller Prop. Only.)



GRAPH E1. RESULTS OF SIMULATION
 (Both Controllers P + I.)

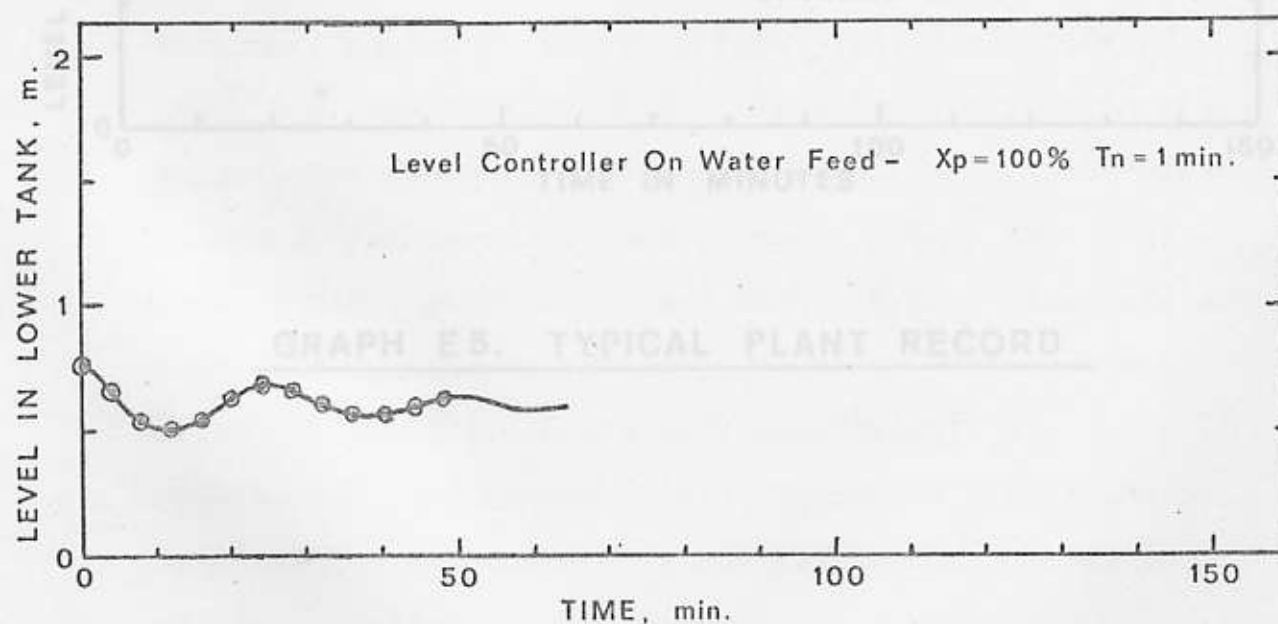


GRAPH E2. RESULTS OF SIMULATION
 (Density Controller PI, Level Controller Prop. Only.)



GRAPH E3. RESULTS OF SIMULATION.

(Both Controllers Prop. Only)



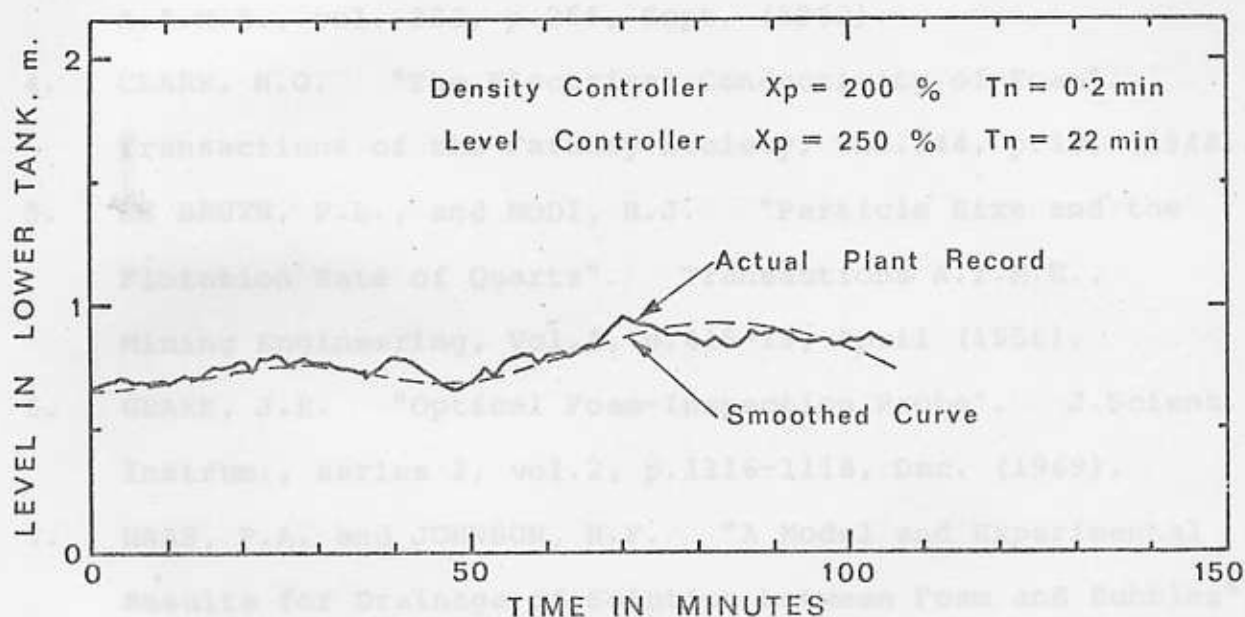
GRAPH E4. RESULTS OF SIMULATION.

(Level Controlling Water Feed.)

APPENDIX F

REFERENCES

1. ARMITAGE, W., and HARRIS, C.G. "Flotation Kinetics".
Froth Flotation 50th Anniversary Volume, Paper 9,
A.I.M.M.E., N.Y., (1963).
2. BIRNBAUM, J.B. "Foams: Theory and Industrial
Applications". Published by Reinhold, N.Y., (1953).
3. HARRIS, C.G. "Kinetics of Flotation" Transactions



GRAPH E5. TYPICAL PLANT RECORD

4. HARRIS, C.G. "Optical Foam Analysis".
Transactions, Series 2, vol. 2, p. 1216-1218, Dec. (1969).
5. HARRIS, C.G. and BIRNBAUM, J.B. "A Study of 2 Phase Model
of Flotation Process". Trans. Instn. Min. Metall.,
vol. 75, p. C153-C162, (1966).
6. HARRIS, C.G. and BIRNBAUM, J.B. "Flow Regimes of Stable
Foams". I. & E.C. Fundamentals, vol. 8, no. 3, p. 483-490,
Aug. (1969).

APPENDIX F

REFERENCES

1. ARBITER, N., and HARRIS, C.C. "Flotation Kinetics" Froth Flotation 50th Anniversary Volume, Paper 8, A.I.M.M.E., N.Y., (1962).
2. BIKERMAN, J.J. "Foams: Theory and Industrial Applications". Published by Reinhold, N.Y., (1953).
3. BUSHELL, C.H.G. "Kinetics of Flotation" Transactions A.I.M.E., vol. 223, p.266, Sept. (1962).
4. CLARK, N.O. "The Electrical Conductivity of Foam". Transactions of the Faraday Society, Vol. 44, p.13, (1948).
5. DE BRUYN, P.L., and MODI, H.J. "Particle Size and the Flotation Rate of Quartz". Transactions A.I.M.E., Mining Engineering, Vol.8, p.415-19, April (1956).
6. GEAKE, J.E. "Optical Foam-Inspection Probe". J.Scient. Instrum., series 2, vol.2, p.1116-1118, Dec. (1969).
7. HAAS, P.A. and JOHNSON, H.F. "A Model and Experimental Results for Drainage of Solution between Foam and Bubbles". I. & E.C. Fundamentals, vol.6, no.2, p.225, May (1967).
8. HARRIS, C.C., JOWETT, A., and GHOSH, S.K. "Analysis of Data from Continuous Flotation Tests". Transactions A.I.M.E., vol.226, p.444-447, Dec. (1963).
9. HARRIS, C.C. and RIMMER, H.W. "Study of 2 Phase Model of Flotation Process". Trans. Instn. Min. Metall., vol.75, p.C153-C162, (1966).
10. HOFFER, M.S. and RUBIN, E. "Flow Regimes of Stable Foams". I. & E.C. Fundamentals, vol.8, no.3, p.483-490, Aug. (1969).

11. I.B.M. Reference Manual. "Continuous Systems Modelling Program". (1130-CX-13X) Publication H20-0282-0, (1966).
12. JAKOBI, W.M., WOODCOCK, K.E., and GROVE, C.S., Jr.
"Theoretical Investigation of Foam Drainage" I.E.C.,
vol. 48, p.2045, (1956).
13. JOWETT, A. "Gangue Mineral Contamination of Froth"
Brit.Chem.Eng., vol. 2, no.5, p.330-333, May (1966).
14. KING, R.P., TE RIELE, W.A.M., and BUCHALTER, E.M.
"An Improved Distributed-Parameter Model for the
Kinetics of Mineral Flotation". Report no. 996,
Johannesburg, National Inst. for Metallurgy, Aug. (1970).
15. KLASSEN, V.I. and MOKROUSOV, V.A. "An Introduction
to the Theory of Flotation". Published by Butterworths,
London, (1963).
16. LEMLICH, R. "Foam Overflow Rate; Comparison of
Theory with Experiment". (Reply to ref. 21), Chem.
Eng. Sci., Vol.23, no.8, p.932-3, (1968).
17. LEONARD, R.A., and LEMLICH, R. "A Study of Inter-
stitial Liquid Flow in Foams". A.I.Ch.E. Journal,
vol. 2, no.1, p.18, Jan. (1965).
18. LIVSHITS, A.K., and DUDENKOV, S.V. "Some Factors in
Flotation Froth Stability". Part 7 of 7th International
Mineral Processing Congress, vol. 1, p.367-371.
19. LOVEDAY, B.K. "Analysis of Froth Flotation Kinetics"
Trans. Instn. Min. Metall., vol.C75, p.C219, (1966).
20. MAKSIMOV, I.I. and KHAINMAN, V.Ya. "Effects of Processes
Occurring in the Froth Layer, on the Rate and Selectivity
of Flotation". Tsvet. Met., vol.6, no.5, p.8, (1965).

21. ROSS, S. "Bubbles and Foam: New General Law". I.E.C. vol.61, p.48-57, Oct. (1969).
22. RUBIN, E., LA MANTIA, C.R. and GADEN, E.L. "Properties of Dynamic Foam Columns". Chem. Eng. Sci., vol.22, p.1117-1125, (1967).

| | |
|--------------|---|
| A | Surface area in flotation cell. |
| A' | Surface area of bubbles. |
| $C_p(D)$ | Concentration of entrained particles in froth in particle size range D to $D + dD$. |
| $C_p^*(D)$ | Concentration of entrainable particles in pulp in particle size range D to $D + dD$. |
| d_b | Mean bubble diameter. |
| D | Particle size. |
| E_p | Entrainment fraction for particle diameter D . |
| f | Liquid fraction. |
| $f(k, g, D)$ | Rate constant distribution density function. |
| $f_w(u)$ | Distribution density function for water drainage velocity. |
| $f_D(u)$ | Distribution density function for solids settling velocity. |
| g | Grads (also gravity constant). |
| h | Height of froth layer. |
| k | Rate constant. |
| k' | Proportionality constant. |
| K | Constant defined by $v_D = K.f.d$ |
| n | Number of stages. |
| P | Pressure. |
| Q_a | Air rate. |
| Q_w | Liquid overflow rate in froth. |

APPENDIX G

NOMENCLATURETheory

| | |
|--------------|--|
| A | Surface area in flotation cell. |
| A' | Surface area of bubbles. |
| $C_F(D)$ | Concentration of entrained particles in froth in particle size range D to $D + dD$. |
| $C_P(D)$ | Concentration of entrainable particles in pulp in particle size range D to $D + dD$. |
| d_m | Mean bubble diameter. |
| D | Particle size. |
| E_D | Entrainment fraction for particle diameter D . |
| f | Liquid fraction. |
| $f(k, g, D)$ | Rate constant distribution density function. |
| $f_W(u)$ | Distribution density function for water drainage velocity. |
| $f_D(u)$ | Distribution density function for solids settling velocity. |
| g | Grade (also gravity constant). |
| h | Height of froth layer. |
| k | Rate constant. |
| k' | Proportionality constant |
| K | Constant defined by $v_d = K \cdot f \cdot d_m$ |
| n | Number of stages. |
| p | Pressure. |
| Q_A | Air rate. |
| Q_W | Liquid overflow rate in froth. |


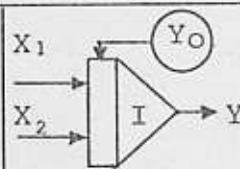
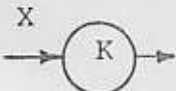
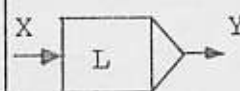
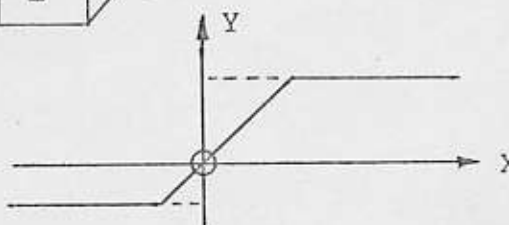
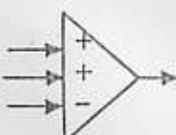
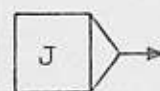
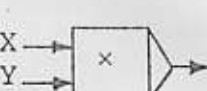
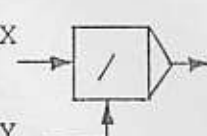
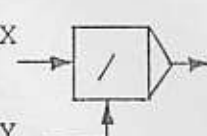
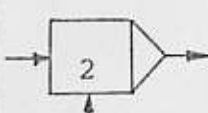
| | |
|--------------|---|
| r | Radius (of Plateau Border). |
| $R(k,g,D,h)$ | Function describing return from froth. |
| S | Fraction uncovered. |
| u | Downward velocity. |
| u_s | Stokes settling velocity. |
| v_d | Drainage velocity. |
| \bar{v}_i | Mean interstitial velocity for water. |
| v_{\max} | $\bar{v}_i + v_d$ |
| v_{\min} | $\bar{v}_i - v_d$ |
| W | Mass of solids in the cell. |
| z | Level in froth layer from froth-liquid interface. |
| μ | Viscosity of water. |
| ρ_L | Density of water. |
| ρ_s | Density of solids. |
| σ | Surface tension. |
| $\phi(D)$ | Function of D in flotation rate expression. |

Controller Study (Appendix E)

| | |
|----------|--|
| A_L | Cross sectional area of lower mixing tank. |
| C_L | Solids concentration in lower tank. |
| C_V | Solids concentration in upper tank. |
| $G(s)$ | Transfer function. |
| h_L | Slurry level in lower mixing tank. |
| K | Gain constant. |
| P | Pressure signal (usually subscripted). |
| s | Variable defined by Laplace Transform. |
| S | Solids feed rate. |
| T_n | Integral time of controller. |
| v_{io} | Recirculation rate: lower to upper tank. |

| | |
|----------|--|
| v_r | Overflow return rate: upper to lower tank. |
| v_{so} | Slurry withdrawal rate from upper tank. |
| v_w | Water feed rate. |
| V_L | Volume of lower mixing tank = $A_L h_L$. |
| V_u | Volume of upper mixing tank. |
| X_p | Proportional band of controller, %. |
| τ | Time constant. |

Symbols Used in Controller Study. (Appendix E.)

| | |
|---|--|
|  constant "A" |  Integrator $Y = Y_O + \int (X_1 + X_2) dt$ |
|  $Y = KX$ |  limiter  |
|  summing block |  random signal generator |
|  multiply $X \times Y$ |  divide X by Y |
|  divide X by Y |  user written block (see note 2 p.E5) |